NRC·CNRC

NRC Publications Archive
Archives des publications du CNRC

An experimental investigation of side intake cooling for passenger cars

Schaub, U. W.; Bassett, R. W.

For the publisher's version, please access the DOI link below./ Pour consulter la version de l'éditeur, utilisez le lien DOI ci-dessous.

Publisher's version / Version de l'éditeur:
https://doi.org/10.4224/40003606

Laboratory Technical Report (National Research Council Canada. Division of Mechanical Engineering. Engine Laboratory); no. LTR-ENG-100, 1981-04

NRC Publications Archive Record / Notice des Archives des publications du CNRC :
https://nrc-publications.canada.ca/eng/view/object/?id=5d7be100-13d0-4d5e-a364-fb31f0544f97
https://publications-cnrc.canada.ca/fra/voir/objet/?id=5d7be100-13d0-4d5e-a364-fb31f0544f97

Access and use of this website and the material on it are subject to the Terms and Conditions set forth at
https://nrc-publications.canada.ca/eng/copyright
READ THESE TERMS AND CONDITIONS CAREFULLY BEFORE USING THIS WEBSITE.

L'accès à ce site Web et l'utilisation de son contenu sont assujettis aux conditions présentées dans le site
https://publications-cnrc.canada.ca/fra/droits
LISEZ CES CONDITIONS ATTENTIVEMENT AVANT D'UTILISER CE SITE WEB.

Questions? Contact the NRC Publications Archive team at PublicationsArchive-ArchivesPublications@nrc-cnrc.gc.ca. If you wish to email the authors directly, please see the first page of the publication for their contact information.

Vous avez des questions? Nous pouvons vous aider. Pour communiquer directement avec un auteur, consultez la première page de la revue dans laquelle son article a été publié afin de trouver ses coordonnées. Si vous n'arrivez pas à les repérer, communiquez avec nous à PublicationsArchive-ArchivesPublications@nrc-cnrc.gc.ca.

National Research Council Canada | Conseil national de recherches Canada

Canada

DECLASSIFIED
DÉCLASSIFIÉ

National Research Council Canada | Conseil national de recherches Canada

DIVISION OF MECHANICAL ENGINEERING

DIVISION DE GÉNIE MÉCANIQUE

PAGES 24
PAGES

FIG.
DIAG.

TABLES
TABLES

REPORT
RAPPORT

LABORATORY / LABORATOIRE

ENGINE LABORATORY

REPORT LTR-ENG-100
RAPPORT

DATE APRIL 1981
DATE

LAB. ORDER 21744
COMM. LAB.

FILE 3641-3 (L)
DOSSIER

FOR
POUR

REFERENCE
RÉFÉRENCE

LTR-ENG-100

AN EXPERIMENTAL INVESTIGATION OF SIDE INTAKE COOLING FOR PASSENGER CARS

SUBMITTED BY H. S. Fowler
PRÉSENTÉ PAR
LABORATORY HEAD
CHEF DE LABORATOIRE

APPROVED E. H. Dudgeon
APPROUVÉ
DIRECTOR
DIRECTEUR

AUTHOR (s) U. W. Schaub, R. W. Bassett
AUTEUR

Distribution: Limited
Classification: Limited

THIS REPORT MAY NOT BE PUBLISHED WHOLLY OR IN PART WITHOUT THE WRITTEN CONSENT OF THE DIVISION OF MECHANICAL ENGINEERING

CE RAPPORT NE DOIT PAS ÊTRE REPRODUIT, NI EN ENTIER NI EN PARTIE, SANS UNE AUTORISATION ÉCRITE DE LA DIVISION DE GÉNIE MÉCANIQUE

COPY NO. 1
COPIE NR.

SUMMARY

A side intake cooling system, operating entirely without the aid of ram air, was compared to a standard frontal intake cooling system with respect to aerodynamic performance and total energy requirements. The study was made on a full scale standard North American passenger car in the 30 ft NRC wind tunnel.

The study showed that side intake cooling systems could be at least as effective and as efficient as standard cooling systems. On the whole the side intake cooling system was observed to be less sensitive to variations in the approach air velocity and to improve the overall vehicle aerodynamics.

The investigation was only an evaluation of a concept and not an optimization in any sense. The side intake concept seems fundamentally sound and considerable potential remains to develop the idea with respect to energy saving.

Logical extensions to the present work include the following options:

- An aerodynamic optimization of the side intake and associated internal air ducting, including repositioning the radiator and A/C condenser.

- Development of a more suitably matched and more efficient cooling fan unit.

- A complete revision of the aerodynamic styling of the front end (in the absence of frontal intakes and heat exchanger constraints) to reduce vehicle drag. Estimates showed that a 5% reduction in this vehicle's drag would reduce the fuel consumption by 3%.

FOREWORD

This work reports on the second part of on-going research on the aerodynamics of automotive engine cooling systems. The first part dealt with ram air effects on the air side cooling system performance of a typical North American passenger car and was reported in References 4 and 5. Although the investigation involved only one vehicle, the present work demonstrates that the interpretive methods derived are applicable generally. The present work investigates the performance of and compares the energy requirements for two types of automotive cooling system concepts: a conventional one using both ram and fan cooling (frontal intakes), and a novel side intake cooling system concept based on 100% fan cooling. Both parts of the completed work were done under ambient cooling system temperature. Complementary (hot) cooling tests under loaded engine conditions are scheduled to be done by Canadian Fram Limited in Chatham, Ontario.

The research was aided by Canadian Fram Limited, who provided the test vehicle and spare parts. Support in the form of company test data and specifications was given by the Ford Motor Company. The continuing support and interest of these firms has been most valuable.

The experimental work was done at NRC, in the test facilities of the Division of Mechanical Engineering and the National Aeronautical Establishment. Supplementary funding by the Strategic Studies Branch of Transport Canada for special equipment purchases is especially gratefully acknowledged.

The personnel associated with the research and their specific responsibilities were as follows:

National Research Council

Mr. E. H. Dudgeon, Director of the Division of Mechanical Engineering
- program definition, direction
- overall responsibility

Mr. H. S. Fowler, Section Head, Engine Laboratory
- program management
- financial responsibility for project

Dr. U. W. Schaub, Senior Research Officer
- project engineer
- project definition and direction

Mr. R. W. Bassett, Senior Technical Officer
- technologist in charge of testing and instrumentation, data system, data handling and reduction

Mr. R. J. Rimmer, Senior Technical Officer
- crew chief, preparation and installation of hardware, operation and transport of equipment, testing, safety

Mr. G. A. Fowler, Senior Designer
- design of experimental hardware
- technical photography

Mr. G. R. Matthews, Technical Officer
- experimental assistant

Canadian Fram Limited

Mr. H. N. Charles, Cooling Products Engineering Manager
- technical consultant

Transport Canada

Mr. G. B. Maund, Program Manager for the Strategic Studies Branch
- project review, Transport Canada

TABLE OF CONTENTS

LIST OF ILLUSTRATIONS

1. INTRODUCTION

The widespread use of ram air for automotive engine cooling had its origin in the early history of the motor car. Radiators were placed up front, where ram air was "freely" available. Because the vehicles moved slowly the ram pressure was minimal and generated very low radiator face velocities. This necessitated large radiator face areas. The radiator and its shell came to serve more than just a strictly functional purpose; they had such an imposing looking and distinctive appearance that they quickly became the identifying symbol or marque of the automobile's maker.

The growing demand for more power eventually necessitated adding cooling fans to augment ram cooling. Most cars today of course still rely on ram and the cooling fan to achieve engine cooling jointly.

The radiator shell evolved into a grilled intake, which is continuing to characterize the vehicle model as well as to offer a strong decorative appeal to both stylists and customers.

In recent years, models have been downsized and replaced in response to restrictive demands for meeting legislated Corporate Average Fuel Economy (CAFE) requirements. Cars are becoming smaller and more fuel efficient - and their grilles less distinctive.

Although frontal intakes are still used almost universally for cooling purposes there is a growing appreciation that the active intake area changes drastically with approach air speed. A wind tunnel study of ram effects on the cooling system performance of an actual car demonstrated that front end resistance is created not only by cooling flow but also by approach air speed[1]. Consequently, not only is it most difficult to make one intake satisfy the requirements for minimum loss of both ram and 100% fan cooling, but it seems as well that the energy costs due to the additional ram losses and momentum drag are not insignificant. The same study showed that the power necessary to overcome ram momentum and drive the cooling fan could exceed the input power required if the cooling fan delivered the same rate of cooling flow without the assistance of ram.

The power demands to drive the cooling fan and to overcome ram air momentum were independently estimated by Hawes[2] on the basis of simple momentum and energy theory. By assuming reasonable component and drive train efficiencies it was shown that ram air cooling required more engine power than fan cooling did.

It has of course been known for a long time that frontal intake cars usually experience a significant reduction in drag when the intakes are covered up. The reference that documents this observation[3] also

shows that one rear-engined car, using 100% fan cooling, actually increased drag when the cooling air intakes were covered up.

There is a great deal of evidence which shows the drag and energy penalties of the cooling system[4,5,6]; but the energy needs of a standard cooling system (a combination of ram and fan) have not been compared experimentally with that of 100% fan cooling.

A frontal intake always receives some ram and therefore cannot be used to investigate 100% fan cooling. Placing the intake axis normal to the approach flow creates opportunities. Modern passenger car design has achieved more efficient air flow over the vehicle than round its sides; the wedge shape is one good example. Good streamlining round the sides of the vehicle is usually not possible because of the need for front wheel openings and the practical limits placed on the vehicle's plan view aspect ratio. The sides of the vehicle therefore suggest themselves as the most promising location for cooling inlets because they usually feature large regions of poor surface flow, i.e. considerably degraded total pressure and little kinetic energy in the air.

The above rationale leads to the side intake concept which will now be described.

2. EXPERIMENTAL METHOD

2.1 TEST SITES

The research described herein was primarily a wind tunnel study making use of NRC's V/STOL tunnel at NAE Uplands in Ottawa. A limited number of supportive tests were also done on a divided four-lane public highway under selected weather conditions with police support in managing control over normal traffic flow.

The wind tunnel, shown in Figure 1, features a closed air circuit and a 9 x 9 m (30 x 30 ft) closed test section. The tunnel's force balance is located directly beneath the test section and is terminated at the tunnel floor in four wheel pads for automotive applications. A complete description of this facility is given in Reference 7.

An exhaust gas extraction system mounted in the test section turntable floor and isolated from the active balance elements and the test vehicle was used for live vehicle (engine running) experiments, see Figure 2. Fuel flow to the engine was provided by the vehicle's own fuel storage and delivery system.

2.2 TEST VEHICLE

The test vehicle had to satisfy the following requirements:

- wheel well liners with adequate space between the liner and the front outer fender to serve as an air duct,

- sufficient space between the frontal grille and the horse collar to act as an entry plenum to the A/C condenser,

- a reasonably spacious engine bay that would permit relocating accessories and installation of instrumentation,

- adequate external access to the passenger compartment for convenient installation and service of the data acquisition system,

- a vehicle size that would be typical of a popular North American passenger car during the eighties,

- the vehicle had to have a directly driven cooling fan with an unvented fan shroud.

The vehicle chosen for the tests was a 1980 3-door Ford Mustang with a 2.3 ℓ four cylinder engine, four speed transmission, air conditioning, and sport suspension. Figure 3 shows the test vehicle inside the working section of the tunnel.

To modify the test vehicle from standard frontal to side intakes involved the following changes:

- closing and sealing off all of the frontal intakes,

- replacing the plastic headlight reinforcement assembly with a more space-conserving transverse steel brace,

- closing off and fairing in all headlight recesses and parking lights,

- sealing up all holes and joints along the air path that communicate with either the outside or the engine bay,

- removing the reinforcement plates underneath the bumper isolators,

- cutting new intake openings in the front fender panels.

As outlined in Section 4, three side intake openings were chosen and three holes were cut in each front fender. One so modified front

fender is depicted in Figure 4. Since the prime purpose of this investigation was to examine the concept of side intakes, no effort was made to provide a low loss air path for cooling air. The side intakes were simple sharp edged cutouts in the fenders of more or less rectangular shape and varying in area from 15 to 43% of the radiator area. The dry space between the outer fender and its plastic liner served as the duct passage to carry cooling air from the intake to the front of the A/C condenser.

The side intake concept was tested by exposing pairs (r.h. and l.h. sides) in sequence and using fitted blanking plates over those not in use. The intake illustrated in Figure 5 had a smooth lip and was part of a test sequence to investigate effects of varying entrance losses.

The tests were done almost exclusively with the vehicle's suspension pulled down and restrained to give standard manufacturer's vehicle height: rocker panel drain dimples to ground clearance front to back 7-1/4 and 6-1/2 ins., respectively. The effects on aerodynamic forces of unrestrained and 0.44 deg. nose-up vehicle height were also investigated.

The test vehicle was secured in the wind tunnel by locked foot and hand brakes. The coolant thermostat was blocked wide open. The vehicle was tested in the following configurations:

- standard car,
- with frontal intakes faired in,
- with frontal intakes, head and parking lights faired in,
- with frontal intakes, head and parking lights faired in and new side intakes open.

Except when collecting balance force data the vehicle was manned by a test crew comprising a "driver" and a data system operator.

2.3 IN-CAR INSTRUMENTATION AND DATA ACQUISITION SYSTEM

2.3.1 Data Acquisition System

With the exception of balance forces data was collected by a pre-programmed on-board acquisition system located directly behind the driver's seat, as illustrated in Figure 6. Data was recorded on magnetic tape and transmitted after each test series to the central NRC computing facility for reduction and printing.

2.3.2 Measurements

Fan Speed - Fan speed was sensed with a slotted disk mounted on the fan pulley and a L.E.D./photo-transistor pickup. It was measured on a standard frequency counter.

Torque - A torquemeter developed jointly by Canadian Fram Limited and NRC was used to measure fan input torque. It was installed in place of the distance piece normally mounted between the fan spider and the drive pulley. Figures 7 and 8 show parts of this meter with its two strain gauged cantilever beams. The gauges arranged in a Wheatstone bridge configuration were excited and transmitted the unbalance voltage output signal via a standard commercial slipring unit. The meter, which was originally developed for use on smoother V-8 engines was modified mechanically with internal damping for use on the rougher 4 cylinder engine under test. The cooling fan and torquemeter assembly was balanced statically and dynamically prior to installation. The torquemeter was calibrated statically on the vehicle before and between experiments.

Pressures - Pressures were sensed by means of Scanivalve mounted differential pressure transducers using the approach air total pressure as a backing pressure.

Engine bay static pressure was sensed by pressure lines capped with small porous foam turbulence shields, under the engine bay on the tunnel floor by thin multitube pressure tape, and on the body panels by standard detail static pressure taps.

Side intake total pressure was sensed with a number of internally chamfered Kiel type probes in the fender panel plane. Due to considerable non-uniformity in flow direction and total pressure in the intake region, a number of probes were distributed around one intake and aligned individually at approach air speeds through use of wool tufts. A probe rake using several total pressure heads was mounted at right angles to the front fender of the standard car to assist in finding the most suitable locations for side intakes. Total pressure was sensed also in the radiator exit plane in order to determine front end losses and for the general purpose of establishing detailed stream properties of the cooling flow. The nature of the flow immediately downstream of the radiator core called for large diameter (6 mm) total pressure probes[8].

Temperatures - Measurements included temperatures in the approach air stream, engine bay environment, and cooling air at the radiator exit plane. All temperatures were sensed with chromel-alumel thermocouples using cold junction compensation.

Cooling Air Flow - Air speed at the radiator exit plane was sensed with free propeller anemometers developed by NRC. The units illustrated in Figure 9 had a diameter of 50 mm (2 ins.) and were designed to have a sensitivity of 33 Hz per metre per second in order to be able to indicate very low air speeds. The propeller blades were flat plates twisted to satisfy the free vortex rule. Independent experimental work at NRC[8] had shown that these anemometers supported in a vertical frame rotated nearly 6% faster in the highly non-uniform flow immediately downstream of the radiator core than in smooth flow having the same average velocity.

Six individual anemometer units were arranged in the vertical frame which was traversed horizontally to eight sampling positions across the radiator face inside the fan shroud. This gave an array of 48 sampling stations. Figure 10 shows the configuration including five unshielded thermocouples and five total pressure probes spaced midway between the anemometers.

Approach Air Speed - Tunnel air approach speed was derived from tunnel total and static pressures and was corrected for blockage using the 1/4 area ratio correction given in Pope[9]. The frontal area of the test vehicle was 2.3% of the tunnel working section area.

Other Measurements - Balance forces along with tunnel velocity and vehicle yaw angle were measured and recorded by the tunnel's data acquisition system. Moments were derived from the measured pad forces and appropriate vehicle and tunnel balance dimensions.

Flow visualization studies were made making use of a non-toxic cosmetic oil smoke. The smoke was injected from the tip of a 2.5 m long hand held lance at tunnel air speeds of 20 km/h. Simultaneous colour photographs were taken by two hand held 35 mm cameras in the vertical and horizontal planes.

3. DRAG MEASUREMENTS ON THE STANDARD VEHICLE

3.1 VEHICLE DRAG

The drag coefficient of the standard test vehicle at 80 km/h with the cooling fan speed matched to the 4th gear condition was 0.420, see Figure 11. The same figure shows that the drag coefficient was not constant, but increased rapidly with vehicle yaw: $C_D = 0.430$ for $\psi = \pm 5°$ and $C_D = 0.505$ for $\psi = +15°$. Drag coefficient was observed also to increase, albeit moderately, as approach air speed was reduced,

e.g. C_D = 0.430 and 0.413 for V_∞ = 50 and 150 km/h, respectively. Cooling fan operation had surprisingly little influence on drag coefficient; in fact, a comparison between Figures 12 and 13 shows that it was reduced by only 0.004 while the fan was stopped and ram became the only mover of cooling air.

Cooling system drag was however far from insignificant. In fact, cooling system drag was a major contribution to overall vehicle drag, chiefly because of the role played by momentum or ram drag. This can be seen by comparing the drag of the standard vehicle with 100% ram cooling (stationary cooling fan), Figure 13, with that of the same vehicle when its intakes were completely covered up with closure plates, Figure 14. The drag coefficient was reduced from 0.434 to 0.376 and from 0.411 to 0.360 at 50 and 150 km/h, respectively. A similar trend was observed at +15° of vehicle yaw.

For reasons outlined earlier, most of the drag measurements with non-standard vehicle configurations were made with covered head and parking lights. Consequently, absolute drag coefficients had to be calculated by reducing the measured values by a head and parking light drag decrement. On the other hand, adequate comparisons of drag coefficient are possible without this adjustment. Figure 15 shows the head and parking light drag penalty and enables comparisons of absolute drag coefficients. It is evident that the net ram contribution to aerodynamic drag was 8% at 150 km/h and as high as 10% at 50 km/h.

3.2 RAM DRAG

Ram momentum was calculated independently from measured cooling air flows and the premise that all of the cooling air entering the engine bay was brought to rest relative to the vehicle. On comparing Figure 16 with Figure 15 it can be seen that ram momentum drag was indeed nearly equal to cooling system drag measured by force balance under still fan conditions.

When the cooling fan operated however, it augmented cooling flow substantially (as will be shown in Figure 33) and with it momentum drag, as demonstrated in Figure 16. Despite this increase, the net vehicle drag, as measured by the wind tunnel balance, increased only by a disproportionately small amount - ΔC_D = 0.005 according to Figure 15. It appears therefore, that momentum drag was larger than cooling system drag whenever the cooling fan operated. The difference between these two quantities can be rationalized as follows. Regardless of the magnitude of approach air speed, the jet efflux from the fan impinges fully on the engine and its accessory parts so that no net thrust is produced. The increased momentum

created by the cooling fan is balanced by associated pressure forces acting on various intake surfaces, just as in the case of a stationary vehicle, where the force balance is more easily understood.

4. SELECTION OF BODY AREAS FOR SIDE INTAKES

To minimize cooling system drag, cooling air must be taken from regions of naturally low total pressure and low kinetic energy. To minimize the energy demand of the cooling fan there should be as little loss of total pressure as possible between the intake and discharge faces of the cooling system.

Extensive pressure mapping was done on the sides of the front fenders of the standard test vehicle. Typical pressure coefficient $(\frac{P - P_{S\infty}}{q_\infty})$ isobars are presented in Figures 17 to 22. Those exhibit appreciable change with vehicle yaw but very little variation with approach air and cooling fan speeds. Pressure plots like these, together with smoke flow visualization (see Section 8) and total pressure measurements in the external flow alongside the vehicle, see Figures 23 and 24, were used to identify trial locations for side intakes on both sides of the vehicle above and to the rear of the front wheel fender opening. The identified intake boundaries are indicated as superposed broken lines on the standard vehicle profiles. The shape and size of the openings were dictated to some extent by the available fender structure.

INTAKE	LOCATION OF INTAKE	AREA PER SIDE	
		cm^2	$ins.^2$
A	above the wheel opening	239	37
B	above and to the rear of the wheel opening	555	86
C	to the rear of the wheel opening, at the bottom	194	30

Intake "C" was expected to have the best potential from an aerodynamic point of view and the greatest disadvantage for practical considerations.

5. DRAG MEASUREMENTS ON THE SIDE INTAKE VEHICLE

Although the trial intakes were selected carefully for the purpose of testing the side intake concept, they were not achievements of performance optima with respect to low loss entry and to minimizing vehicle drag. Nevertheless, as will be shown, a considerable measure of success in vehicle drag reduction was achieved relative to the standard vehicle with conventional frontal intakes.

Side intake drag results are shown in Figures 25, 26, and 27. These drag data were obtained for the same basic vehicle, but with its front end completely faired in, except for the exposed licence plate in its standard location. Thus, in order to enable direct comparisons with the standard vehicle drag, a head and parking light drag decrement, measured independently, was removed. Table 1 and Figure 28 summarize the principal experimental results, corrected for normal head and parking light drag effect. The drag coefficients shown include those of the standard vehicle using ram and fan cooling, the frontal inlets covered, and the three side intake configurations A, B, and C.

Evidently all three side intakes achieved significant drag reductions. Side intake "C", drawing wheel outwash air directly, featured the lowest drag coefficient, as low in fact as the best possible for the basic vehicle shape, i.e. with the frontal intakes covered and zero cooling system drag. Side intakes "A" and "B" fell somewhat short of eliminating 100% of the normal cooling system drag. The fact that their respective drag coefficients increased perceptibly with cooling fan speed suggests that these intakes ingested air carrying some residual (ram) momentum at the larger cooling flows.

Side intakes "A" and "B" should be less prone to ingestion of road debris than "C", and despite a slight penalty in the overall aerodynamic performance of the vehicle relative to "C", would be more useful in a practical sense.

Section 8 of this report offers a sample record of photographic flow visualization results. The reader is invited to draw comparisons between the standard and modified vehicle external flow fields.

A study of all of the aerodynamic forces revealed that the chosen standard vehicle had a better than average aerodynamic performance relative to other present North American and foreign passenger car models. Consequently, any benefits shown in drag reduction through elimination of cooling system drag were probably more modest than they would be for other more "boxy" cars. Nevertheless, there seems to be substantial scope for optimization of intake geometry and location and the internal air ducting on the present test vehicle, not to mention the potential advantages of adjusting the basic front end styling when the obvious constraints of frontal inlets are not necessary.

TABLE I

DRAG COEFFICIENT SUMMARY

YAW ANGLE $\psi = 0°$

CONFIGURATION		BASIC*	STAND'D FRONT END	SIDE INTAKE					
				A		B		C	
FAN SPEED (N)		0	N ~ V_∞	2500	4500	2500	4500	2500	4500
APPROACH SPEED = V_∞ (km/h)	50	0.388	0.437	0.404	0.413	0.402	0.407		
	90	0.383	0.420	0.394	0.398	0.391	0.396	0.386	0.382
	128	0.379	0.413	0.388	0.391	0.387	0.390	0.386	0.382

YAW ANGLE $\psi = +15°$

CONFIGURATION		BASIC*	STAND'D FRONT END	SIDE INTAKE					
				A		B		C	
FAN SPEED (N)		0	N ~ V_∞	2500	4500	2500	4500	2500	4500
APPROACH SPEED = V_∞ (km/h)	50	0.470	0.512						
	90	0.477	0.498		0.470		0.468		0.464
	128	0.478	0.500		0.462		0.464		0.456

*BASIC MEANS STANDARD CAR WITH FAIRED IN FRONT END AIR INTAKES, WITH NORMAL HEAD AND PARKING LIGHTS AND STANDARD LICENCE PLATE MOUNT.

6. AERODYNAMIC PERFORMANCE OF THE COOLING SYSTEM

6.1 FRONT END LOSSES

6.1.1 Standard Car

Front end loss was customarily defined as the difference in total pressure between that in the approach air flow and that at the rear face of the radiator. This loss was measured for a number of cooling air flow rates, as shown in Figure 29. The data exhibited a characteristic dependence on the square of cooling air flow (or velocity) and ram dynamic pressure, and were therefore correlated by means of linear regression using Q_a^2 as the independent variable.

TABLE 2

Standard Car Regression Line Fits for Front End Losses
$\Delta P_o = mQ_a^2 + b$

V_∞	m	b
0	6.59×10^{-8}	0.076
50	6.88×10^{-8}	0.387
100	5.77×10^{-8}	1.567
150*	5.20×10^{-8}	3.489

Where V_∞ is in km/h
ΔP_o is in ins. w.g.
Q_a is in ft^3/m

Reference 1 identifies two basic loss mechanisms: the basic loss at zero forward speed having to do with friction effects, which is proportional to Q_a^2, and a ram loss associated with catch flow stream tube contraction effects of the cooling air as it passes through the frontal intakes, which is proportional to V_∞^2. The coefficients of Q_a^2 would be constant if the internal air path losses were independent of approach air speed. The indicated variations relative to the basic ($V_\infty = 0$) loss case, as large as 21% for the

*Due to lack of sufficient data there is considerable uncertainty in the regression fit for 150 km/h.

150 km/h case, are attributed primarily to lack of adequate data and to a lesser extent on stream tube contraction effects.

To a first approximation, with an accuracy of ±2.5% at $Q_a = 0$, the ram losses can be represented by the ordinate intercepts of the above regression lines. Expressed in non-dimensional form the ram loss coefficient in the speed range $0 \leqslant V_\infty \leqslant 150$ km/h was

$$\frac{\Delta P_{oRAM}}{q_\infty} \doteq 0.77$$

The standard frontal intakes are seen to be highly restrictive to cooling flow at forward speed, since 77% of the ram dynamic pressure was destroyed at the frontal grille openings.

6.1.2 Side Intake Car

Because no precautions were taken to avoid the large losses created by the sharp edges of the side intake openings and the rough and cramped fender spaces the pressure losses generated from still surroundings were obviously much greater than in the case of the frontal intake. This can be appreciated by comparing Figure 30 with Figure 29.

Using the customary definition of front end loss, i.e. that based on approach air total pressure, the side intake configuration suffered seemingly large losses with increasing approach air speed, see Figure 30. However, since side intakes are intended to draw air from regions of separated flow (low total pressure), the customary definition is inappropriate. Total pressure loss was instead referenced to independently measured total pressures in the side intake planes, which were, because of external aerodynamic effects, substantially lower than the stagnation pressure of the approach flow.

The side intakes were actually quite well shielded from the approach flow because the so-defined front end loss was much less sensitive to approach air speed and direction than for frontal intakes. Under normal running line conditions, e.g. 4th gear operation, the front end system losses of the side intake configuration tested were very similar to those of the frontal intake system losses at identical conditions. At lower than normal cooling flows the side intake system losses are substantially less. The above observations can be checked in Figure 31.

Intake "C" drew cooling air directly from the outwash of the front wheel, a region of somewhat lower static pressure than higher up on the fender panel near "A" and "B", and potentially subject to considerable dust ingestion. Both intakes "A" and "C" were narrow slits

due to spacial constraints inside the fender. Because of this they experienced very high edge velocities and shed bad flow separations directly into ducts of small cross sectional area, especially so in the case of "A".

While all side intakes suffered from poor entrance flow intake "B" seemed to offer the best location on the present test vehicle because:

- the inside fender space was the least congested and hence availed the largest possible entrance area,

- it contributed to one of the lowest front end losses,

- it was better protected than "C" from wheel outwash and possible debris ingestion.

Bearing in mind that the side intake modifications were strongly influenced by existing hardware constraints, it is reasonable to expect that front end resistance could be lowered measurably by relatively few and simple hardware changes.

6.2 PRESSURE RISE - FLOW CHARACTERISTIC

Figure 32 is a universal plot of cooling fan performance showing the static pressure rise - flow characteristics. This type of plot can be constructed by graphing the fan and ram developed static pressure rises, or by removing the front end resistance from approach flow total pressure[1]. The apparent general lack of data indicates that performance mapping was not a prime objective of this investigation. Nevertheless, the available data define a surprisingly representative characteristic map, including third and fourth gear running lines. Constant fan speed lines were generated from Figure 33, which is a plot of cooling air flow rate against fan speed with approach air speed as a free parameter.

This latter plot shows for 100% fan cooling that the side intake configuration reduced the cooling flow by only 250 cfm relative to the standard frontal intake. Normally the ram provided between 1/2 and 2/3 of the total cooling air (3rd and 4th gear, respectively); but in the case of side inlets ram had no significant contribution to cooling flow. To achieve similar cooling flows through such intakes the same fan had to be operated at much higher speed (approximately 40 to 60% for 3rd and 4th gear, respectively), as can be seen from Figure 33.

Unlike the standard frontal intake, which suffered a 10% loss in air flow at a yaw angle of 15°, the side intake cooling flow was completely insensitive to vehicle yaw, see Figure 34.

Figure 35 shows the ram-only pressure rise and the negative image of the basic (fan only) static pressure running line. Clearly, ram cooling created much greater front end resistance than full fan cooling.

The universal characteristic plot (Figure 32) demonstrates that side intakes offer a fair degree of isolation to the cooling fan from vehicle dynamic effects. This suggests that the side intake cooling system designs may be based simply on still surrounding air, provided the appropriate external pressure boundary conditions are met.

6.3 FAN INPUT POWER

Figure 36 shows the input power of the cooling fan in the standard vehicle configuration. The four cylinder engine ran roughly and torque measurements between the water pump pulley and the cooling fan became possible only after the torquemeter's strain arms were bedded in rubber vibration dampers. The data scatter evident in the figure is due to a residual torque fluctuation of about ±5%. Fan speed fluctuations (time averages) were small; the severest fluctuation was at idle and it amounted to ±1.5%.

Reference 10 showed that cooling fan input power in a standard passenger car was surprisingly insensitive to approach air speed. Figure 37 shows that the same observation was made for the cooling fan in the present standard car. In the case of side intakes input power seemed weakly dependent on approach speed, and the cooling fan required less power (8.5 to 20%, depending on approach speed) than for standard intakes if run at the same speed. The greater system resistance of the present tortuous air path and the aerodynamically deficient duct elements, together with the externally imposed greater head rise across the system, moved the fan's design operating regime to lower flows, closer to stall, and to higher efficiencies.

Figure 38 exhibits the cooling fan's input power as a function of fan r.p.m. for three different vehicle intake configurations: standard frontal intakes, side intakes "B", and side intakes "B" reduced in area (per side) from 555 cm^2 (86 $ins.^2$) to 26 cm^2 (4 $ins.^2$). A fairly severe change in the system resistance implied by such a large decrease in intake area apparently resulted in a surprisingly minor (14%) change in the required input power of the standard cooling fan.

7. VEHICLE POWER CONTRIBUTIONS

7.1 POWER NEEDED TO OVERCOME AERODYNAMIC DRAG

The power required to overcome aerodynamic drag is proportional to drag force times approach air speed. To make a comparison of that power between the standard and the side intake vehicle, correct cooling

system drag with identical cooling flows must be included. Figure 39 offers such a comparison. At rated cooling flows the "B" intake equipped car needed 6% less power than the standard car with frontal intakes. This apparent saving in power is however not a true one because of the additional work the fan has to do if ram is not there.

7.2 POWER NEEDED TO DRIVE THE COOLING FAN

Figure 33 shows how much cooling flow was generated over a range of fan and approach air speeds by the standard car and the car modified with side intakes. Cooling flows produced by ram only for frontal intakes are given by the intercepts along the ordinate axis. Then, following any constant approach air speed line with increasing fan speed it is possible to observe how much flow was augmented by fan operation. Side intake cooling flows had, of course, no help from ram. At any given fan speed it was also observed that side intake cooling flows were appreciably less than fan-only cooling flows through conventional frontal intakes. It was in fact necessary to overspeed the same cooling fan in order to draw rated cooling flows. This figure was used in the process of estimating fan running speed and required input power to achieve a given cooling air flow when side intakes were employed.

The cooling air flow and required power for the "B" intake equipped test vehicle as a function of fan speed are shown in Figure 40.

7.3 POWER COMPARISONS BETWEEN THE STANDARD AND THE SIDE INTAKE VEHICLES

To get a true measure of the energy demand of both systems it does not suffice to compare fan powers directly because in the one case the fan is the only mover of cooling air, and in the other it is assisted by ram. Moreover, orientation and location of intakes were shown to have a profound effect on vehicle drag. Figure 41 is a plot of power of the standard vehicle comprising both the power necessary to overcome vehicle drag and to power the fan in simulated 3rd and 4th gear operation. Since drive train transmission losses were not known the measured fan power was added directly to aerodynamic power calculated from force balance measurements. To obtain comparable data for the side intake car rated 3rd and 4th gear cooling flows were selected in Figure 33. "B" intake fan speeds necessary to achieve these cooling flows were located in Figure 40, and appropriate "B" intake fan powers were then located in the same figure as indicated. Note that the "B" intake fan speeds were always greater. These power data were then added to the aerodynamic drag power of the "B" intake car at the approach air speeds previously selected in Figure 33. Figure 42 is the total power resulting from this cross plotting procedure and necessary for the "B" intake vehicle.

Finally, Figures 41 and 42 can be compared to find that no energy penalty had been incurred in switching the location of the cooling air intake from the front to the sides.

The single most important result of this investigation is the finding that frontal air intakes are not necessary for engine cooling. For energy conservation reasons it seems best to optimize the vehicle's front end shape to give the lowest possible C_D, and then to resort to side intakes as a separate solution for engine cooling purposes. Since all comparisons were made on the basis of the same basic vehicle shape, the potential created by eliminating frontal inlets for significant reductions in overall power has really not been explored. However, Reference 5 reports that aerodynamic optimization of front end shape can lead to significant drag reduction of approximately $\Delta C_D = 0.02$.

7.4 ESTIMATED FUEL SAVING

The fuel saving implied by the proposed drag reduction of 0.02 can be calculated for a known rolling resistance, road and wind speeds, hill grade and vehicle acceleration. This has been done during other investigations[5,6]. In the present case a simple estimate was made for the special conditions of:

- constant road speed,
- still ambient air,
- horizontal flat road.

The relative fuel saving expression, derived in the Appendix, is:

$$\frac{\Delta\mu}{\mu} = \frac{\Delta C_D/C_D}{1 + R_r/D_a}$$

Where R_r/D_a is the ratio of rolling resistance to aerodynamic drag force.

$$D_a = C_D A_f \frac{\rho V_\infty^2}{2g_o}$$

$$R_r = (r_o + r_1 V_\infty)W$$

for estimating purposes the normal modest speed dependency may be omitted, so that

$$R_r = r_o W$$

W = defined vehicle weight

Since there is no universally applicable value of r_o, three values (a generally used number: $r_o = 0.01$, G.M.[11]: $r_o = 0.015$, V.W.[5]: $r_o = 0.0405$) were used in Figure 43.

It is noteworthy that the variables characterizing the vehicle appear combined in one parameter $\frac{C_D A_f}{W}$ with the units of m^2/kg or ft^2/lb.

Using the specifications of the present test vehicle

$A_f = 1.89\ m^2\ (20.3\ ft^2)$

W = 1361 kg (3000 lbs), estimated EPA cost-down for the basic Mustang weight of 1142 kg (2517 lbs)

and the measured drag coefficients given in Figure 11, the fuel fraction saved due to a drag reduction of $\Delta C_D = 0.01$ was plotted in Figure 43.

Assuming that the Mustang has a rolling resistance similar to a G.M. car ($r_o = 0.015$), a proposed reduction of $\Delta C_D = 0.02$ is therefore expected to give a fuel saving of 3.1% at 100 km/h.

8. FLOW VISUALIZATION EXPERIMENTS

Figure 44 shows typical close-up plan and elevation views of smoke being drawn into side intake "B" with a trial bellmouth lip. The vehicle was yawed +15° relative to the approach flow and the shown intake was on the lee side, where the flow normally separated on the standard vehicle. The smoke, which left the smoke lance 3 cm (1 in.) off the surface upstream of the intake, adhered to the fender and got drawn into the side intake. Inside the intake the smoke appeared to be unable to follow the leading lip surface and separated inside the duct.

Figures 45, 46, and Figures 47, 48, are sets of paired photographs. The upper illustrations in each figure show the standard car, the lower illustrations the side intake car, and the smoke trail skirts the same spot near the fender in each figure. The odd number figures (Figures 45 and 47) are plan views and the even number figures (Figures 46 and 48) are elevation views. The flip chart test sequence numbers shown (most often in the window of the car) indicate paired plan and elevation views of the same situation taken at the same time.

In Figures 45 and 46 the test vehicles were aligned with the wind direction and the smoke was injected aft of and high up on the front wheel opening, i.e. at the 10 o'clock position. On the standard car

(upper illustrations, run 002) the smoke rapidly spread or diffused as it was carried along the side of the car. This depicts a region of separated flow. In the lower illustrations (run 093), i.e. at the side intake, the smoke diffused at first, but was ultimately drawn completely into the intake.

In Figures 47 and 48 the cars were at +15° of yaw and the smoke trail passed over the front fender near the windshield on the lee side of the cars. In the standard car case (upper illustration, run 021) the smoke was carried by the air in the original stream direction. This shows fully separated flow at the lee side door of the standard car. In the side intake car case (lower illustration, run 069) the side intake suction caused the smoke filament to be deflected from its original direction towards the lee side door. The flow appeared to adhere to the lee side of the car, and if there was any flow separation it was certainly smaller than in the standard car case.

These illustrations typically show how effectively the side intake draws off dead air and explain in a qualitative sense the improved aerodynamics of the side intake car while the vehicle was yawed.

9. CONCLUSIONS

(1) Cooling system drag was caused by ram momentum. Cooling fan operation increased drag only in a very minor way.

(2) Cooling system drag was equal to ram momentum drag only under pure ram cooling conditions, at all other conditions it was less.

(3) Cooling system drag was equal to 8 to 10% of the overall vehicle drag. Drawing cooling air in through side inlets virtually eliminated cooling system drag.

(4) Front end losses of the standard car were well correlated if expressed as the sum of a basic system loss which is proportional to the square of the cooling flow face dynamic pressure and a ram loss which is proportional to the approach flow dynamic pressure.

(5) In still ambient surroundings the trial side intake front end losses were almost twice those of the standard frontal intake system losses. Under running line conditions the trial side intake front end losses were about equal to the standard front end losses. At lower than rated cooling flows side intake front end loss was less.

(6) The side intake cooling system had no measurable ram recovery so that the cooling fan had to generate a much larger pressure rise in order to deliver the same cooling flow. It was able to achieve this by running at about 40% greater speed.

(7) Side intakes made the cooling flow rate much less sensitive to approach flow direction than frontal intakes did.

(8) Side intakes made the fan power demand slightly sensitive to approach air speed. Frontal intakes increased the fan power demand, but the power demand was virtually insensitive to approach air speed.

(9) Side intake cooling systems were found to be at least as energy efficient as standard (frontal intake) cooling systems given:

- the same cooling air flow rate,
- the same basic vehicle shape,
- the same cooling fan,
- non-optimized cooling air intake and internal air ducting.

(10) The tested side intakes seemed to be so well isolated from approach flow effects that other side intake cooling system designs may be based on still surrounding air, provided the appropriate external pressure boundary conditions are satisfied.

(11) Side intakes enable at least as effective and efficient engine cooling as frontal intakes. Consequently, the frontal intake can be done away with and the front end of the vehicle can be restyled aerodynamically to give a lower drag coefficient than possible for the previous basic shape. A 5% drag reduction in the present vehicle would assure a fuel saving of about 3% at a vehicle speed of 100 km/h.

10. RECOMMENDATIONS

The research done so far has shown that the side intake cooling concept is fundamentally sound and feasible. The concept compares favourably with the standard frontal intake cooling system and has considerable unexplored potential with respect to energy saving. Consequently the research should be extended into the following areas of investigation.

- An aerodynamic optimization of the side intake and associated internal air ducting.

• Development of a complete cooling package including a more suitably matched and more efficient cooling fan and directly coupled compact heat exchangers, which replace the conventional frontal radiator and A/C condenser.

• A complete revision of the aerodynamic styling of the front end (in the absence of frontal intakes and heat exchanger constraints) to reduce vehicle drag.

• Development of a concept car incorporating the above items.

11. REFERENCES

(1) Schaub, U. W., Charles, H. N., "Ram Air Effects on the Air Side Cooling System Performance of a Typical North American Passenger Car", S.A.E. paper 800032, February 1980

(2) Hawes, S. P., "Improved Passenger Car Cooling Systems", S.A.E. paper 760112, February 1976

(3) White, R. G. S., "An Experimental Survey of Vehicle Aerodynamic Characteristics", The Motor Industry Research Association, MIRA Report No. 1969/4

(4) Hucho, W.-H., Janssen, L. J., Emmelmann, H. J., "The Optimization of Body Details - A Method for Reducing the Aerodynamic Drag of Road Vehicles", Automotive Aerodynamics, Progress in Technology Series, S.A.E., Volume 16, 1978, pp. 191-208

(5) Buchheim, R., Deutenbach, K. R., Lückoff, H. J., "Necessity and Premises for Reducing the Aerodynamic Drag of Future Passenger Cars", S.A.E. paper 810185, February 1981

(6) "Study on Reduction of Automotive Accessory Power Requirements - Final Executive Summary", Report 31-2916-1, Energy Research and Development Administration Division, Transportation Energy Conversion, Office of Highway Vehicles, Vehicular Systems Branch, October 1978

(7) "The NRC 30 Foot V/STOL Wind Tunnel", National Research Council of Canada, Ottawa, June 1969

(8) Rimmer, R. J., Bassett, R. W., "A Small Propeller Type Anemometer for Use in Automotive Radiator Air Flow Measurement", Division of Mechanical Engineering Laboratory Report LTR-ENG-85, National Research Council of Canada, August 1978

(9) Pope and Harper, Low Speed Wind Tunnel Testing, New York: Wiley, 1966

(10) Schaub, U. W., "A Wind Tunnel Study of Ram Air Effects on the Air Side Cooling System Performance of a Typical North American Passenger Car", Division of Mechanical Engineering Laboratory Report LTR-ENG-81, National Research Council of Canada, July 1978

(11) Sovran, G., Bohn, M. S., "Formulae for the Tractive - Energy Requirements of Vehicles Driving the EPA Schedules", S.A.E. paper 810184, February 1981

12. APPENDIX

12.1 IN-CAR DATA ACQUISITION SYSTEM

The in-car data acquisition system accepts signals from up to six (6) transducer/pressure scanning valves (each having forty-eight (48) pressure input ports), twenty thermocouples and twenty frequency generators. In addition, a limited amount of binary coded (B.C.D.) information can also be accepted.

All inputs are sequentially scanned under pre-programmed control. Controls permit partially processed data to be examined on a digital display prior to recording on magnetic tape. Recorded data is transferred to NRC's IBM computer for final processing and printing.

12.1.1 System Inputs

Three types of signal are measured - low level d.c. voltages, frequencies and digital codes.

Low Level Voltage Sources - All low level voltages were fed through a system scanner to an integrating digital voltmeter which sampled each signal for a period of 200 milliseconds and provided a time averaged value.

Pressures are measured using scanning values driven by a rotary solenoid. Up to six valves were used, each fitted with a d.c. strain gauge type of pressure transducer, and each capable of handling forty-eight pressures. Signal conditioners, which provide the strain gauge excitation voltage also amplify the signals before they are routed to the system scanner.

Temperatures are measured using chromel/alumel thermocouples connected directly to the system scanner. Cold junction compensation is provided within the scanner.

The fan torquemeter also produces a low level signal derived from d.c. excited strain gauges arranged in a four arm bridge similar to the pressure transducers. This signal is fed directly to the system scanner without amplification.

Frequencies - Rotational speed measurements related to radiator air flow were made by feeding pulse trains from propeller anemometer mounted optical pickups through the system scanner to a frequency counter.

Fan speed was measured in a similar manner.

Digital Codes - B.C.D. signals indicating the position of the pressure scanning valves and the radiator traversing gear are fed directly to the system controller.

12.1.2 System Operation

The data collection sequence and format for the wind tunnel tests were arranged by pre-programming the system controller. Test programs, which were stored on magnetic tape, are loaded into the controller memory prior to testing and then replaced by a data storage tape. As testing proceeds data are stored in the controller memory. After completion of each test and an optional visual inspection the data record is then transferred to magnetic tape upon manual command.

All system operations, such as stepping pressure scanning valves and indexing the radiator traversing gear, are managed automatically by the controller.

12.2 DERIVATION OF EQUATION FOR FUEL SAVING

The power required to propel a car at constant speed on a level flat road in still air is

$$P_e = \frac{1}{550\eta} (R_r + D_a) V_\infty$$

Where P_e = engine power

η = power transfer efficiency

R_r = rolling resistance

D_a = aerodynamic drag

$$= C_D A_f \frac{\rho V_\infty^2}{2g_o}$$

A_f = frontal area of the vehicle

C_D = drag coefficient

The change in power due to a change in drag is

$$\Delta P_e = \frac{1}{550\eta} \Delta D_a V_\infty$$

The ratio of the power ΔP_e and P_e is also equal to the work done ratio because the time interval is the same in both cases. The work ratio is equal to the fuel ratio if it is assumed that the engine's specific fuel consumption is constant for the change in operation due to ΔC_D.

Consequently,

$$\frac{\Delta P_e}{P_e} = \frac{\Delta D_a}{R_r + D_a}$$

$$= \frac{\Delta \mu}{\mu}$$

$$= \frac{\Delta D_a / D_a}{1 + R_r / D_a}$$

$$= \frac{\Delta C_D / C_D}{1 + R_r / D_a}$$

The fuel saving fraction therefore depends on the change in drag coefficient and on the ratio of rolling resistance and drag force. The rule of thumb used that the percent fuel saving is about half the percent drag reduction is exactly right when $R_r = D_a$, which is in the speed range 35 to 60 mph for most cars. When $D_a > R_r$ the percent fuel saving approaches the percent drag reduction. When $D_a < R_r$ the percent fuel saving as a result of drag reduction becomes insignificant.

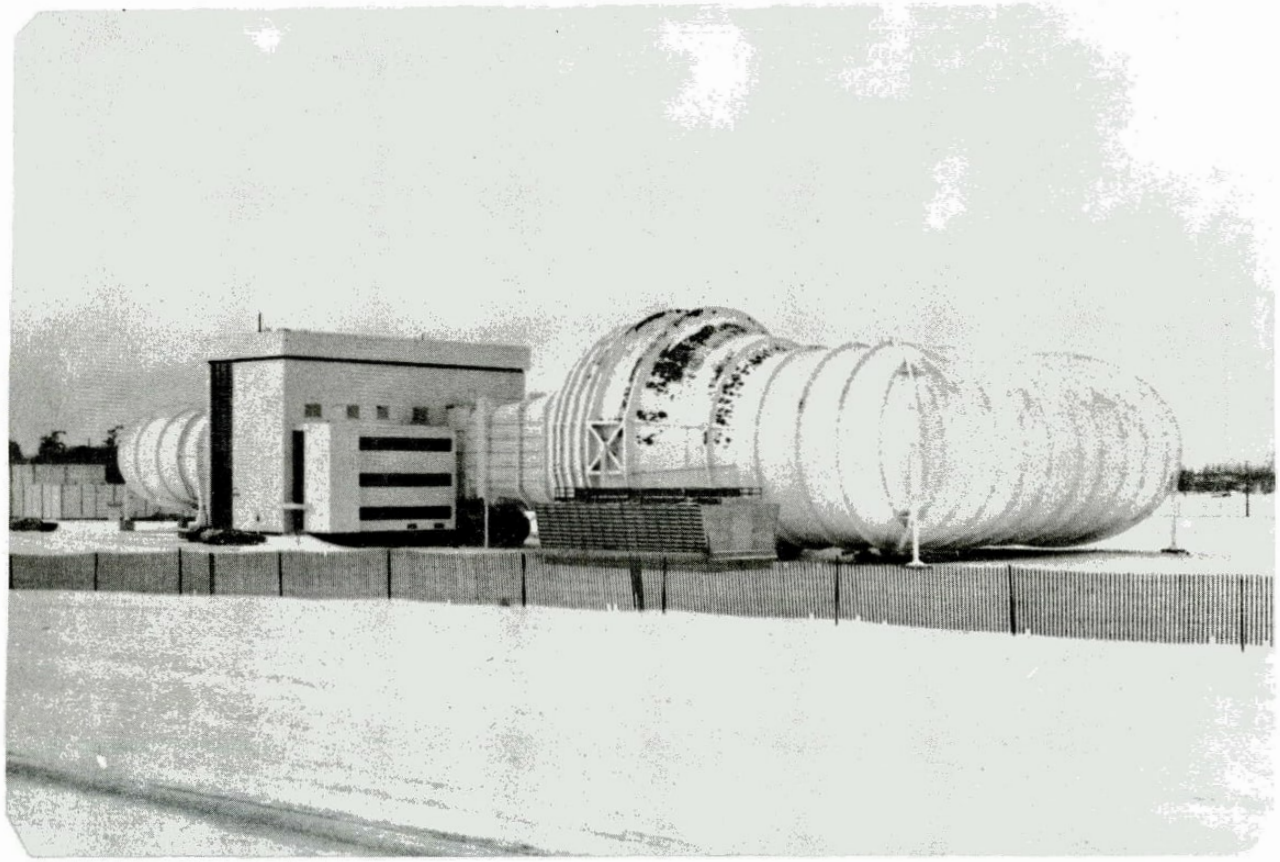

NATIONAL RESEARCH COUNCIL 30 FOOT WIND TUNNEL

FIG.1
LTR-ENG-100

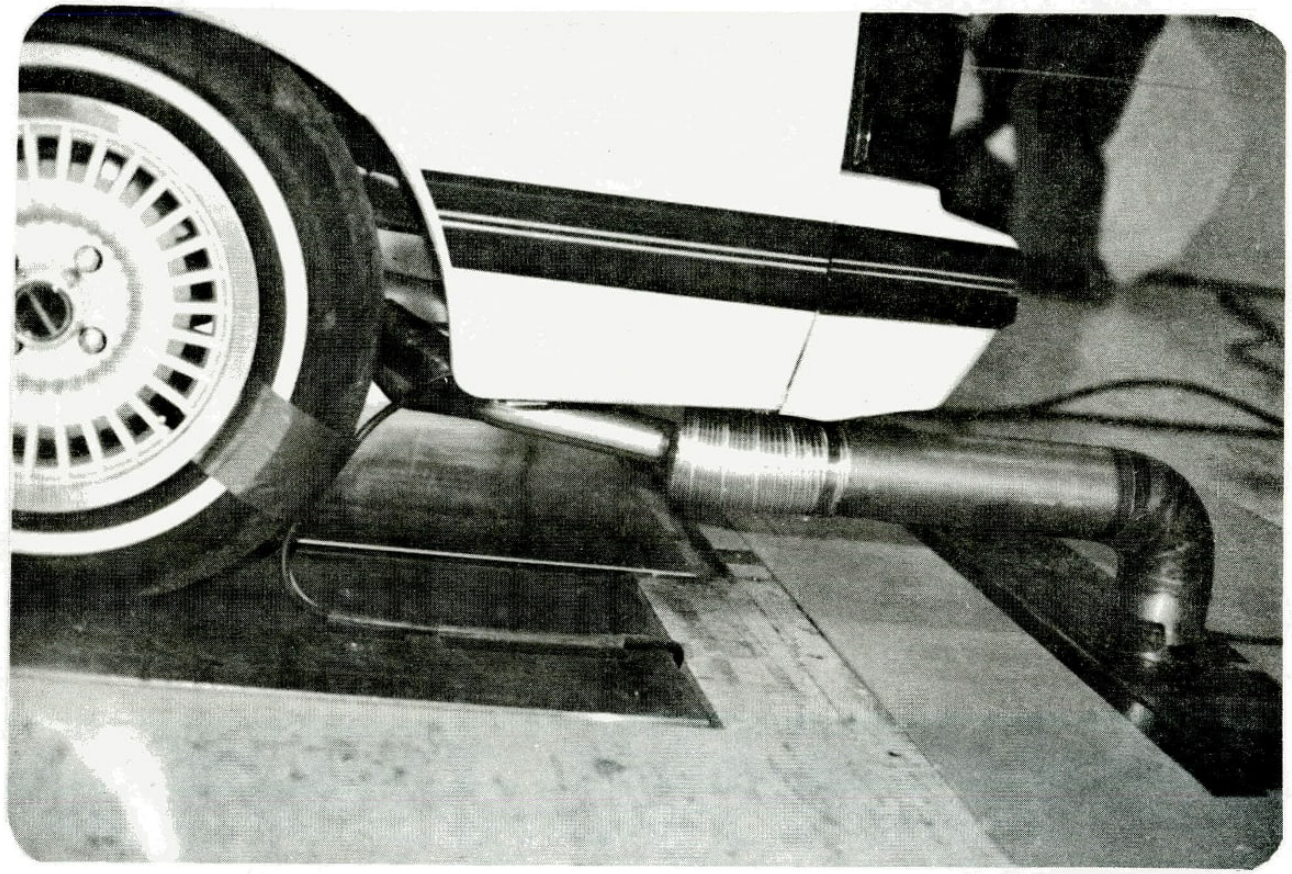

ENGINE EXHAUST COLLECTER

FIG. 2
LTR-ENG-100

1980 FORD MUSTANG TEST VEHICLE IN THE
30 FOOT TUNNEL WORKING SECTION

FIG. 3
LTR-ENG-100

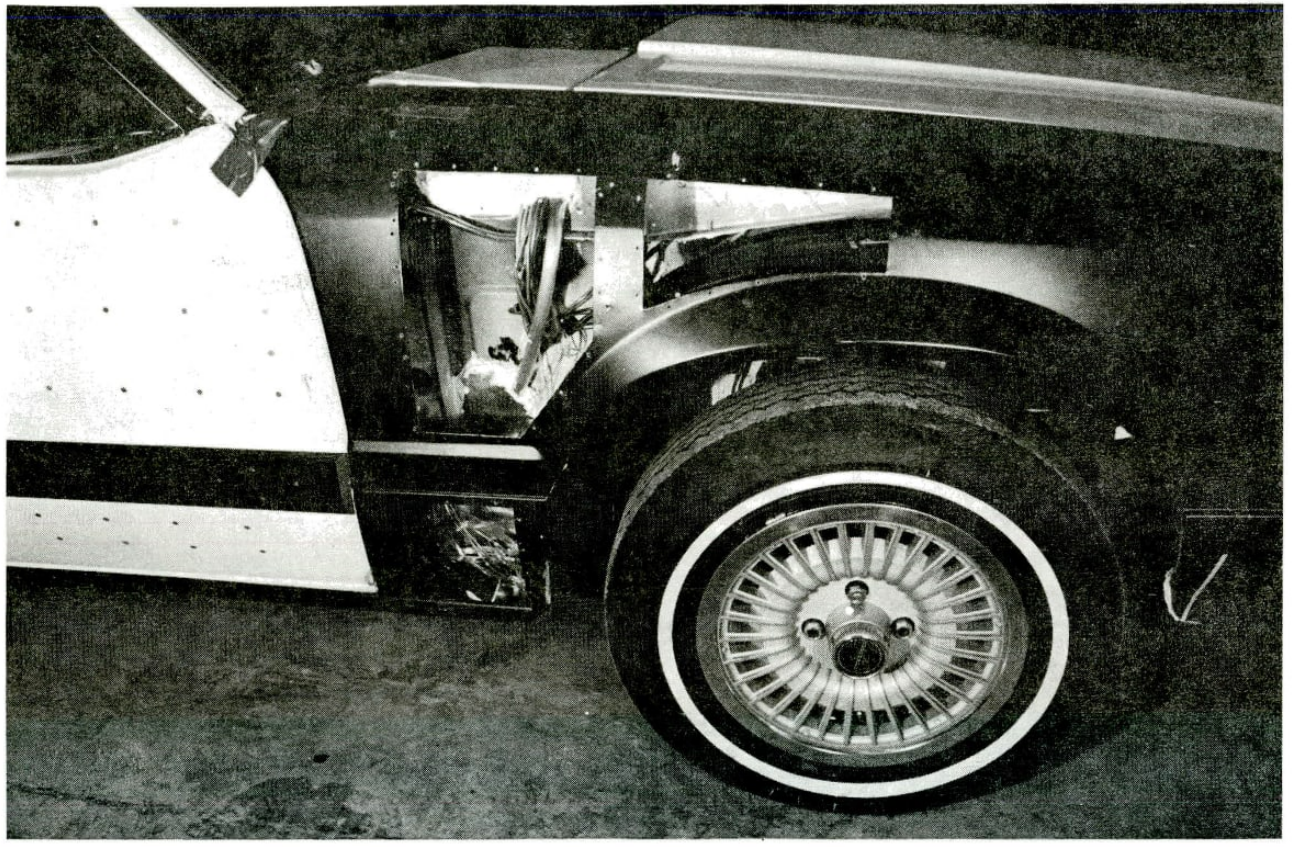

MODIFIED FENDER (R.H.S.) SHOWING THREE
CONFIGURATIONS OF THE SIDE INTAKE

FIG. 4
LTR-ENG-100

FIG. 5
LTR-ENG-100

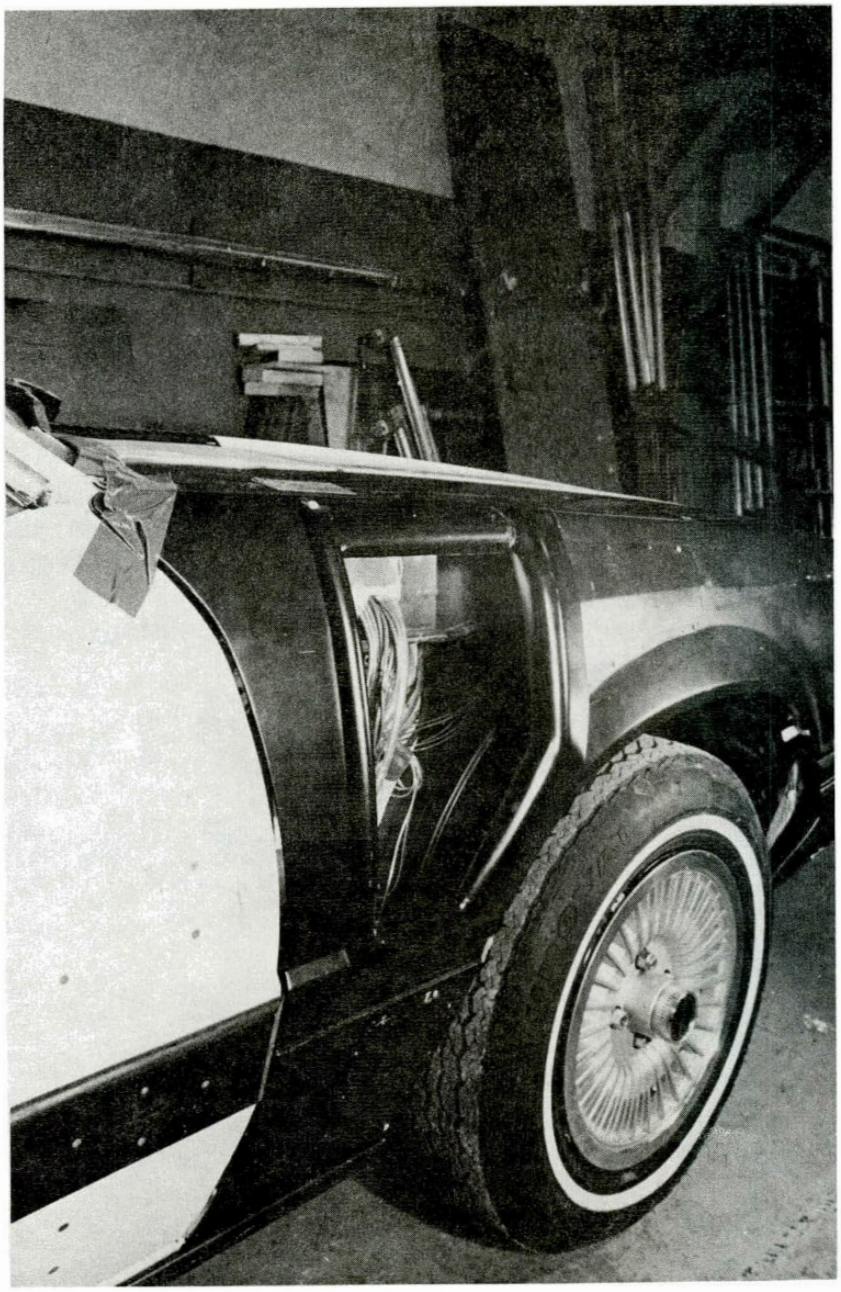

SIDE INTAKE "B" FITTED WITH SMOOTH INLET LIP

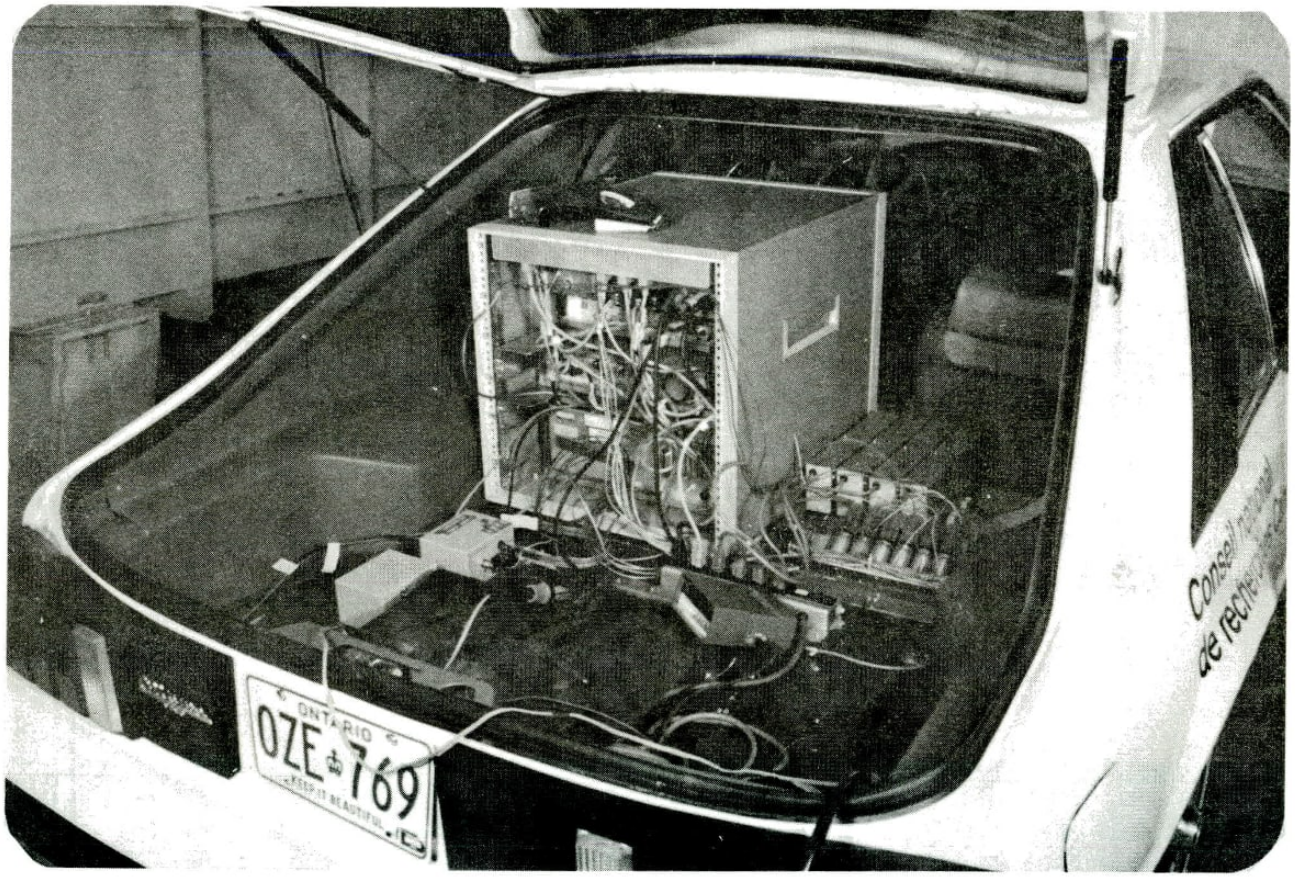

DATA AQUISITION SYSTEM ACCESS VIA
REAR HATCH DOOR

FIG.6
LTR-ENG-100

FIG.7
LTR-ENG-100

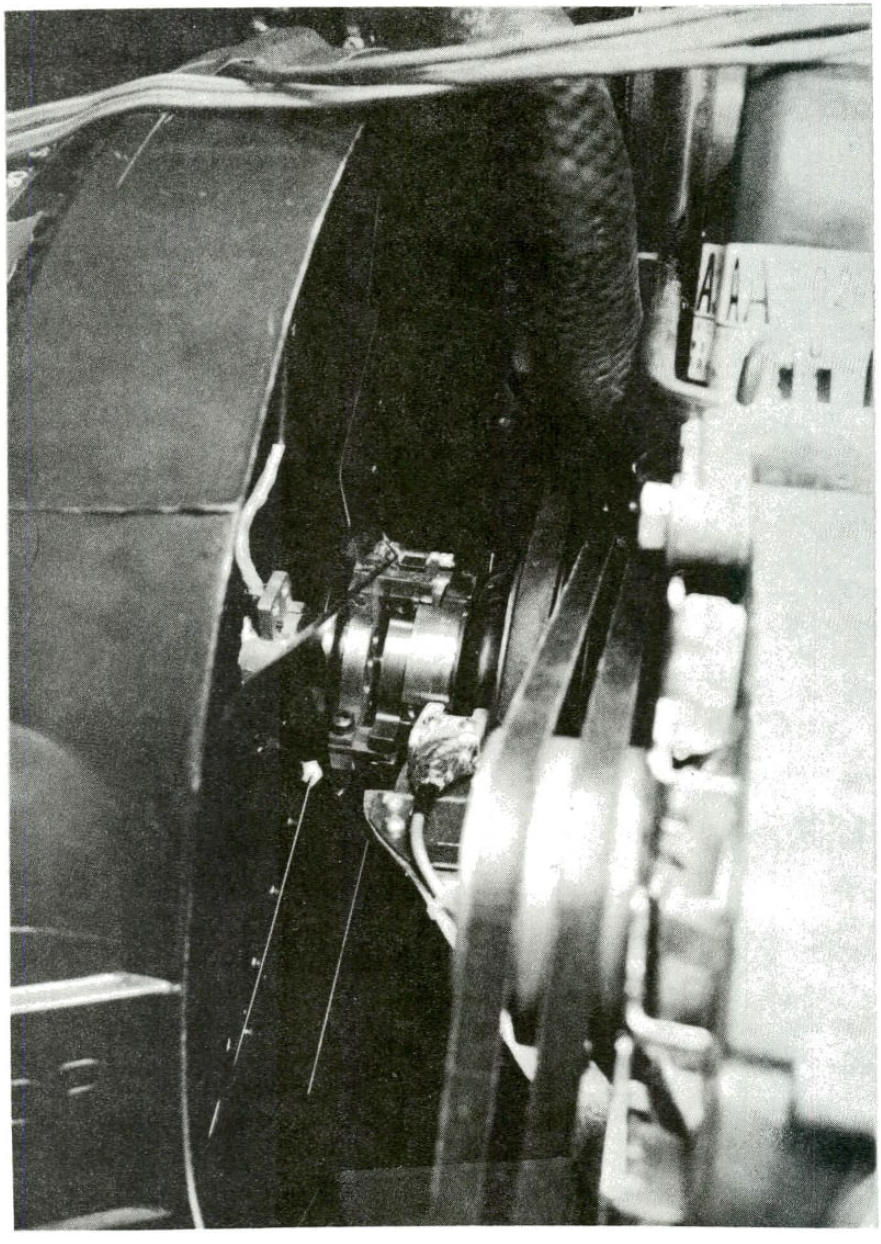

TORQUEMETER LOCATED BETWEEN
FAN AND DRIVE PULLEY

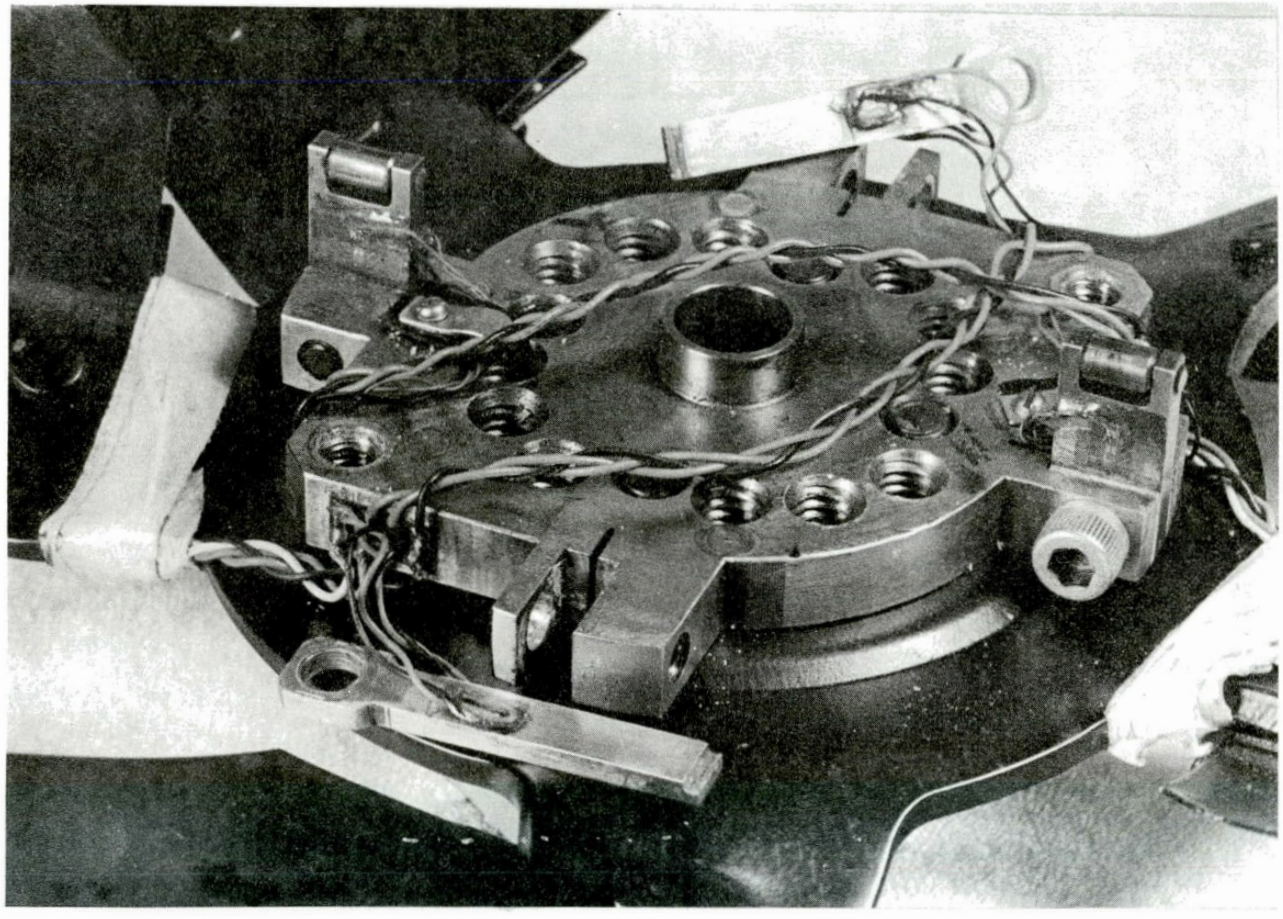

DRIVEN TORQUEMETER MEMBER ATTACHED TO FAN
SHOWING STRAIN GAUGED CANTILEVER ARMS (WITH ROLLERS)

FIG. 8
LTR-ENG-100

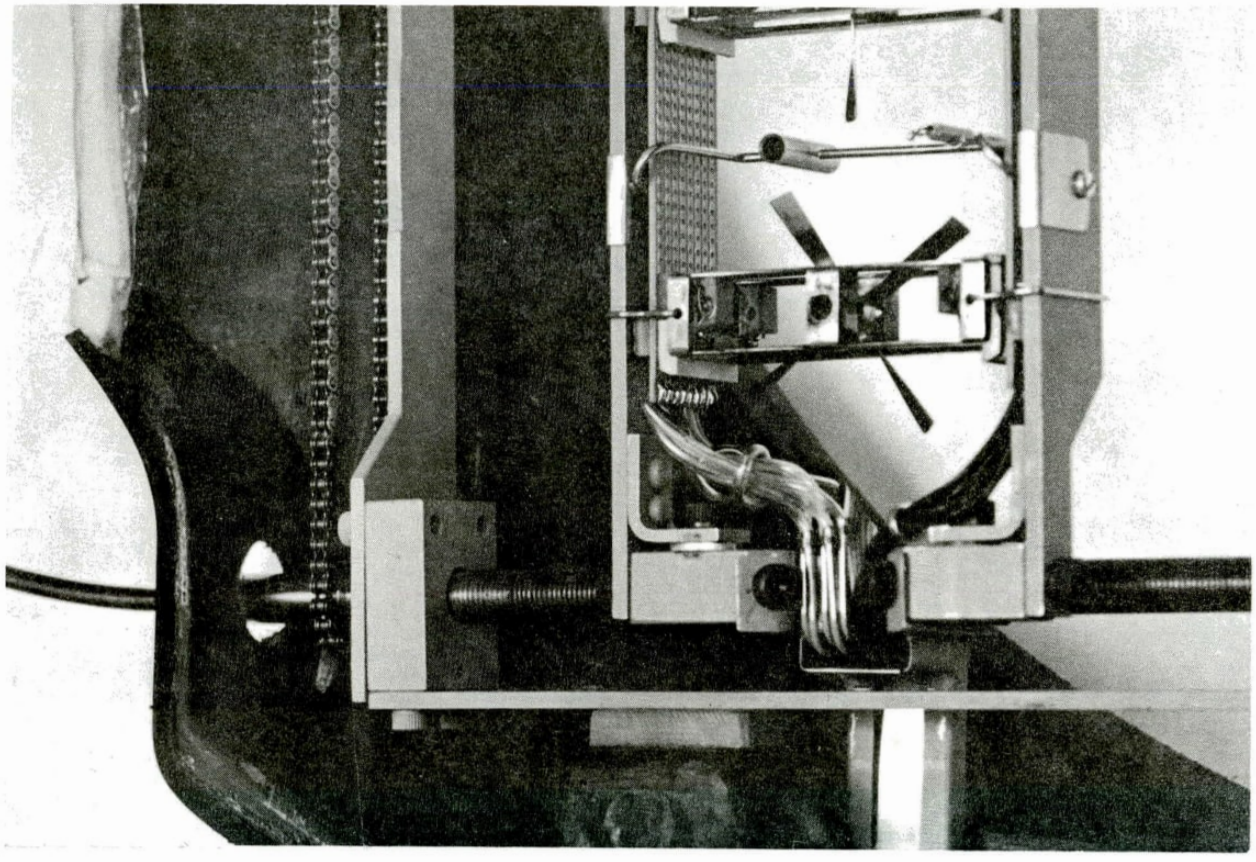

FREE PROPELLER ANEMOMETER MOUNTED IN TRAVERSE FRAME–VIEW FROM RADIATOR SIDE.

FIG.9
LTR-ENG-100

FIG. 10
LTR-ENG-100

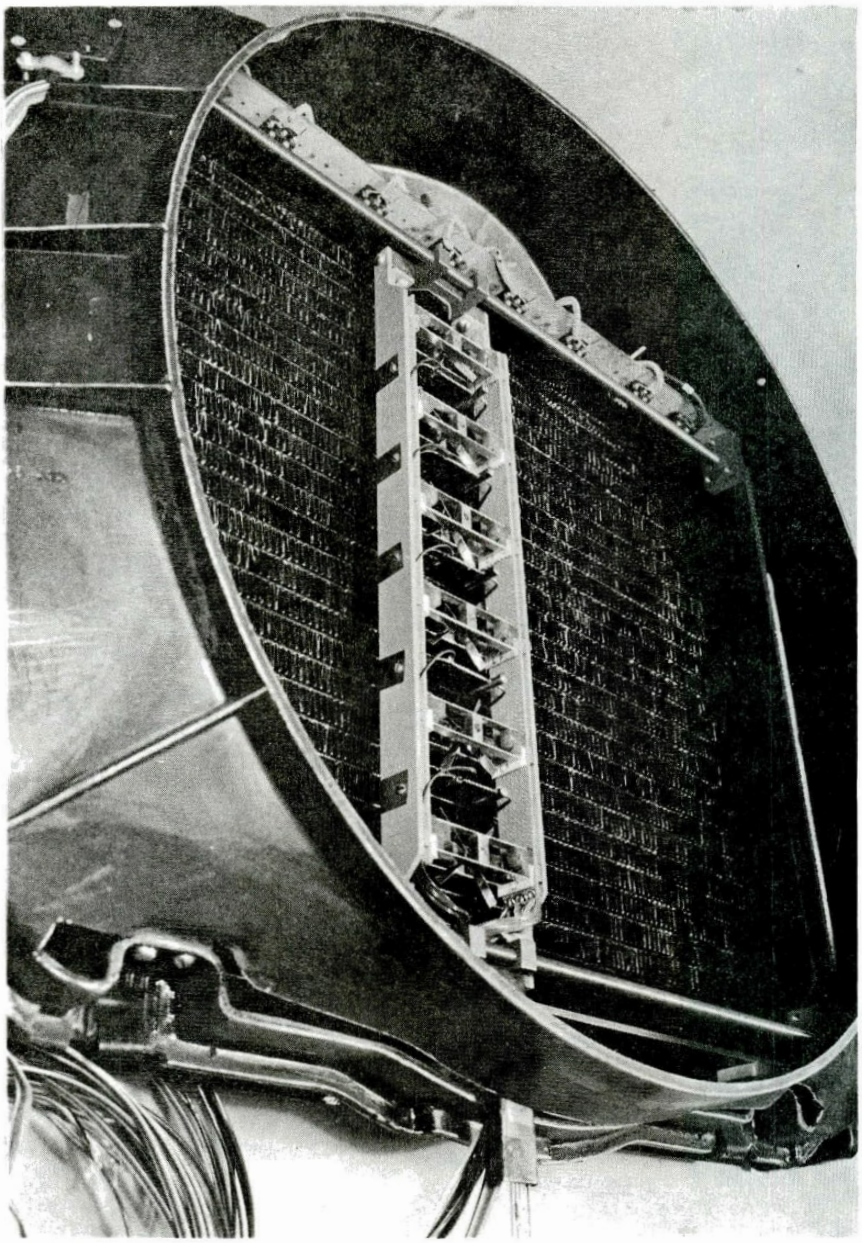

TRAVERSE RAKE CONTAINING SIX ANEMOMETERS, FIVE TOTAL PRESSURE AND TEMPERATURE PROBES MOUNTED INSIDE THE FAN SHROUD-VIEW FROM FAN SIDE.

FIG. 11
LTR-ENG-100

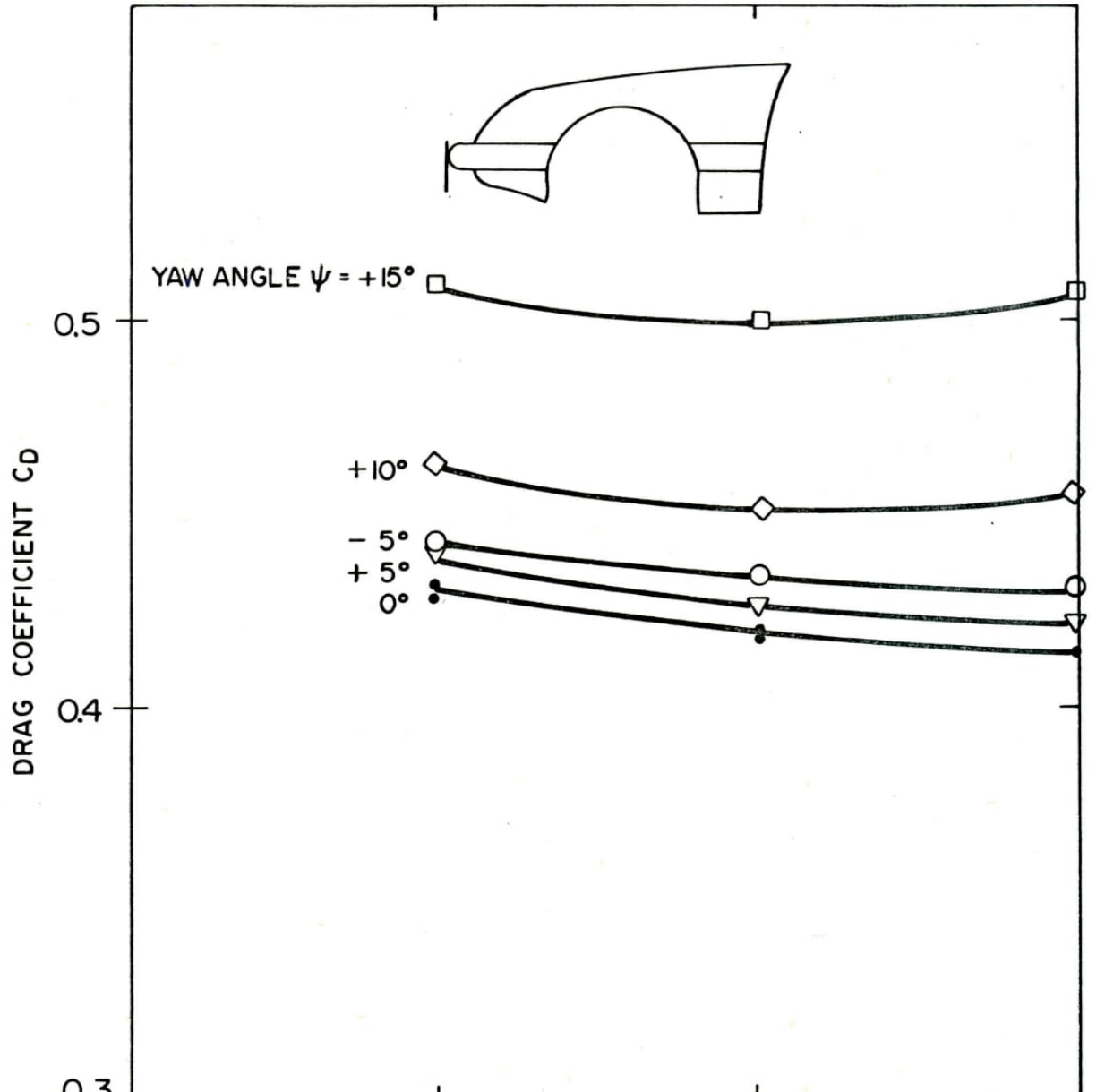

DRAG COEFFICIENT IN VEHICLE STABILITY AXIS – STANDARD FRONTAL INTAKES, 4th GEAR OPERATION

FIG. 12
LTR-ENG-100

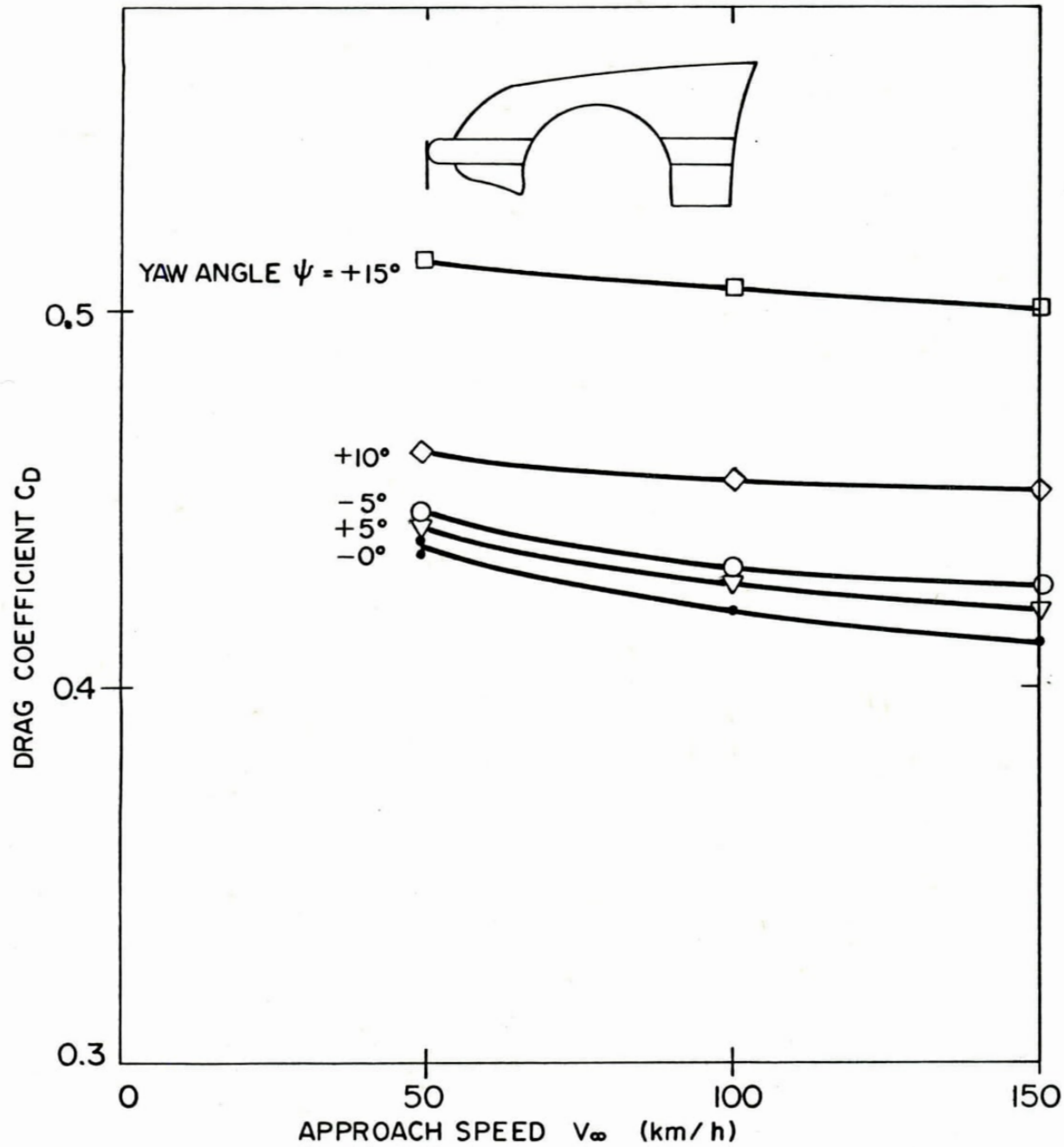

DRAG COEFFICIENT IN VEHICLE STABILITY AXIS-STANDARD FRONTAL INTAKES, 3rd GEAR OPERATION

FIG. 13
LTR-ENG-100

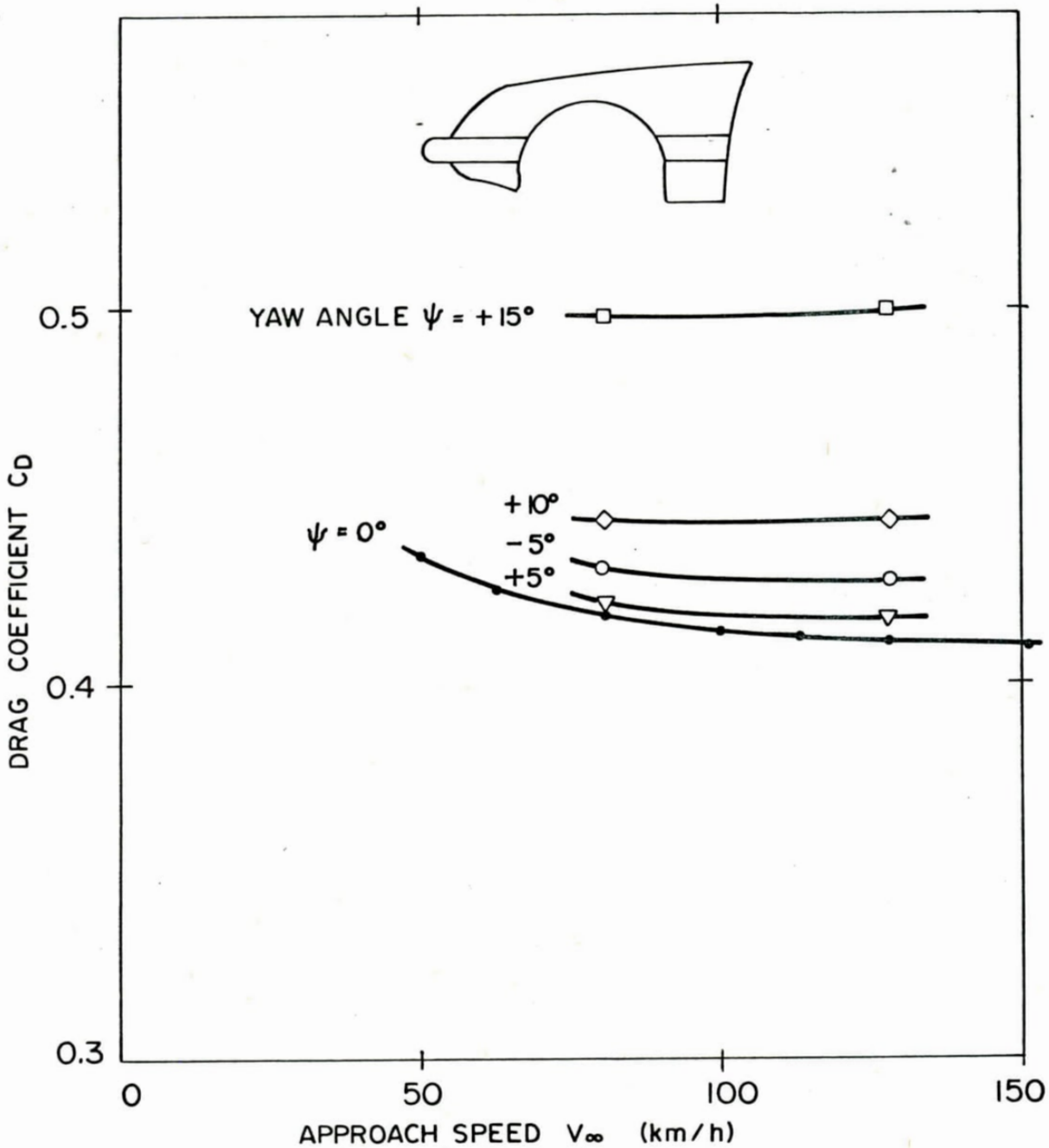

DRAG COEFFICIENT IN VEHICLE STABILITY AXIS – STANDARD FRONTAL INTAKES, STATIONARY COOLING FAN.

FIG. 14
LTR-ENG.-100

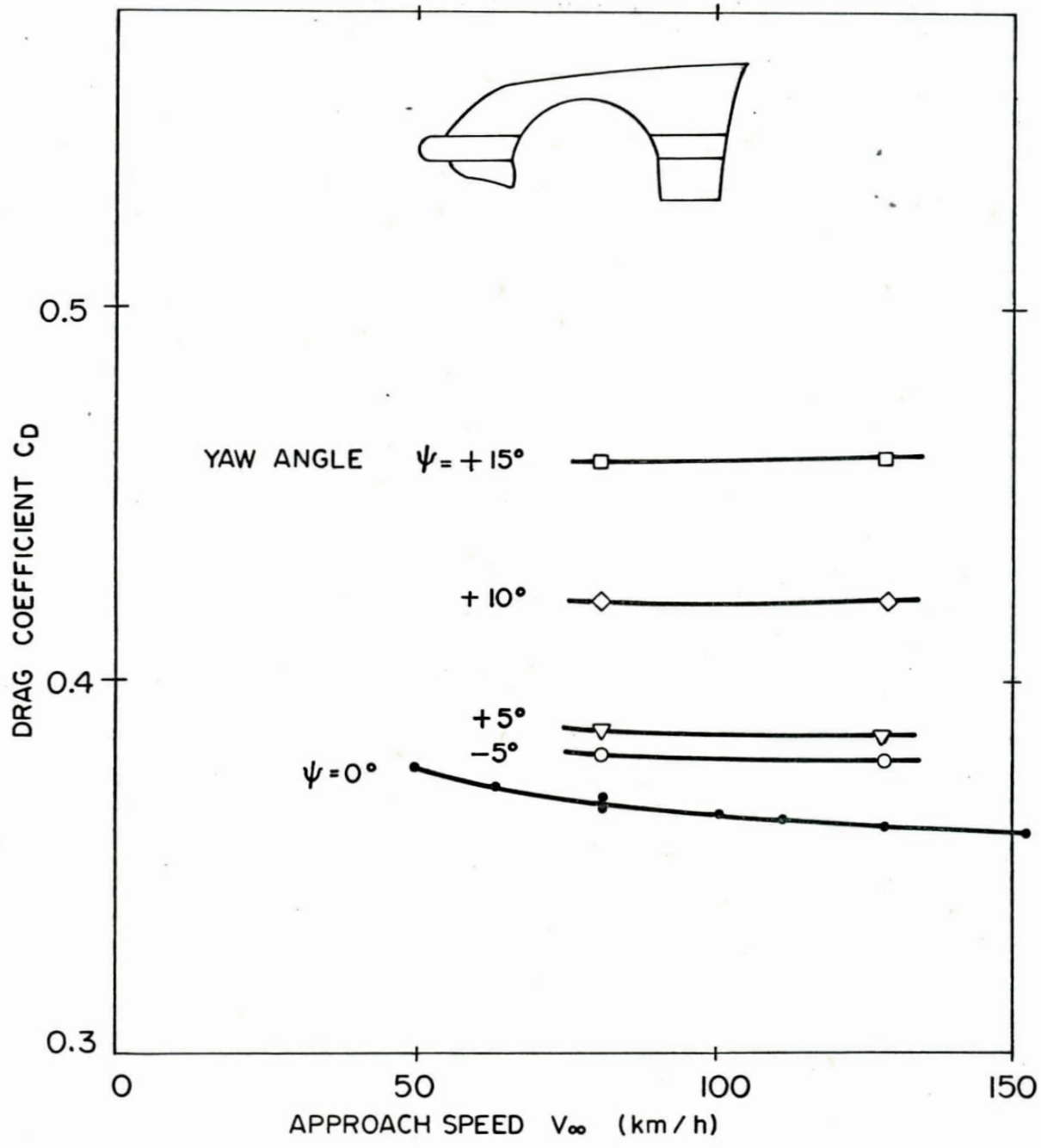

DRAG COEFFICIENT IN VEHICLE STABILITY AXIS– COMPLETELY FAIRED IN FRONT END, EXPOSED LICENCE PLATE, STATIONARY COOLING FAN.

FIG. 15
LTR-ENG-100

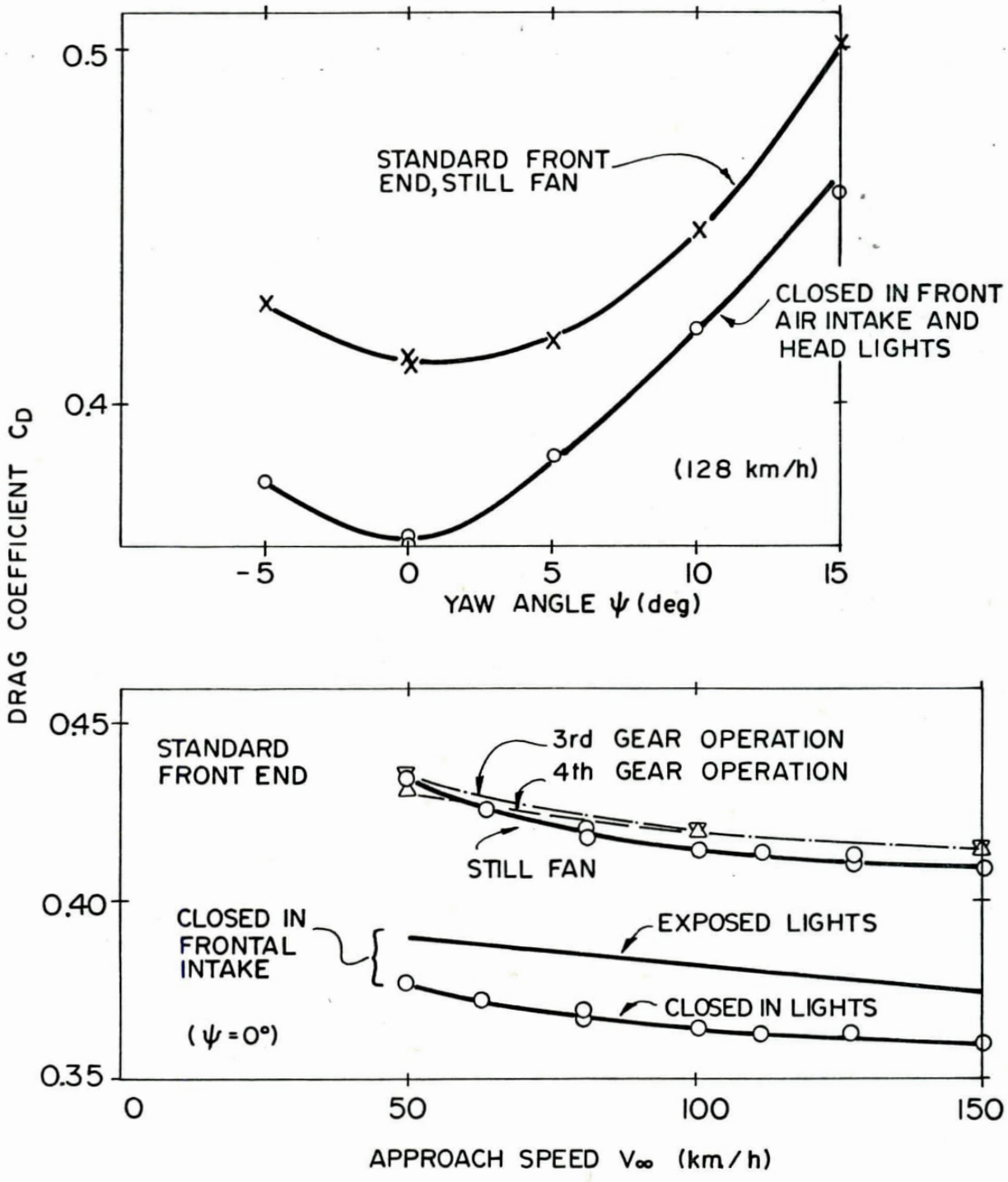

DRAG COEFFICIENT IN VEHICLE STABILITY AXIS–COMPARISONS

FIG.16
LTR-ENG-100

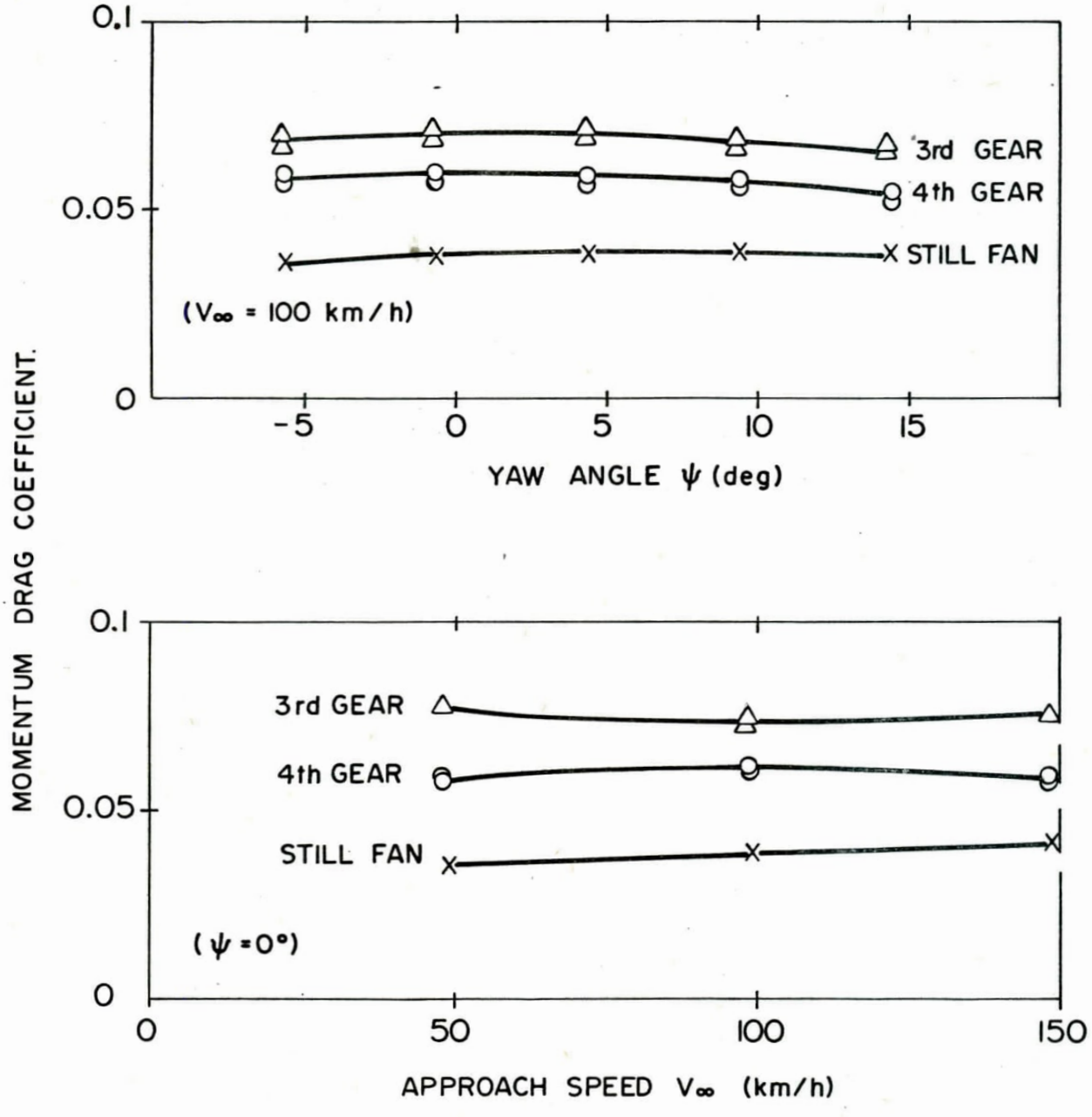

VARIATIONS IN MOMENTUM DRAG COEFFICIENT

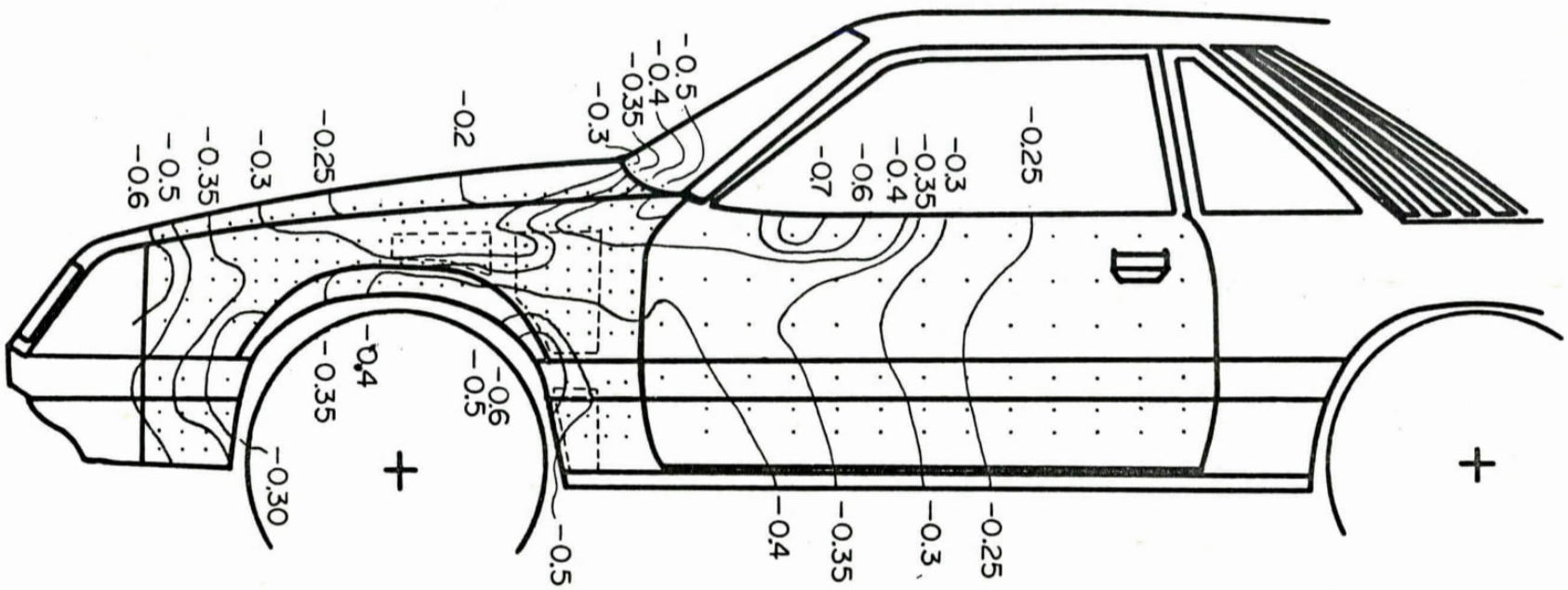

APPROACH SPEED – V_∞ = 100 (km/h)
FAN SPEED – N = 3571 R.P.M.
ANGLE – ψ = +15° Deg.

PRESSURE COEFFICIENT Cp = $\frac{P-P_s}{q_\infty}$

PRESSURE COEFFICIENT ISOBARS – STANDARD VEHICLE CONFIGURATION

FIG. 17
LTR-ENG-100

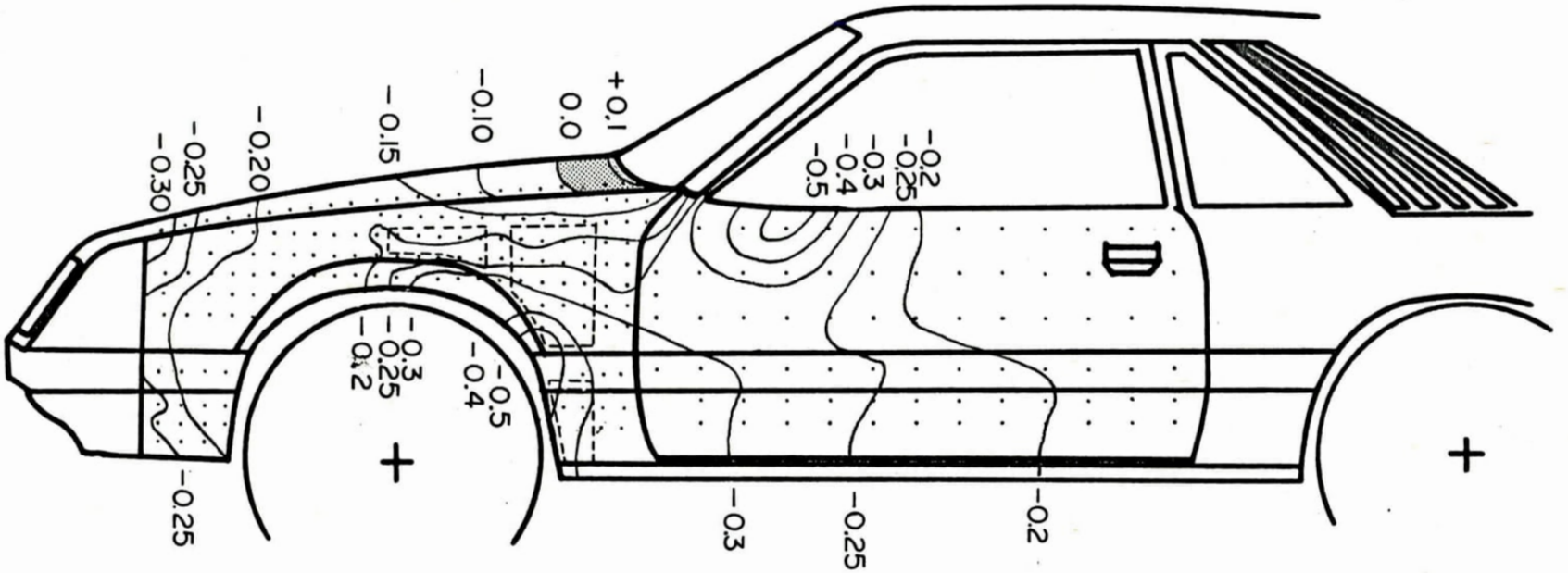

APPROACH SPEED – $V\infty$ = 100 (km/h)
FAN SPEED – N = 3571 R.P.M.
ANGLE – ψ = +5° Deg.

PRESSURE COEFFICIENT Cp = $\frac{P-P_s}{q_\infty}$

PRESSURE COEFFICIENT ISOBARS – STANDARD VEHICLE CONFIGURATION

FIG. 18
LTR-ENG-100

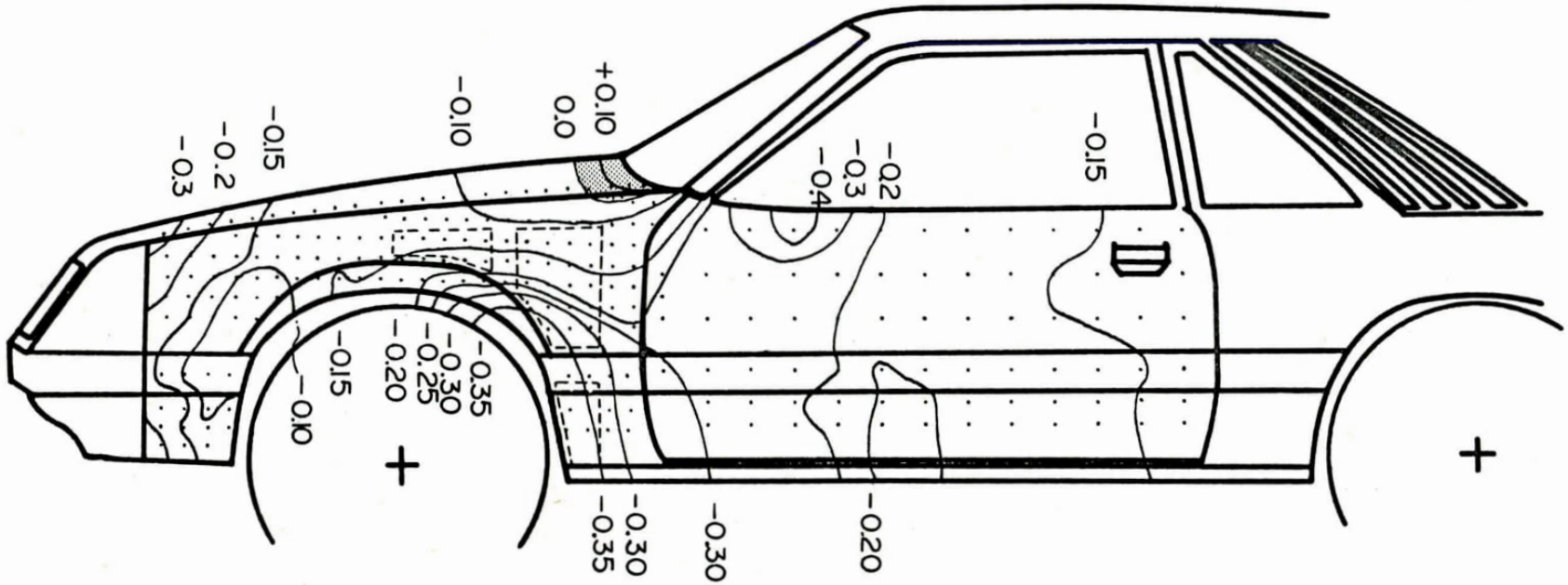

APPROACH SPEED – $V\infty$ = 100 (km/h)
FAN SPEED – N = 3571 R.P.M.
ANGLE – ψ = 0 Deg.

PRESSURE COEFFICIENT Cp = $\frac{P-P_s}{q\infty}$

PRESSURE COEFFICIENT ISOBARS – STANDARD VEHICLE CONFIGURATION

FIG. 19
LTR-ENG-100

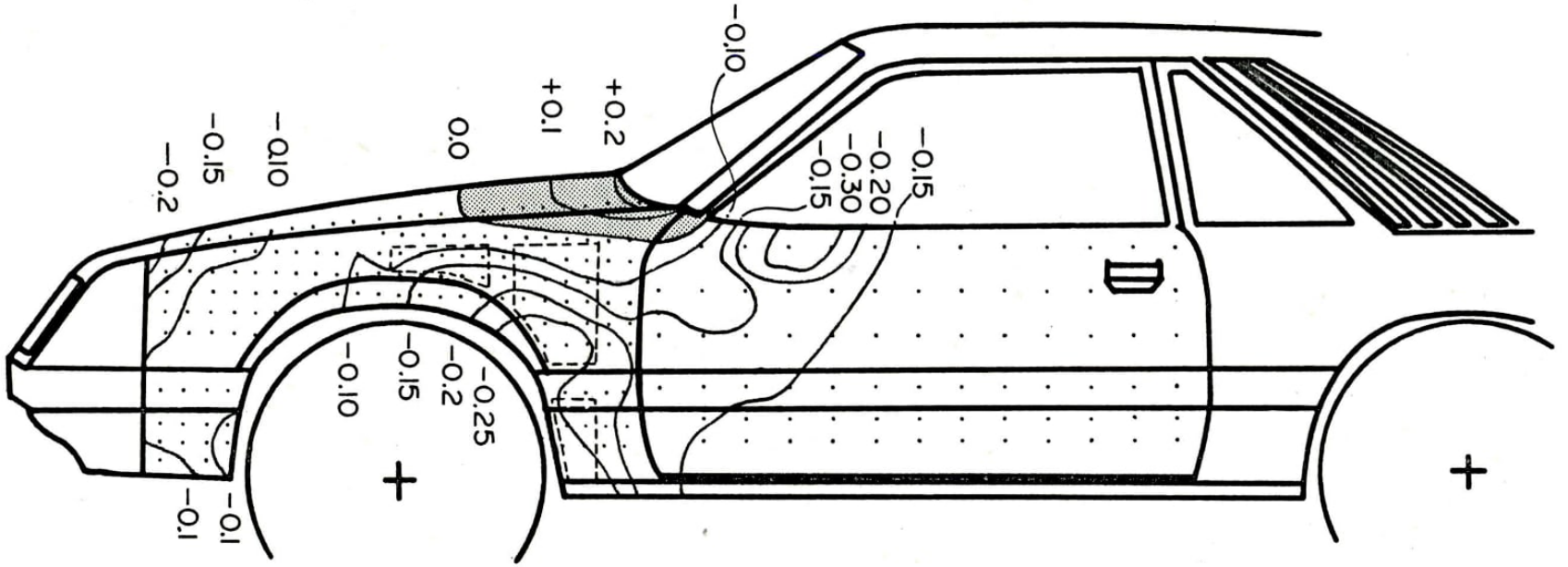

APPROACH SPEED – $V\infty$ = 100 (km/h)
FAN SPEED – N = 3571 R.P.M.
ANGLE – ψ = -5° Deg.

PRESSURE COEFFICIENT $Cp = \frac{P-P_s}{q\infty}$

PRESSURE COEFFICIENT ISOBARS – STANDARD VEHICLE CONFIGURATION

FIG. 20
LTR-ENG-100

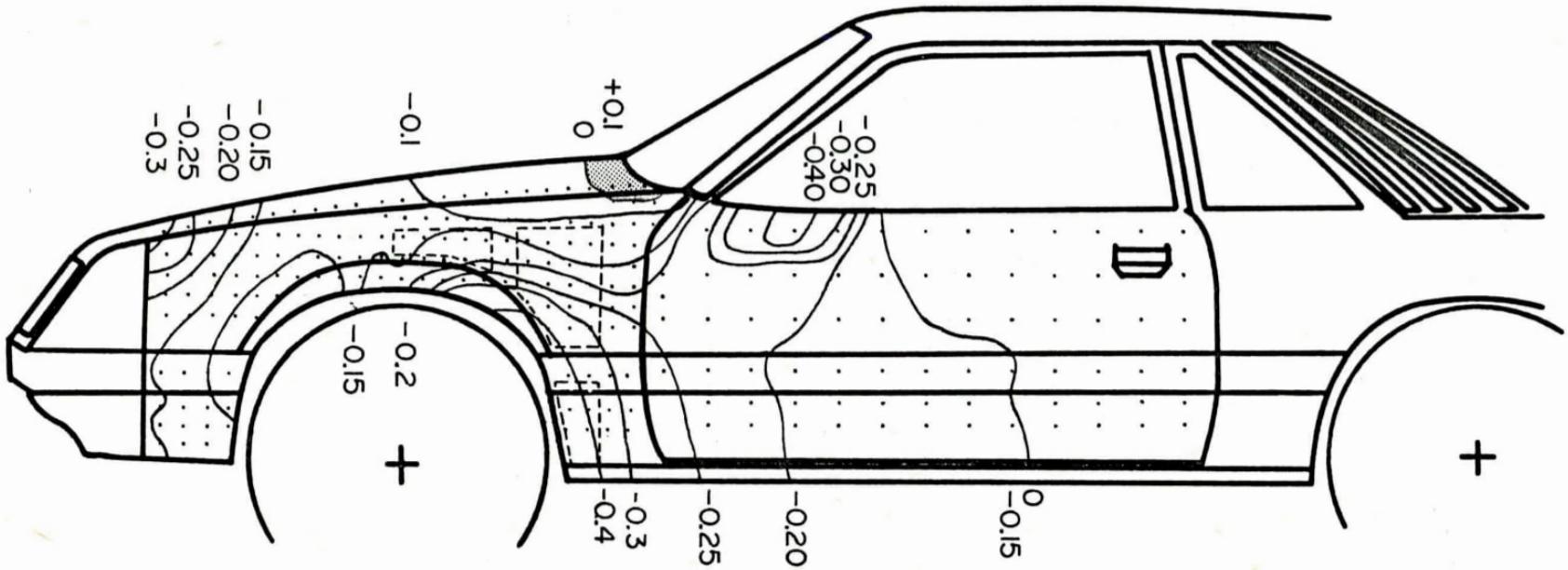

APPROACH SPEED – $V\infty$ = 100 (km/h)
FAN SPEED – N = 2500 R.P.M.
ANGLE – ψ = 0° Deg.

PRESSURE COEFFICIENT $Cp = \frac{P - P_s}{q_\infty}$

PRESSURE COEFFICIENT ISOBARS – STANDARD VEHICLE CONFIGURATION

FIG. 21
LTR-ENG-100

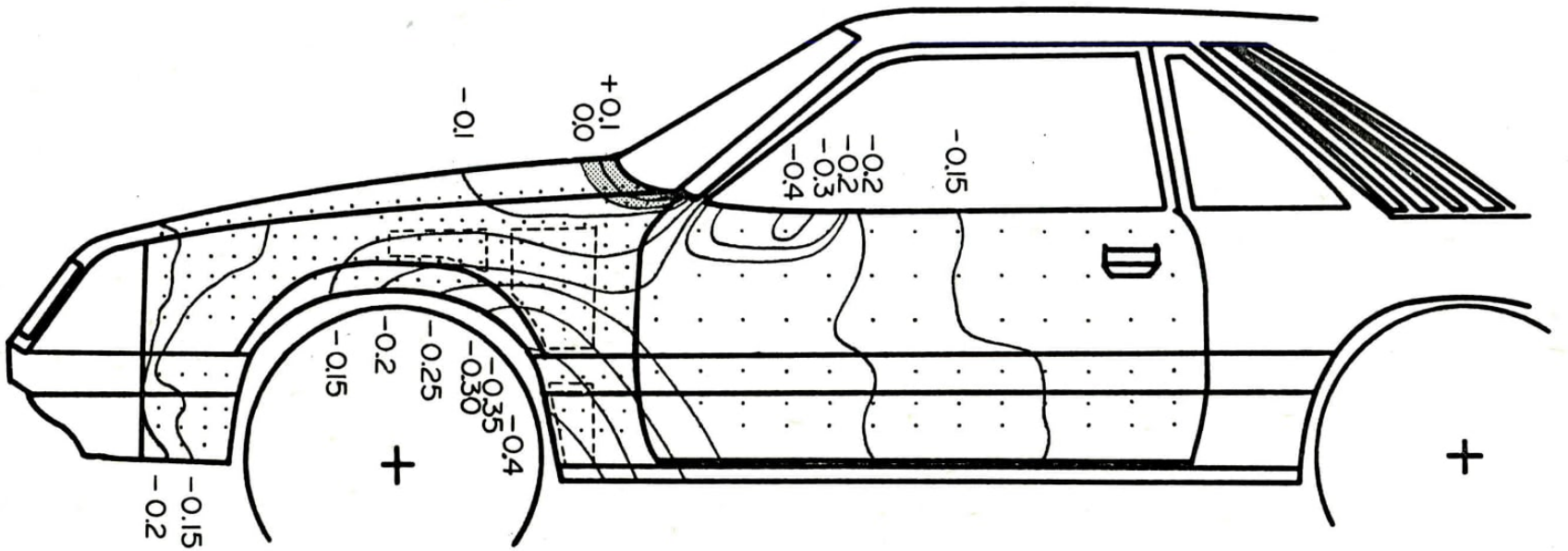

APPROACH SPEED – $V\infty$ = 150 (km/h)
FAN SPEED – N = 3770 R.P.M.
ANGLE – ψ = 0° Deg.

PRESSURE COEFFICIENT Cp = $\frac{P-P_s}{q_\infty}$

PRESSURE COEFFICIENT ISOBARS – STANDARD VEHICLE CONFIGURATION

FIG.22
LTR-ENG-100

FIG. 23
LTR-ENG-100

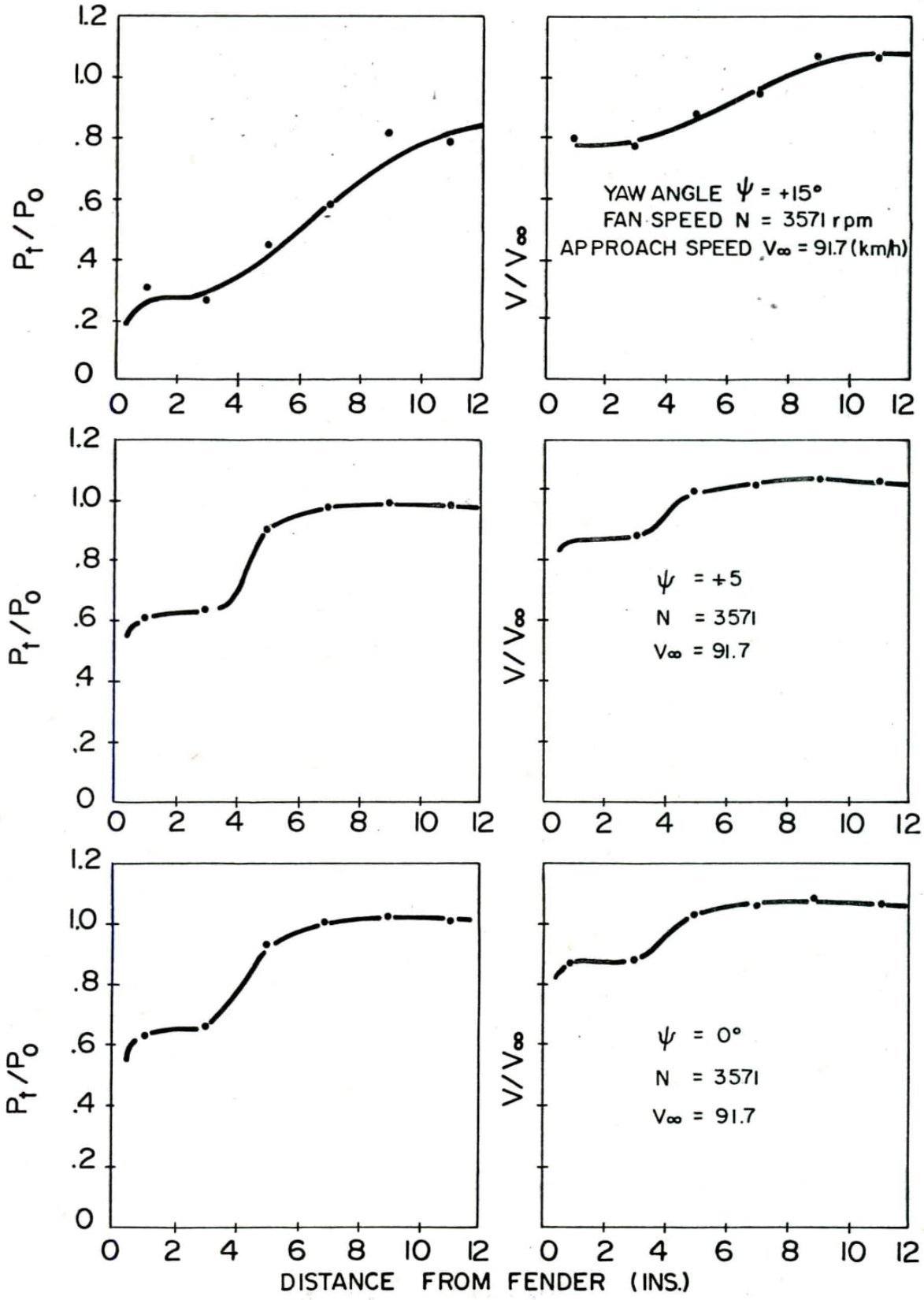

EXTERNAL AIR FLOW AT SIDE OF VEHICLE

FIG. 24
LTR-ENG-100

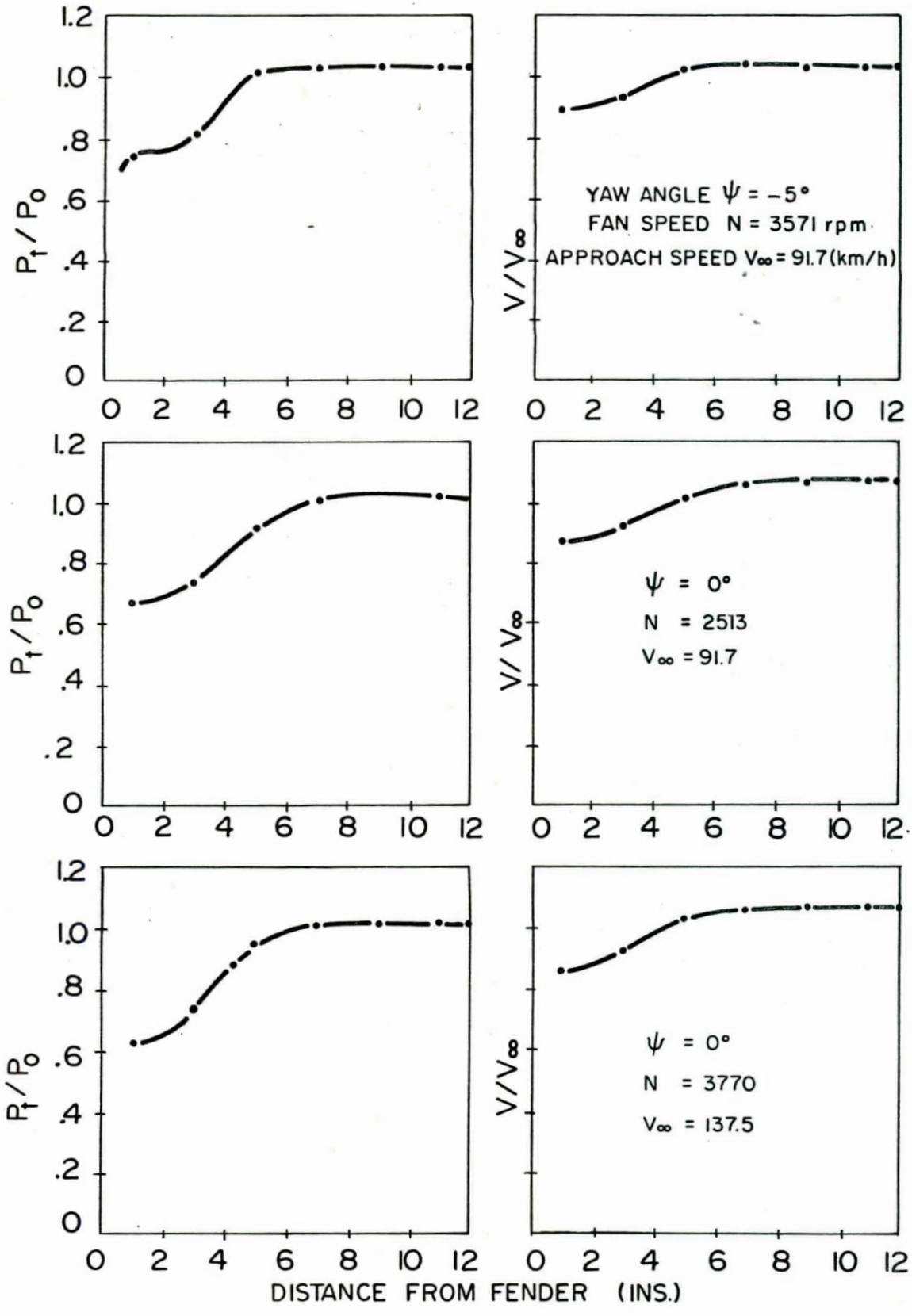

EXTERNAL AIR FLOW AT SIDE OF VEHICLE

FIG. 25
LTR-ENG-100

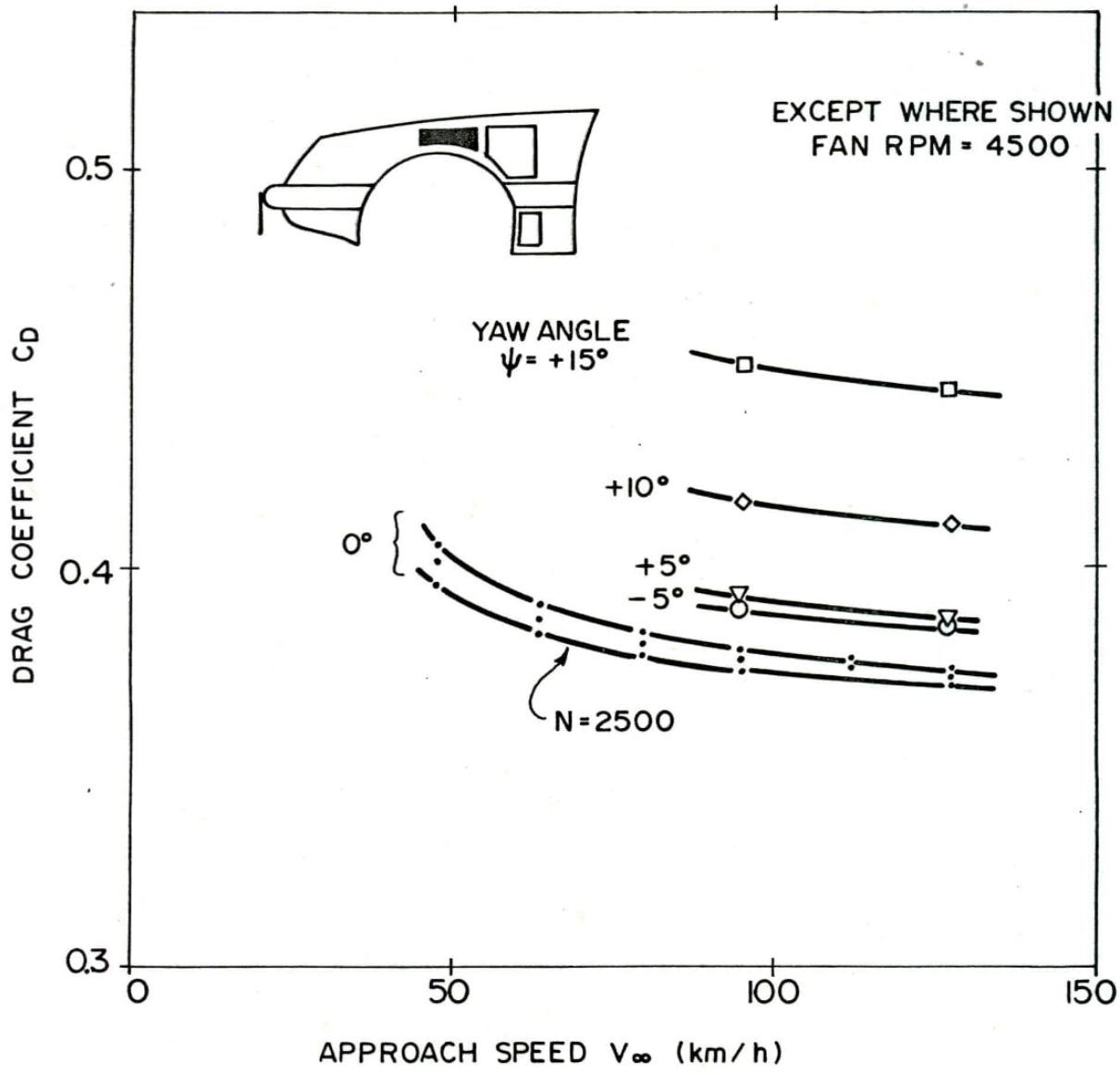

DRAG COEFFICIENT IN VEHICLE STABILITY AXIS-"A" INTAKES, EXPOSED LICENCE PLATE.

FIG. 26
LTR-ENG-100

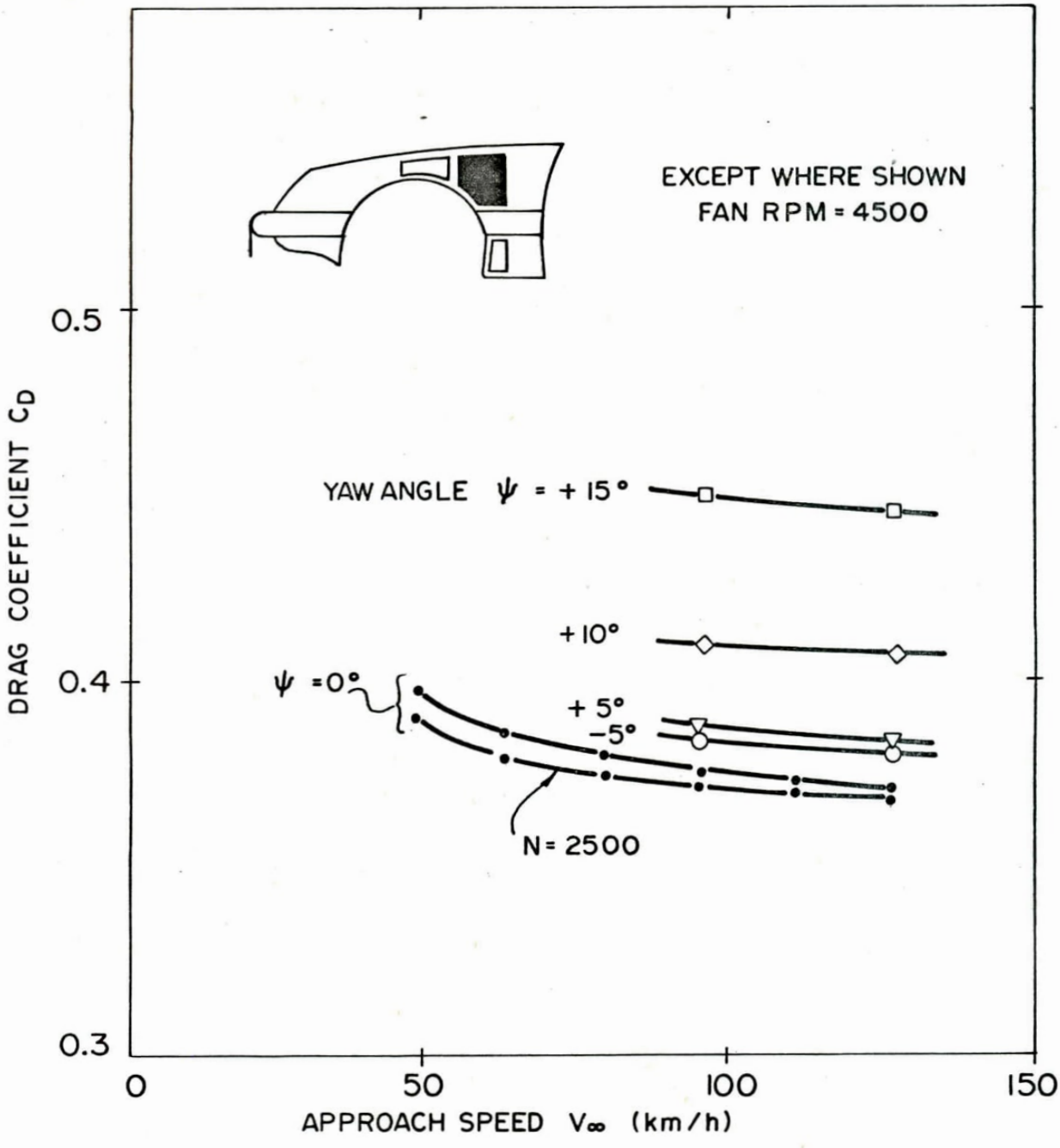

DRAG COEFFICIENT IN VEHICLE STABILITY
AXIS – "B" INTAKES, EXPOSED
LICENCE PLATE

FIG. 27
LTR-ENG-100

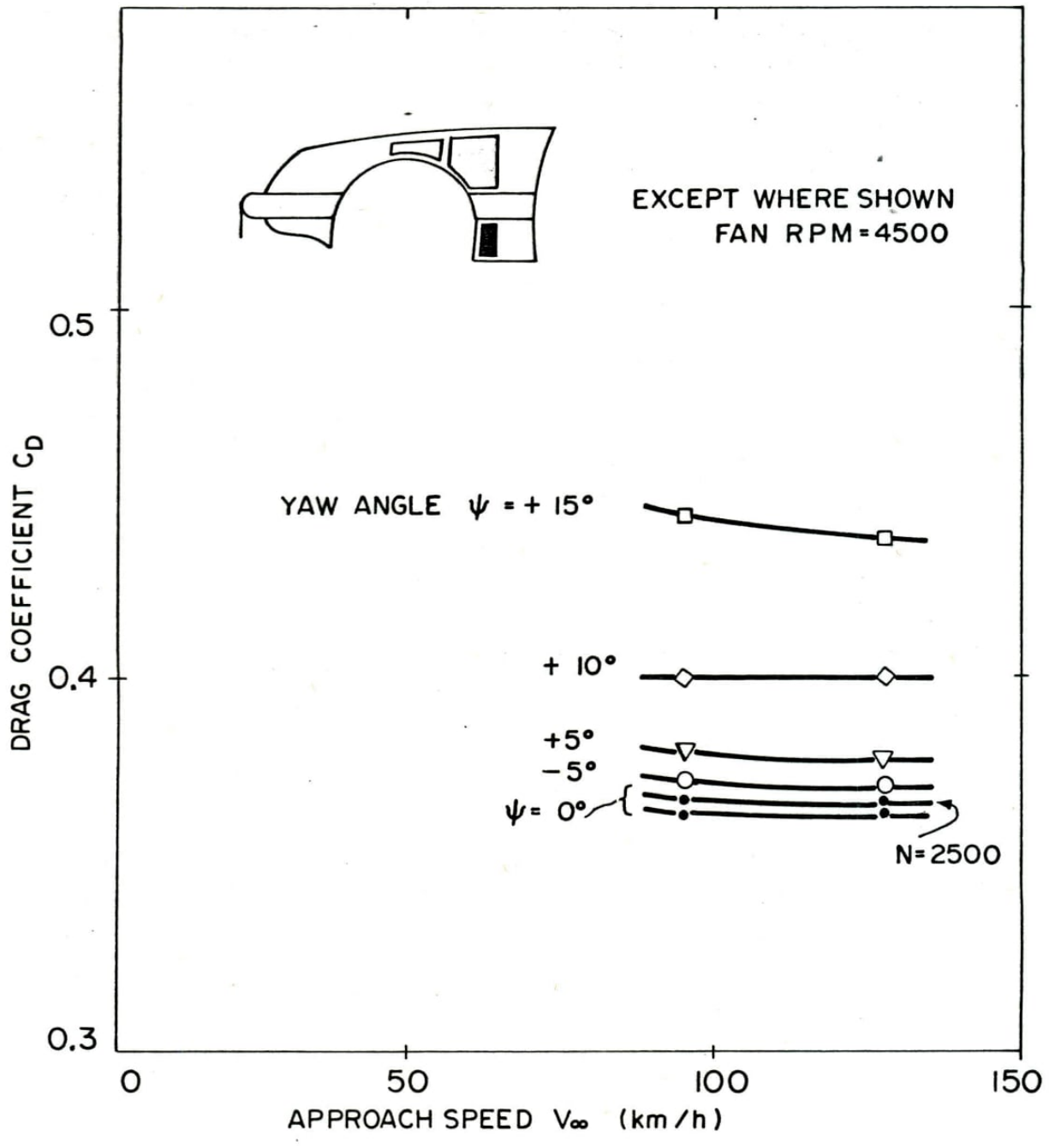

DRAG COEFFICIENT IN VEHICLE STABILITY
AXIS — "C" INTAKES, EXPOSED
LICENCE PLATE

FIG.28
LTR-ENG-100

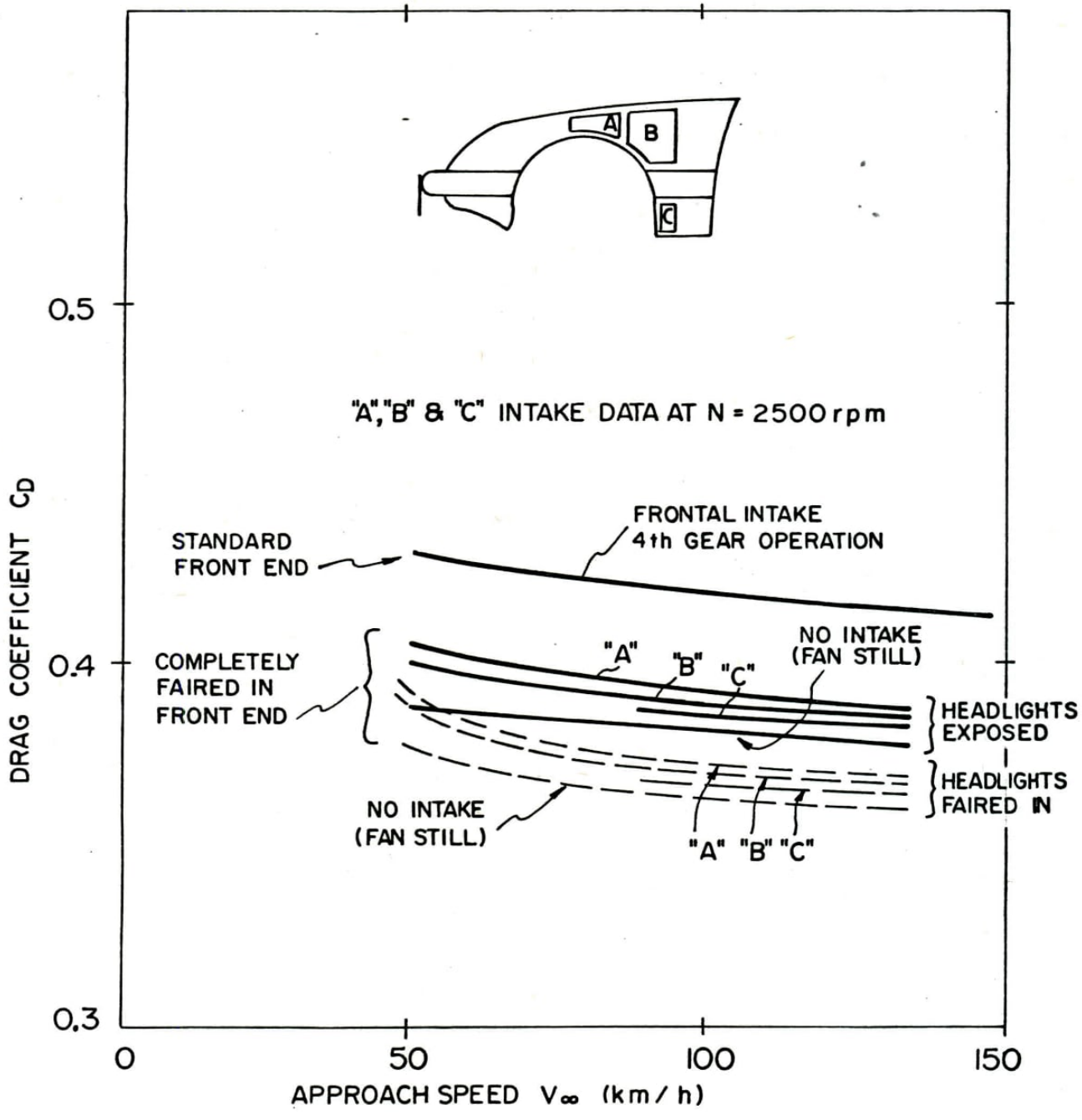

DRAG COEFFICIENT IN VEHICLE STABILITY AXIS – COMPARISONS OF STANDARD FRONTAL INTAKE, AND SIDE INTAKES WITH LIGHTS FAIRED IN AND EXPOSED.

FIG. 29
LTR-ENG-100

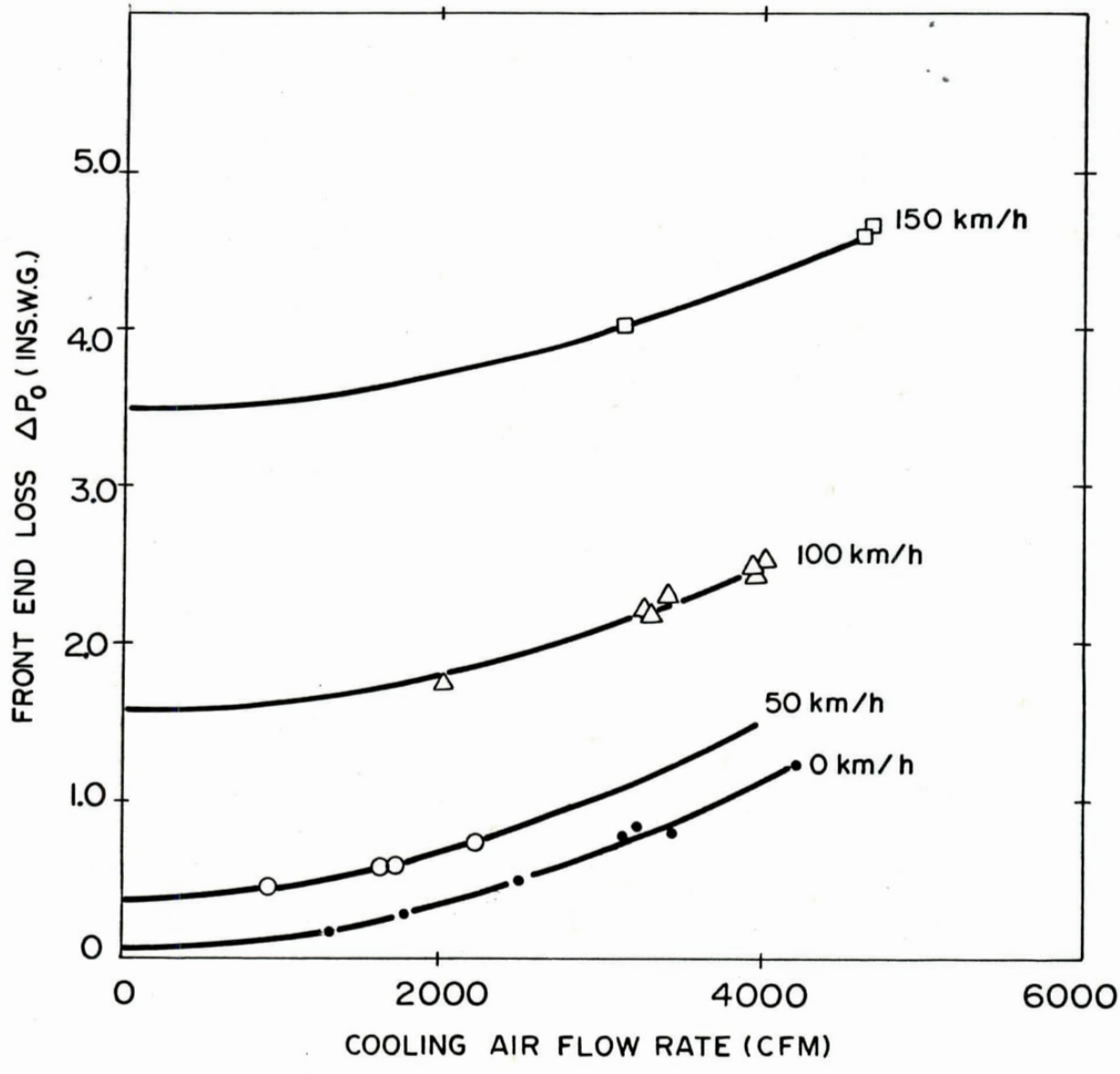

FRONT END LOSS OF
STANDARD VEHICLE

FIG. 30
LTR-ENG-100

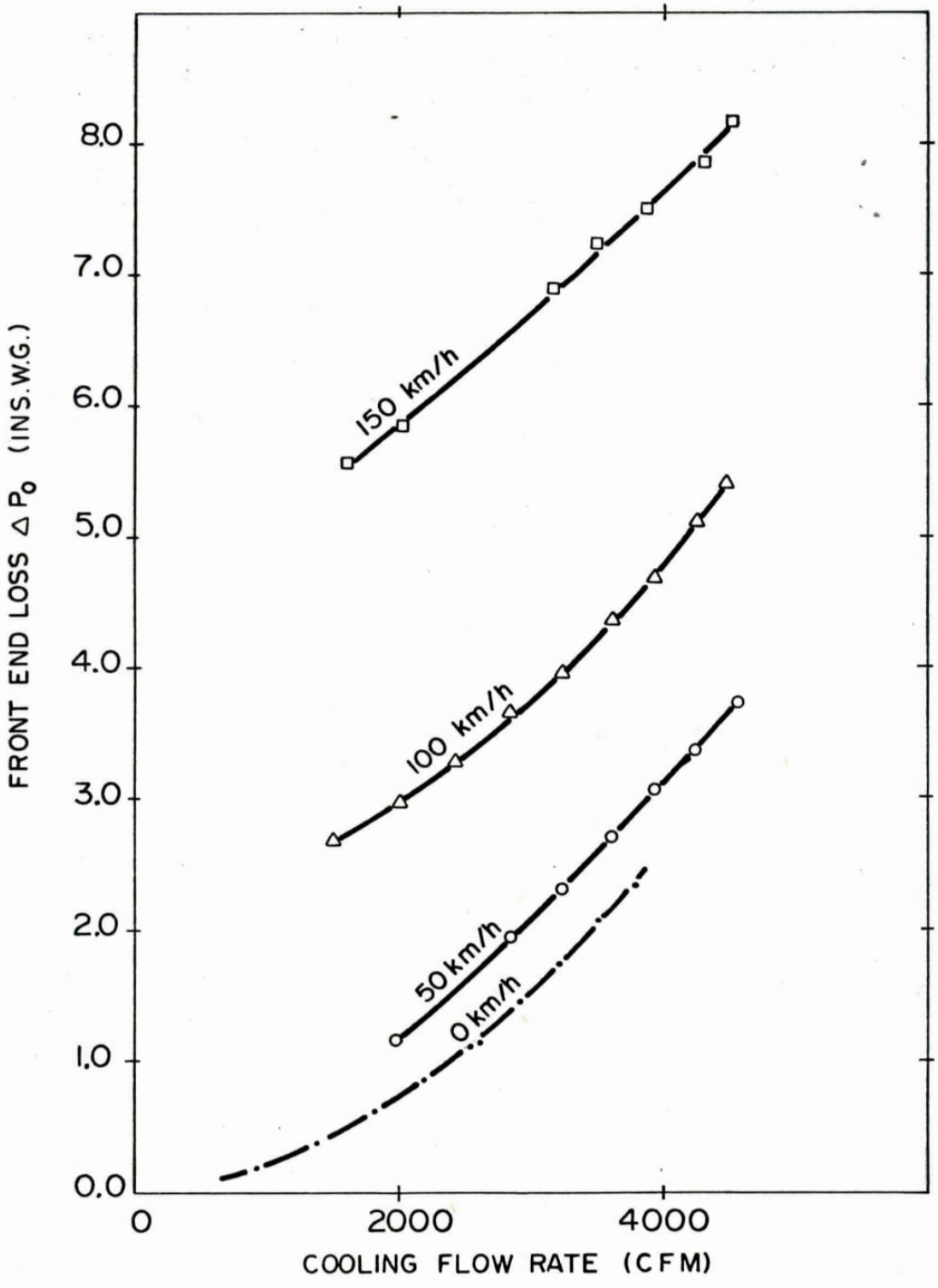

FRONT END LOSS — VEHICLE WITH TYPE "B" SIDE INTAKES

FIG.31
LTR-ENG-100

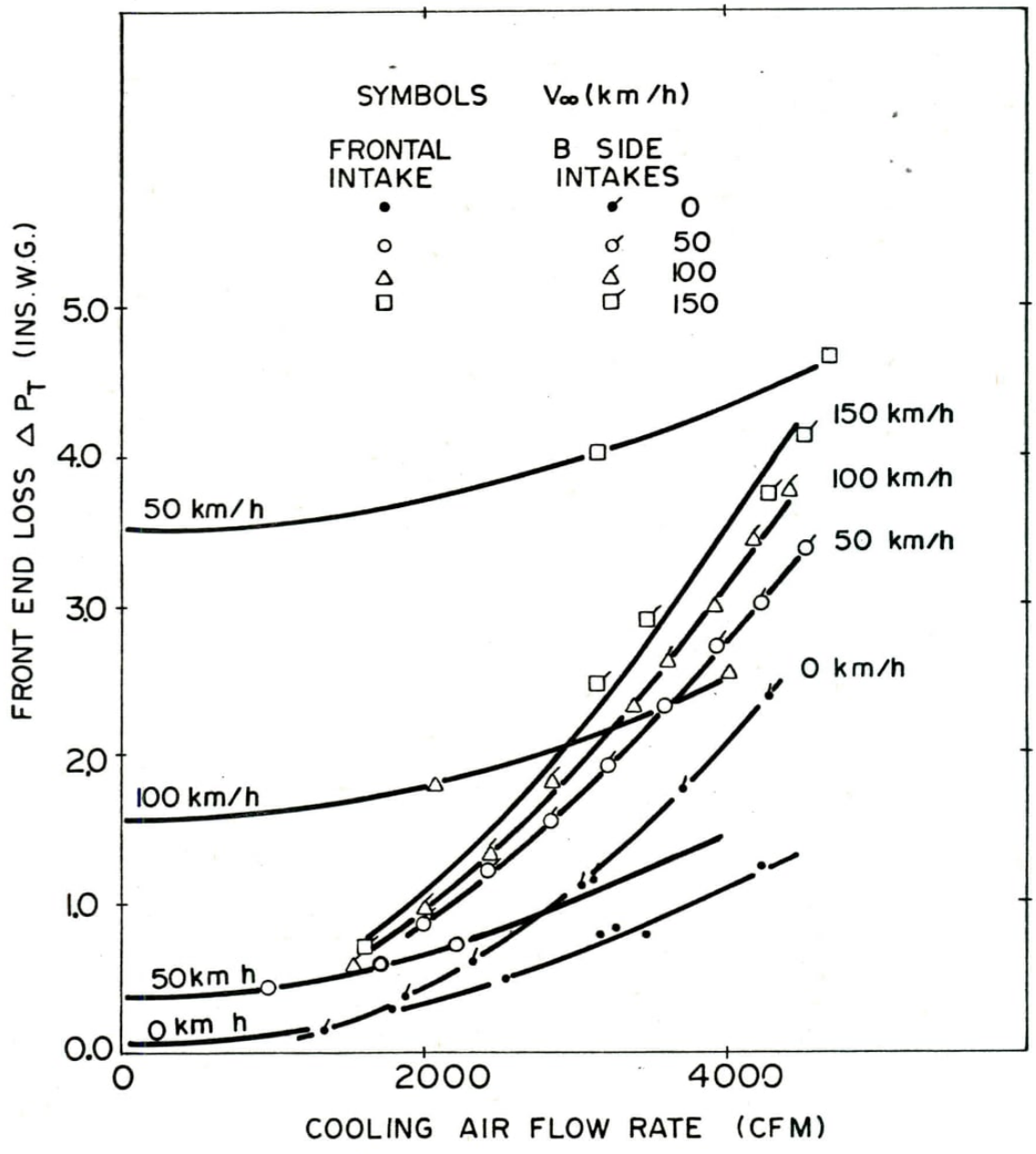

EFFECT OF SIDE INTAKES ON
FRONT END LOSS

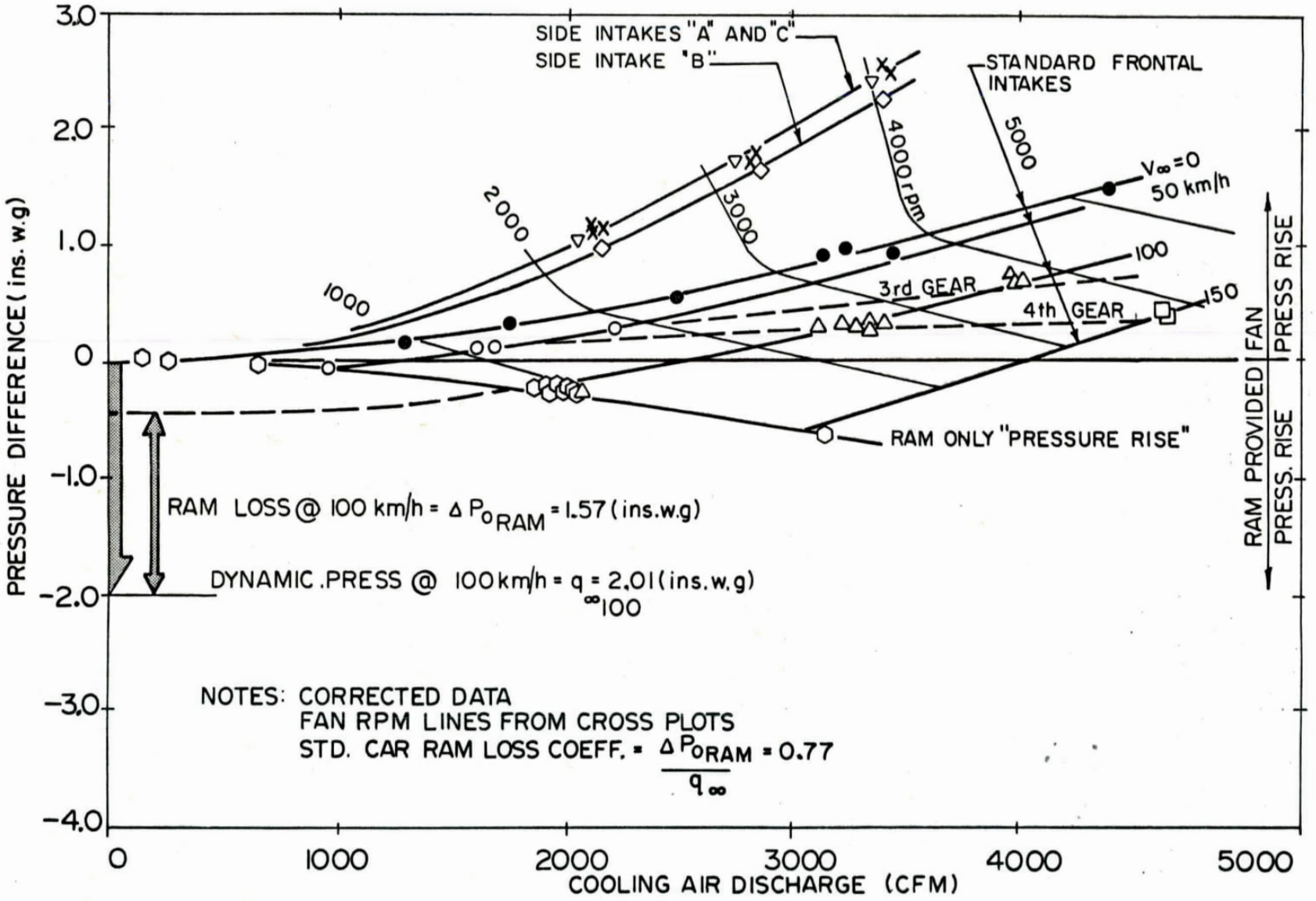

CHARACTERISTIC MAP OF THE COOLING FAN OPERATING WITH RAM.

FIG. 32
LTR-ENG-100

FIG. 33
LTR-ENG-100

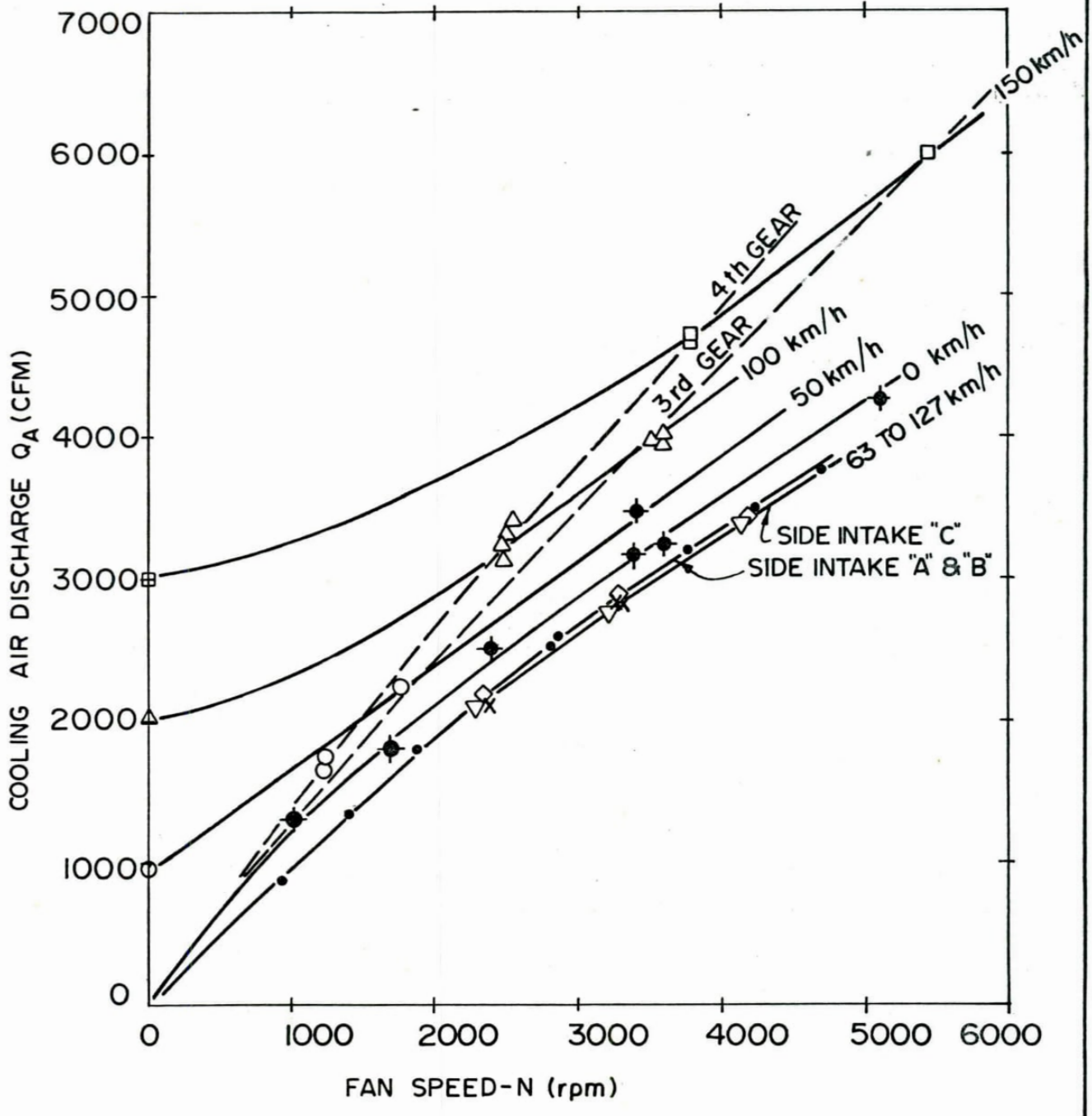

EFFECT OF APPROACH SPEED
ON COOLING FLOW— SIDE AND FRONTAL
INTAKES

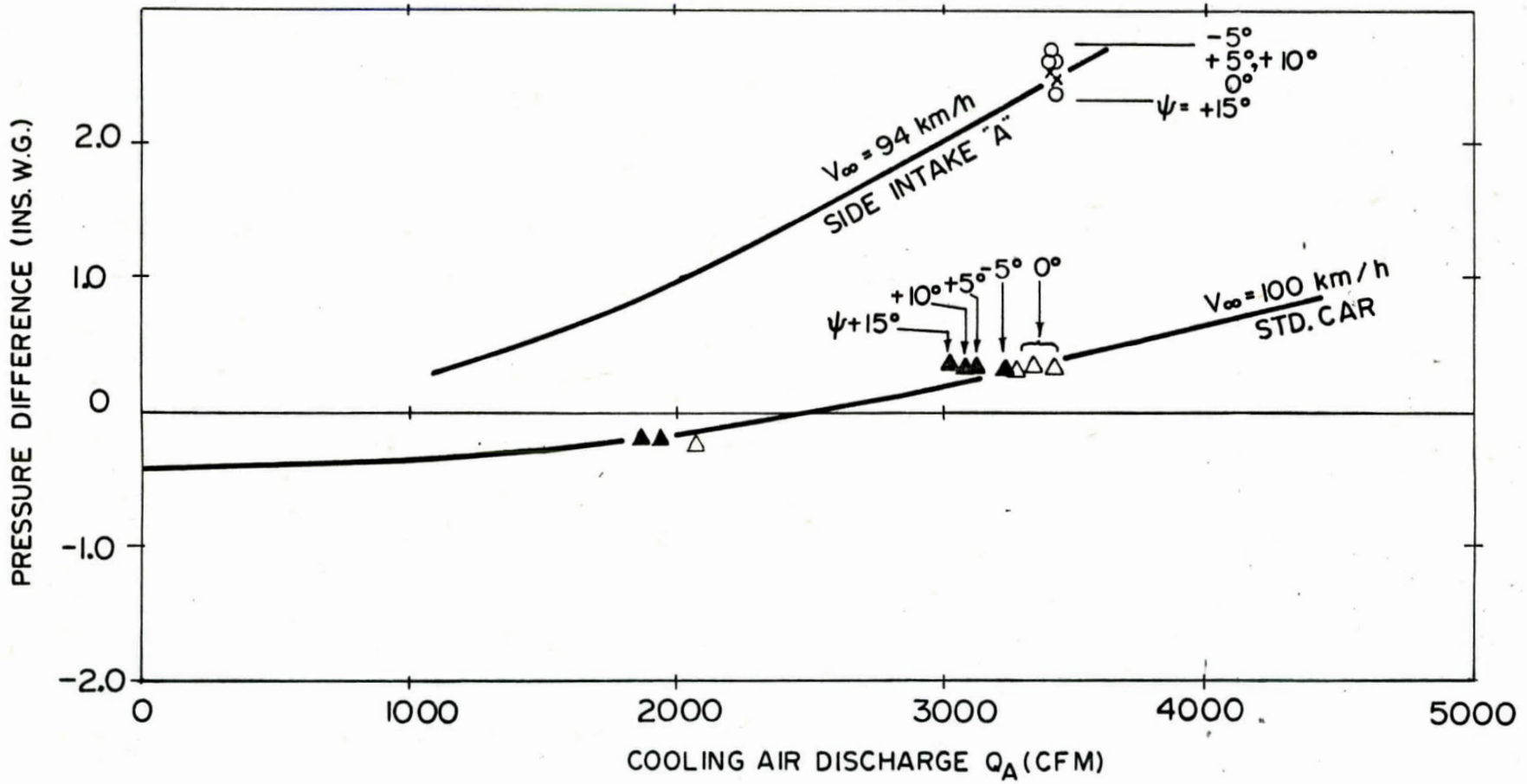

EFFECT OF YAW ON COOLING FLOW

FIG. 34
LTR-ENG-100

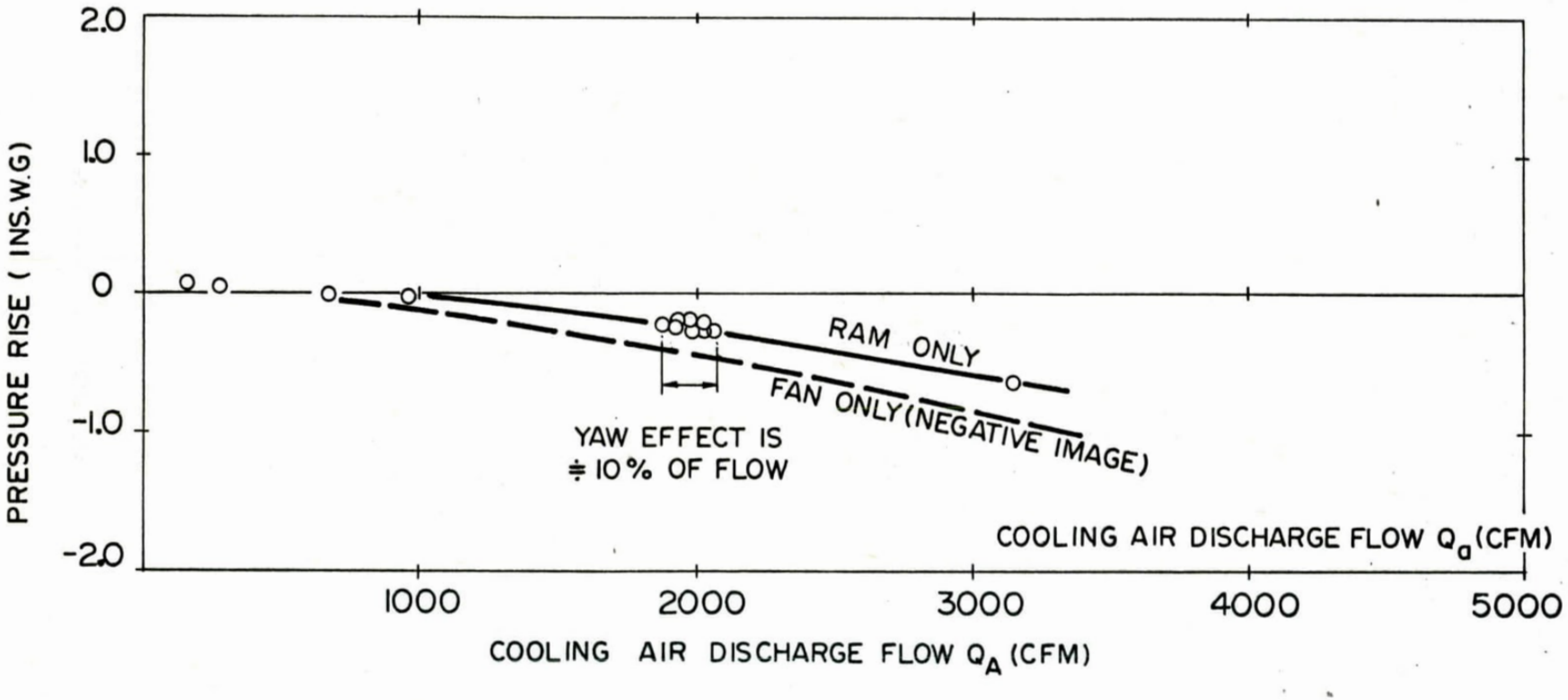

COMPARISON BETWEEN PRESSURE RISES GENERATED IN THE STANDARD CAR BY RAM AND FAN ALONE

FIG. 35
LTR-ENG-100

FIG. 36
LTR-ENG-100

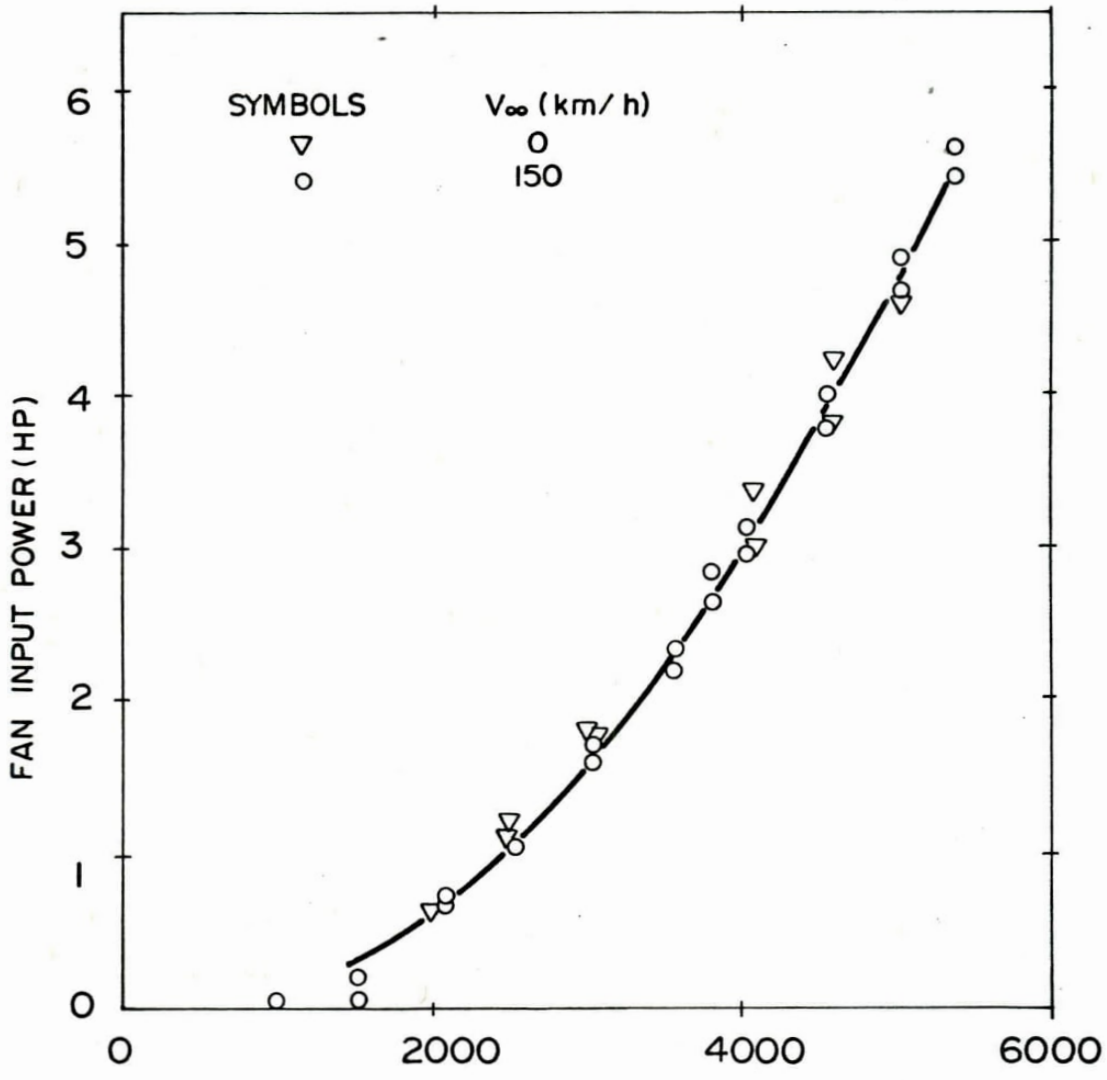

COOLING FAN POWER IN STANDARD VEHICLE AT APPROACH SPEEDS OF ZERO AND 150 km/h

FIG. 37
LTR-ENG-100

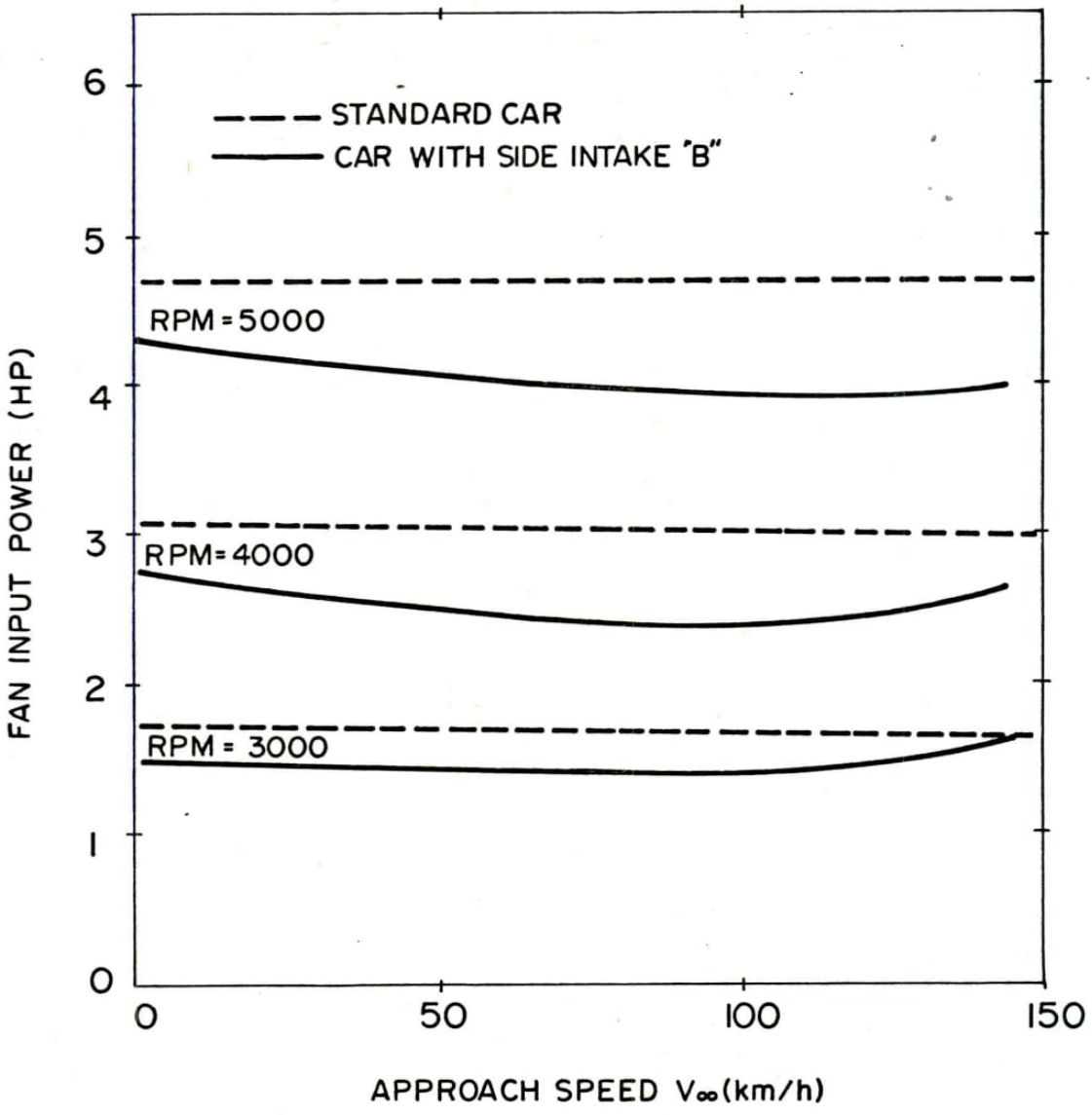

FAN POWER DEPENDENCE
ON APPROACH SPEED

FIG. 38
LTR-ENG-100

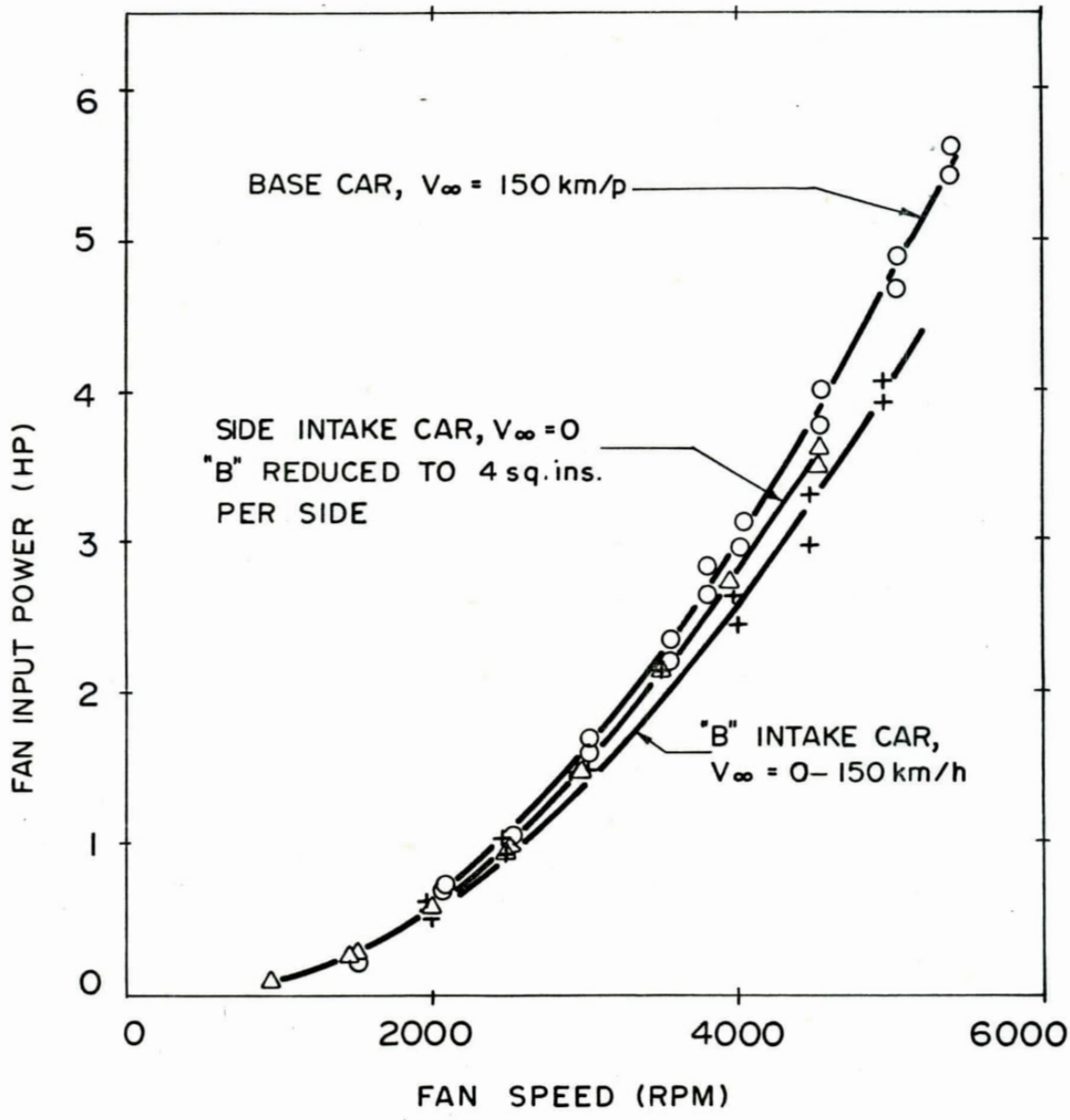

MEASURED COOLING FAN POWER

FIG. 39
LTR-ENG-100

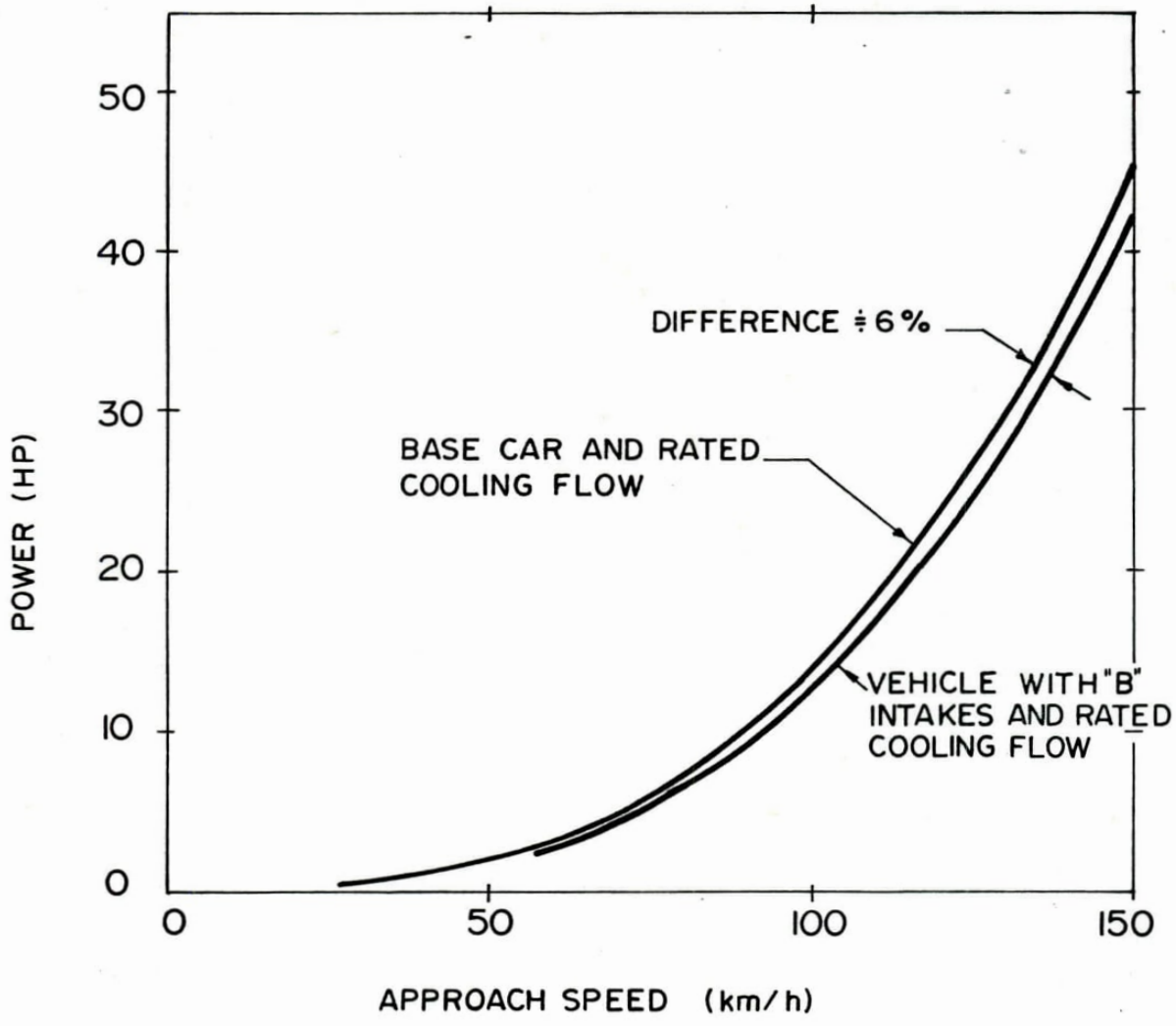

POWER DEMAND TO OVERCOME
AERODYNAMIC DRAG - RATED FLOW
THROUGH COOLING SYSTEM

FIG. 40
LTR-ENG-100

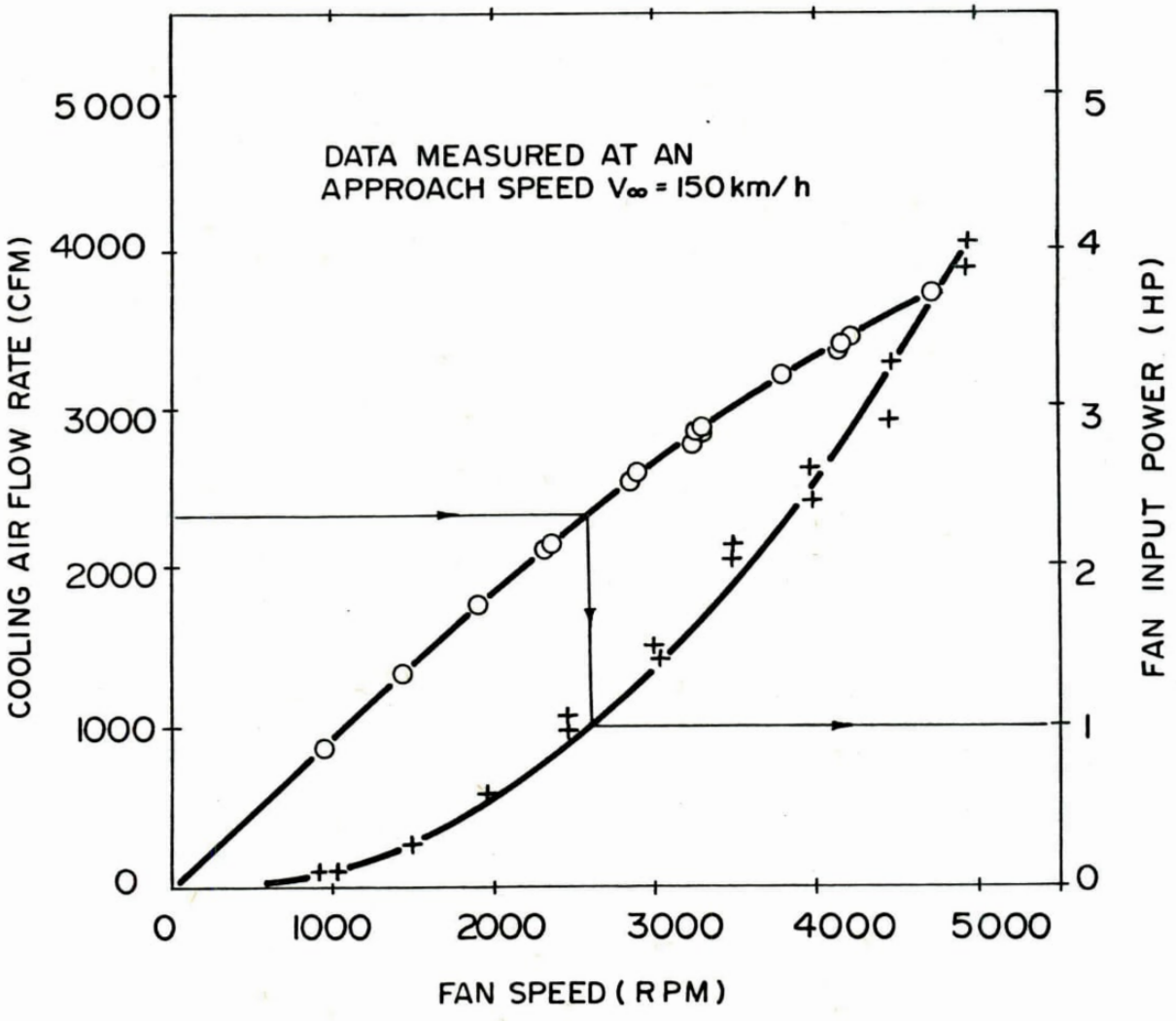

COOLING FAN PERFORMANCE-
TYPICAL FOR "B" INTAKE

FIG. 41
LTR-ENG-100

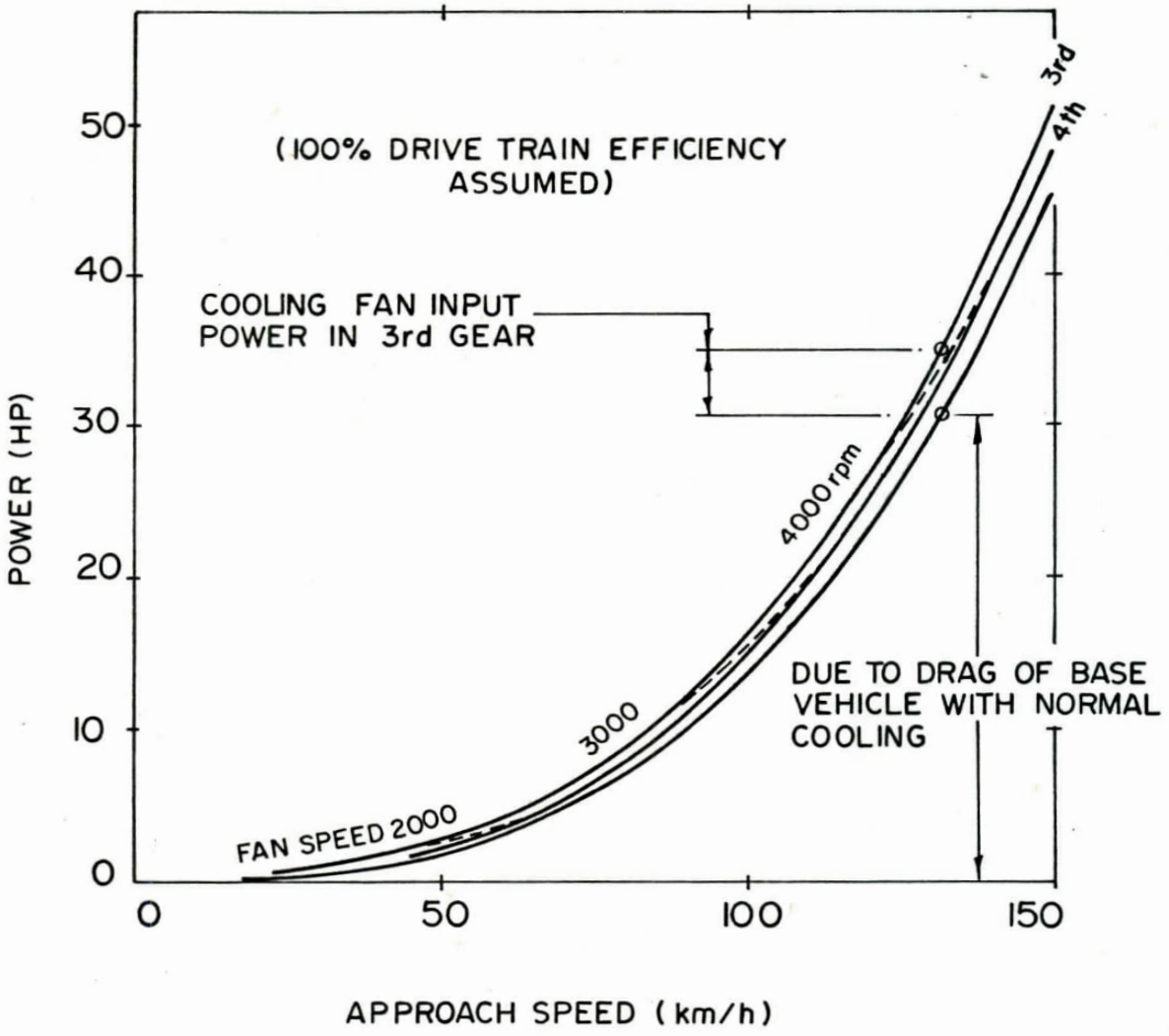

POWER DEMAND TO OVERCOME AERODYNAMIC DRAG AND TO DRIVE THE COOLING FAN – RATED PRODUCTION FLOW THROUGH COOLING SYSTEM OF BASE VEHICLE

FIG. 42
LTR-ENG-100

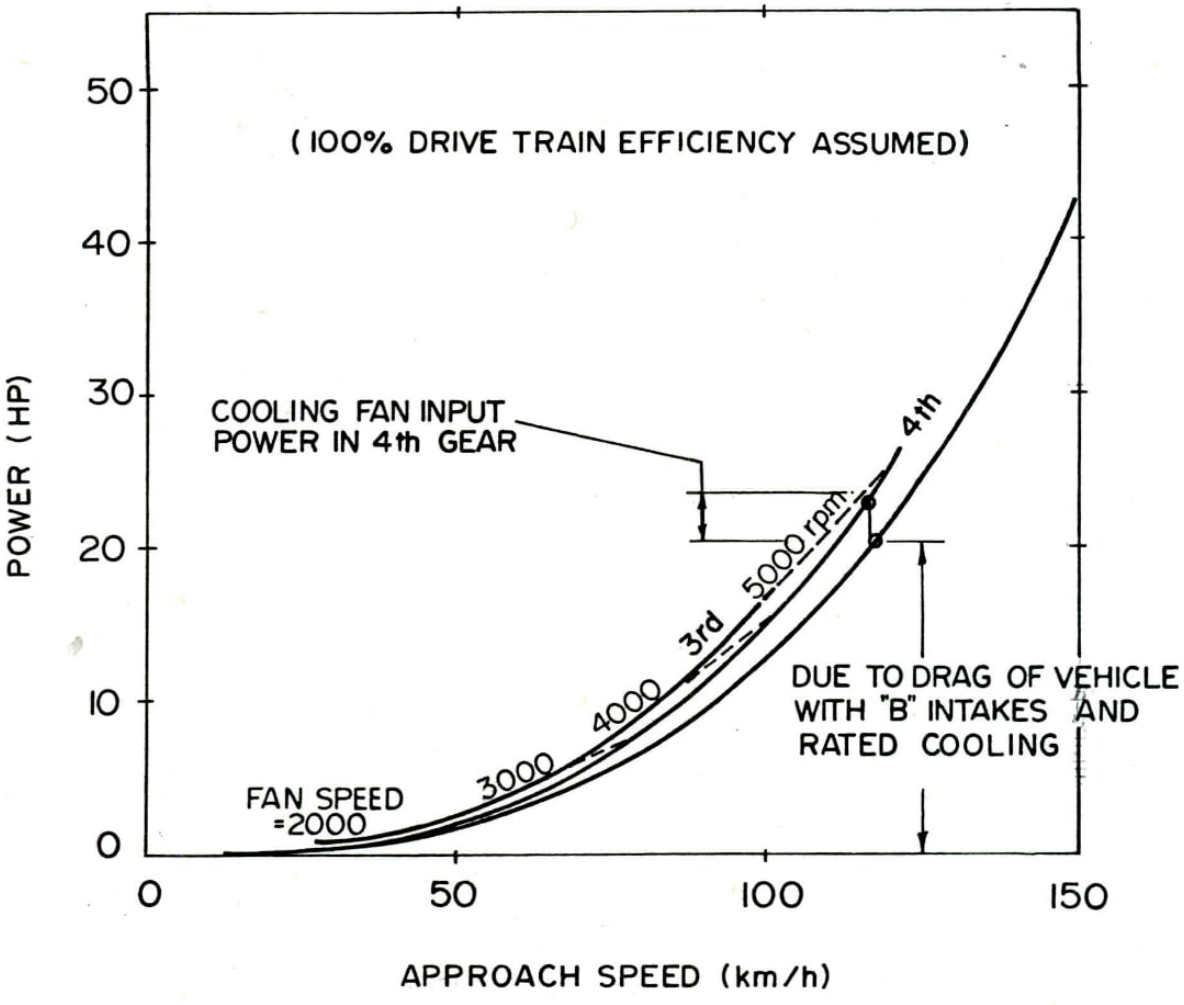

POWER DEMAND TO OVERCOME AERODYNAMIC DRAG AND TO DRIVE THE COOLING FAN—RATED PRODUCTION FLOW THROUGH COOLING SYSTEM OF "B" INTAKE VEHICLE

FIG. 43
LTR-ENG-100

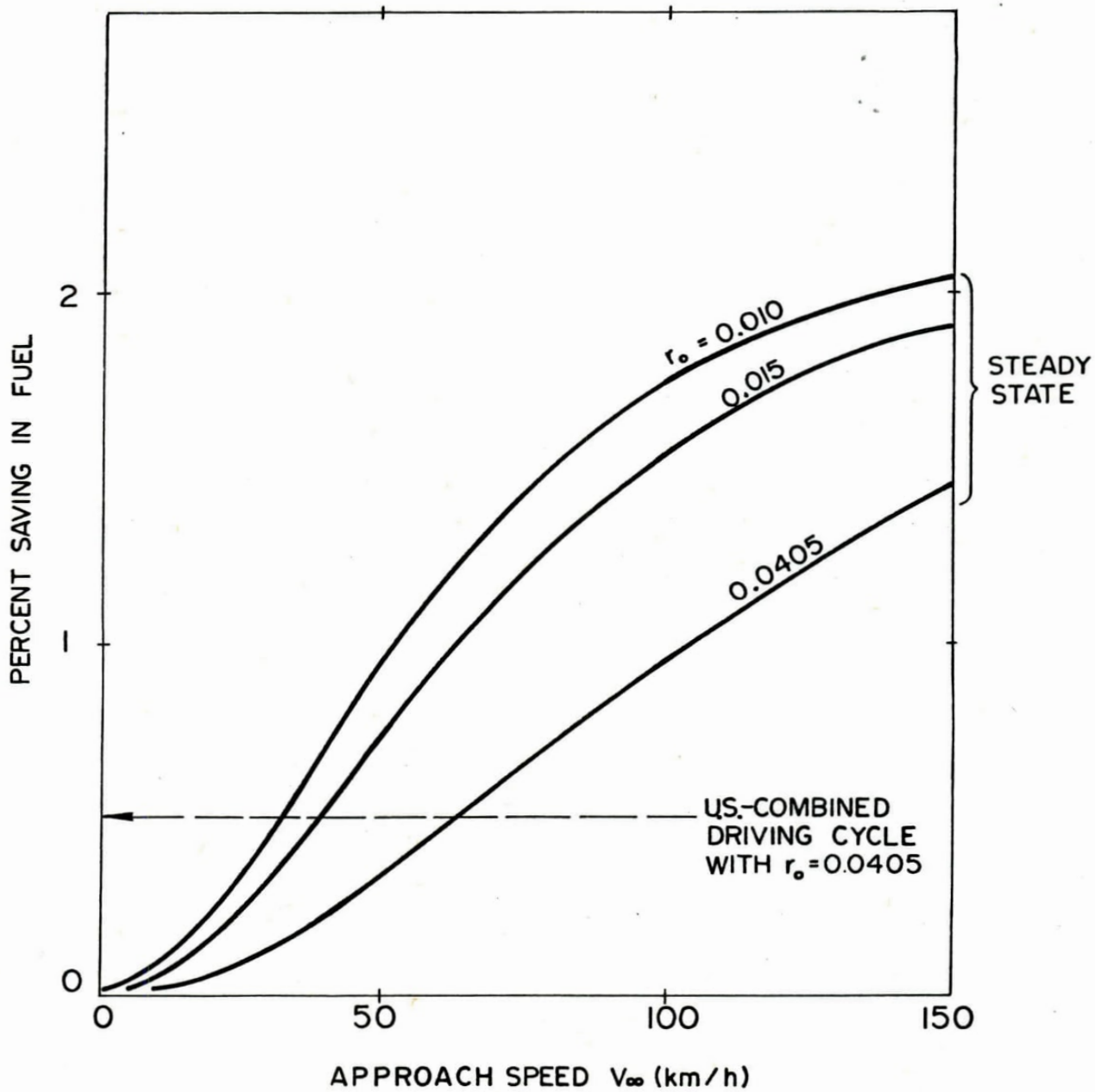

ESTIMATED FUEL SAVINGS FOR $\Delta C_D = 0.01$ REDUCTION IN AERODYNAMIC DRAG FOR VARIOUS ROLLING RESISTANCES

FIG. 44
LTR-ENG-100

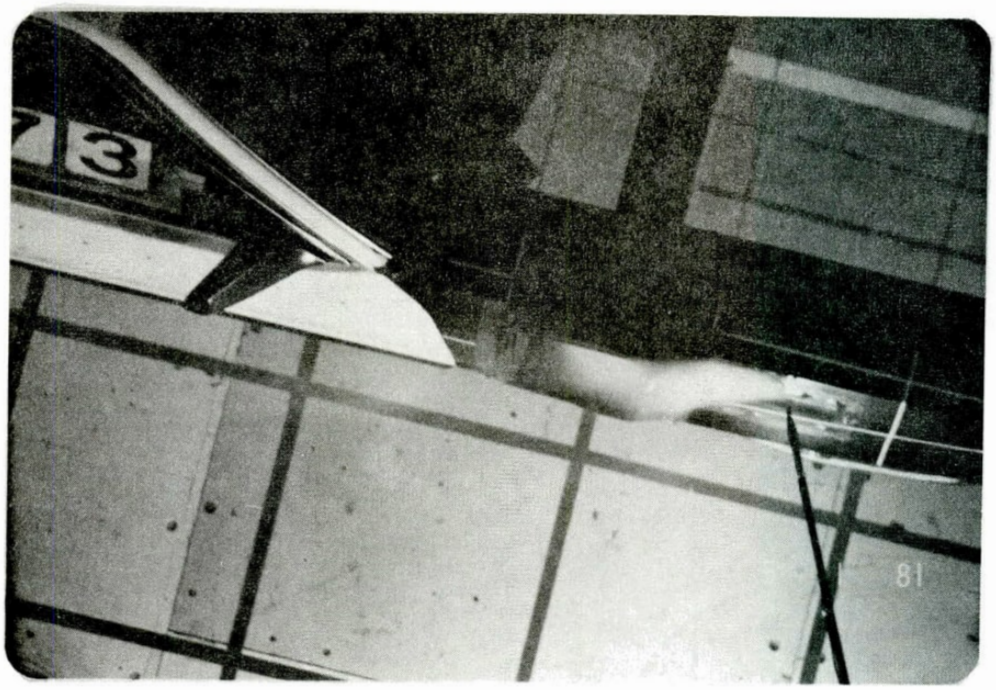

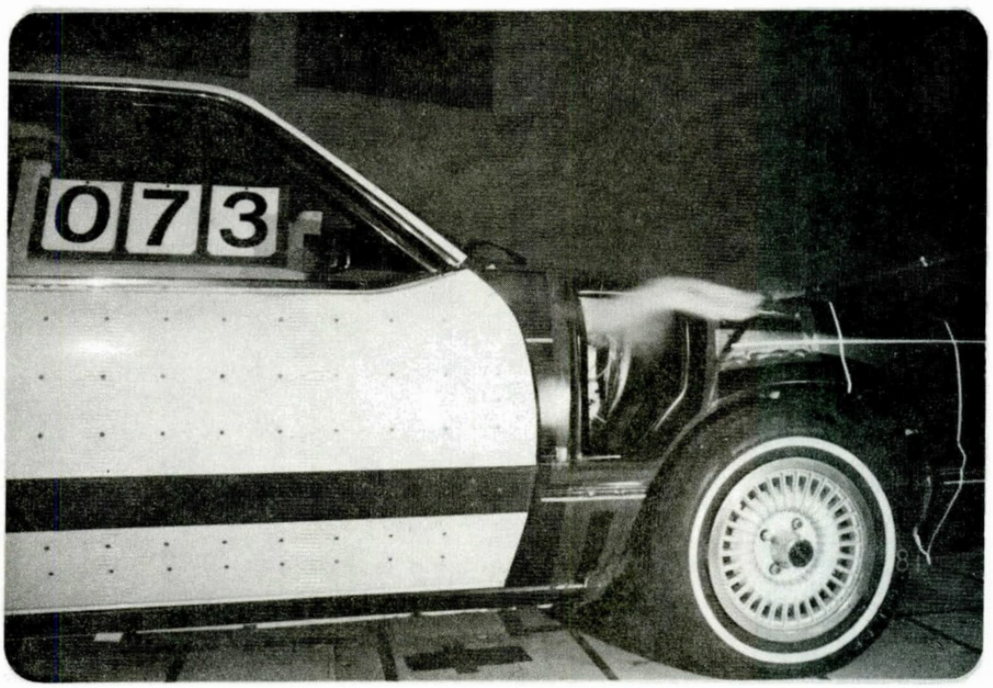

MUSTANG SMOKE STUDIES – TYPE "B" SIDE INTAKES,
LEE SIDE VIEW, YAW ANGLE = + 15 DEGREES.

FIG. 45
LTR-ENG-100

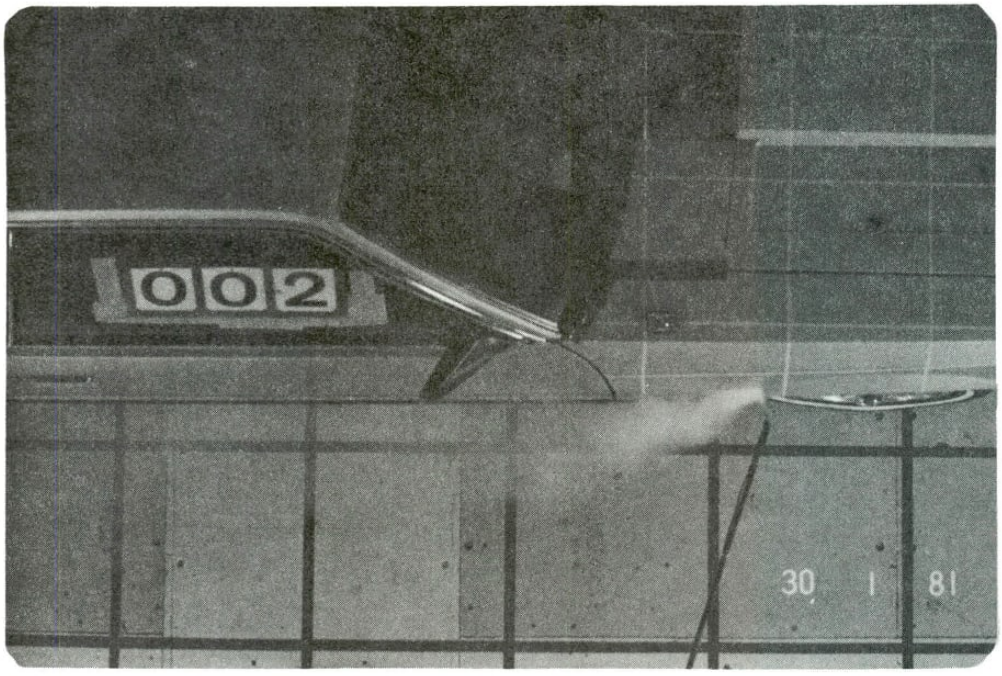

STANDARD FRONTAL INTAKE

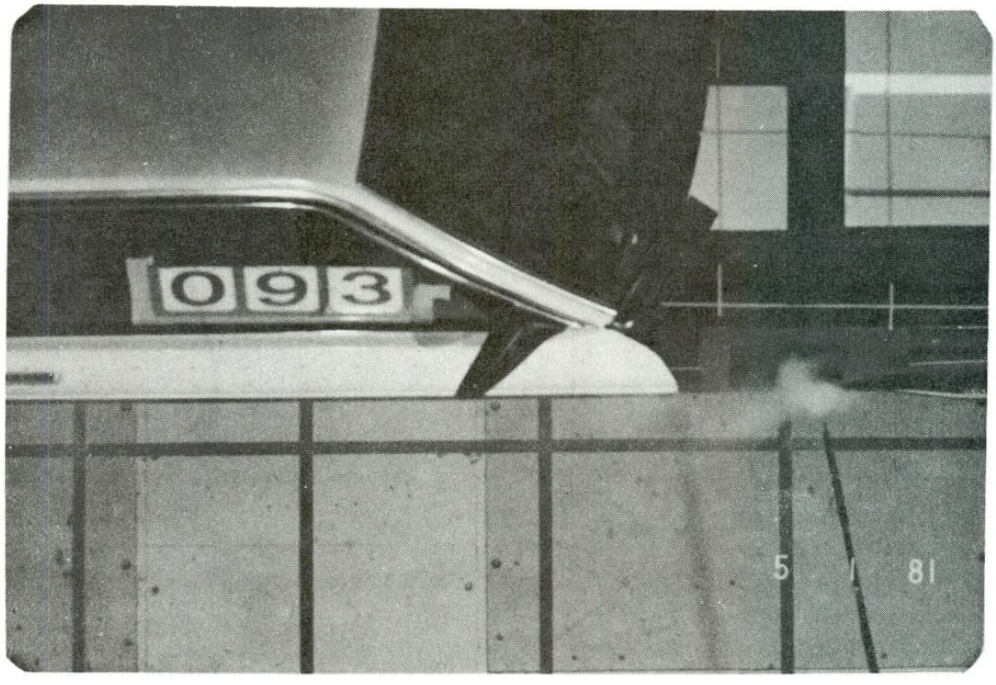

TYPE "B" SIDE INTAKES

MUSTANG SMOKE STUDIES - FRONTAL AND TYPE "B" SIDE INTAKES, OVERHEAD VIEW AT YAW ANGLE OF ZERO DEGREES

FIG. 46
LTR-ENG-100

STANDARD FRONTAL INTAKE

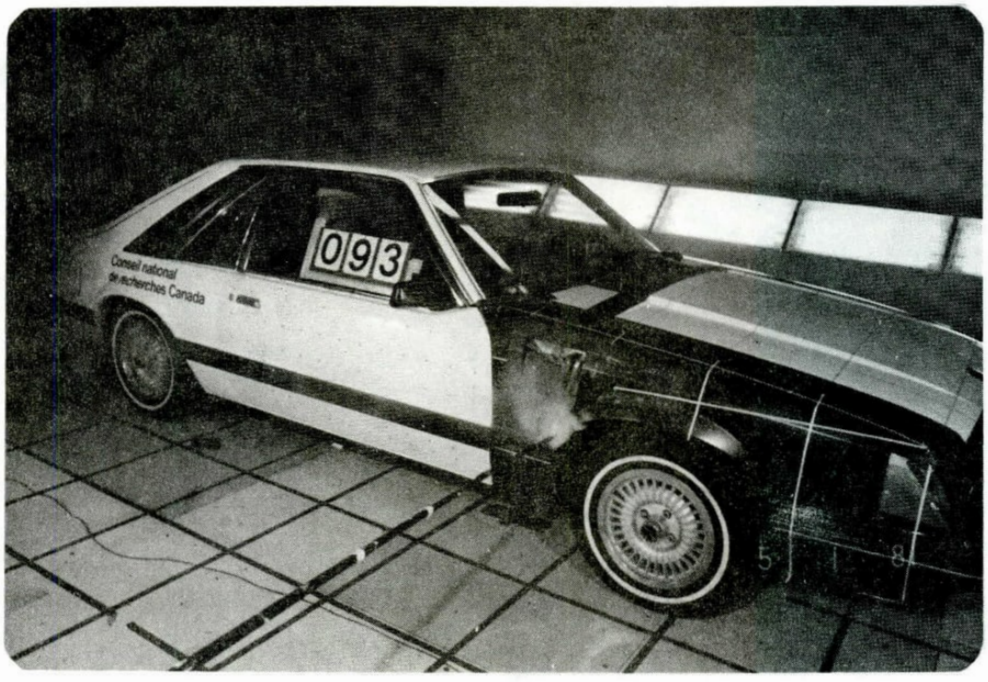

TYPE "B" SIDE INTAKES

MUSTANG SMOKE STUDIES - FRONTAL AND TYPE "B" SIDE INTAKES, SIDE VIEW AT YAW ANGLE OF ZERO DEGREES.

FIG. 47
LTR-ENG-100

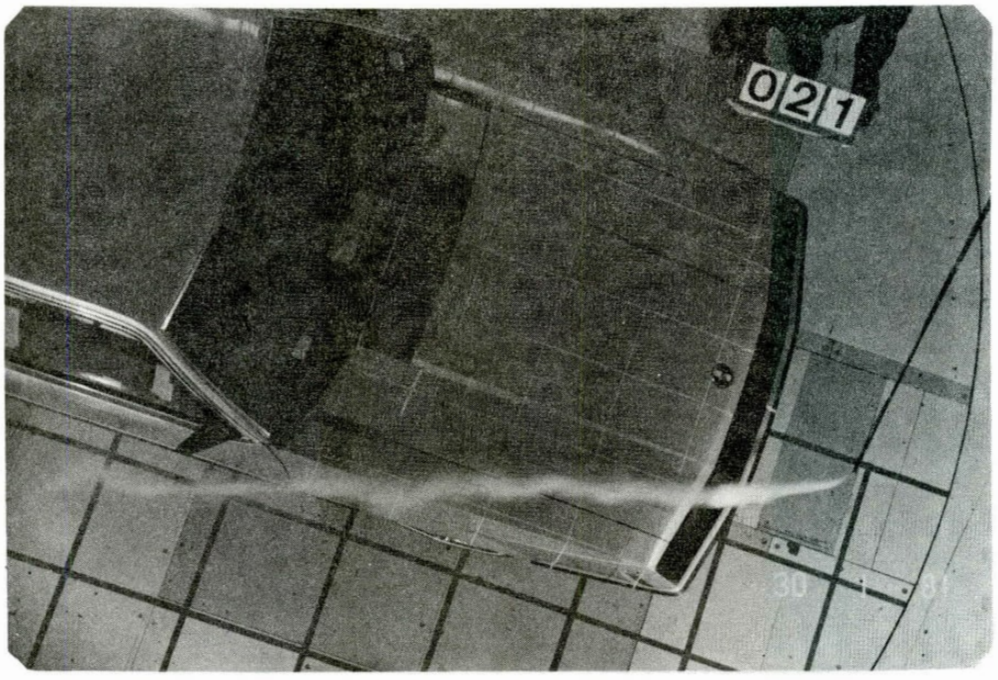

STANDARD FRONTAL INTAKE

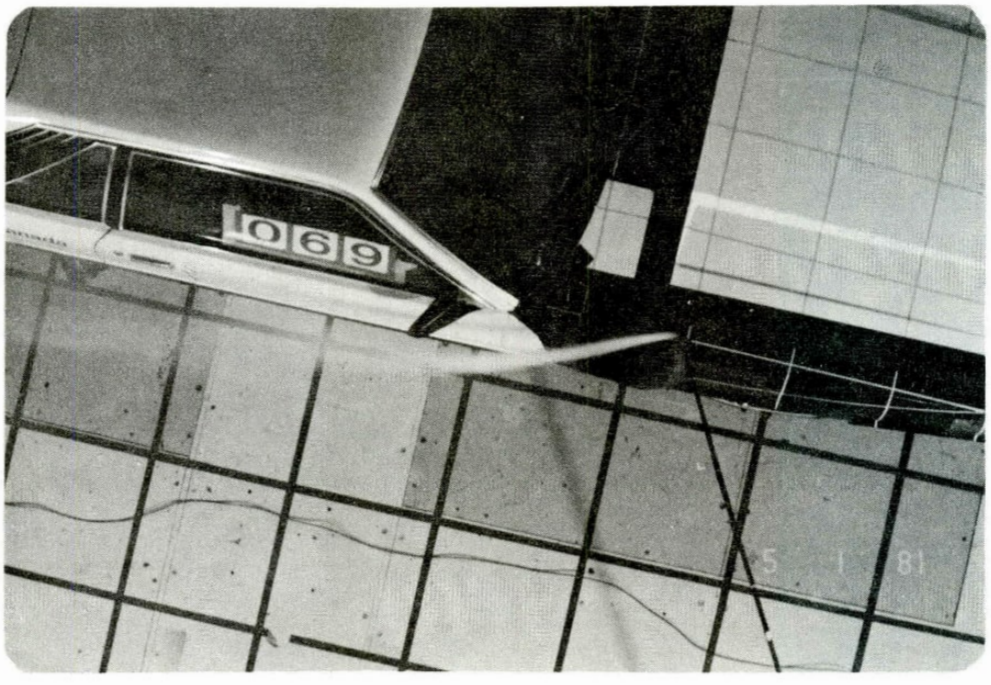

TYPE "B" SIDE INTAKES

MUSTANG SMOKE STUDIES-FRONTAL AND TYPE "B" SIDE INTAKES, LEE SIDE (OVERHEAD) VIEW AT YAW ANGLE OF +15 DEGREES

FIG. 48
LTR-ENG-100

STANDARD FRONTAL INTAKE

TYPE "B" SIDE INTAKES

MUSTANG SMOKE STUDIES – FRONTAL AND TYPE "B" SIDE INTAKES, LEE SIDE VIEW AT YAW ANGLE OF + 15 DEGREES

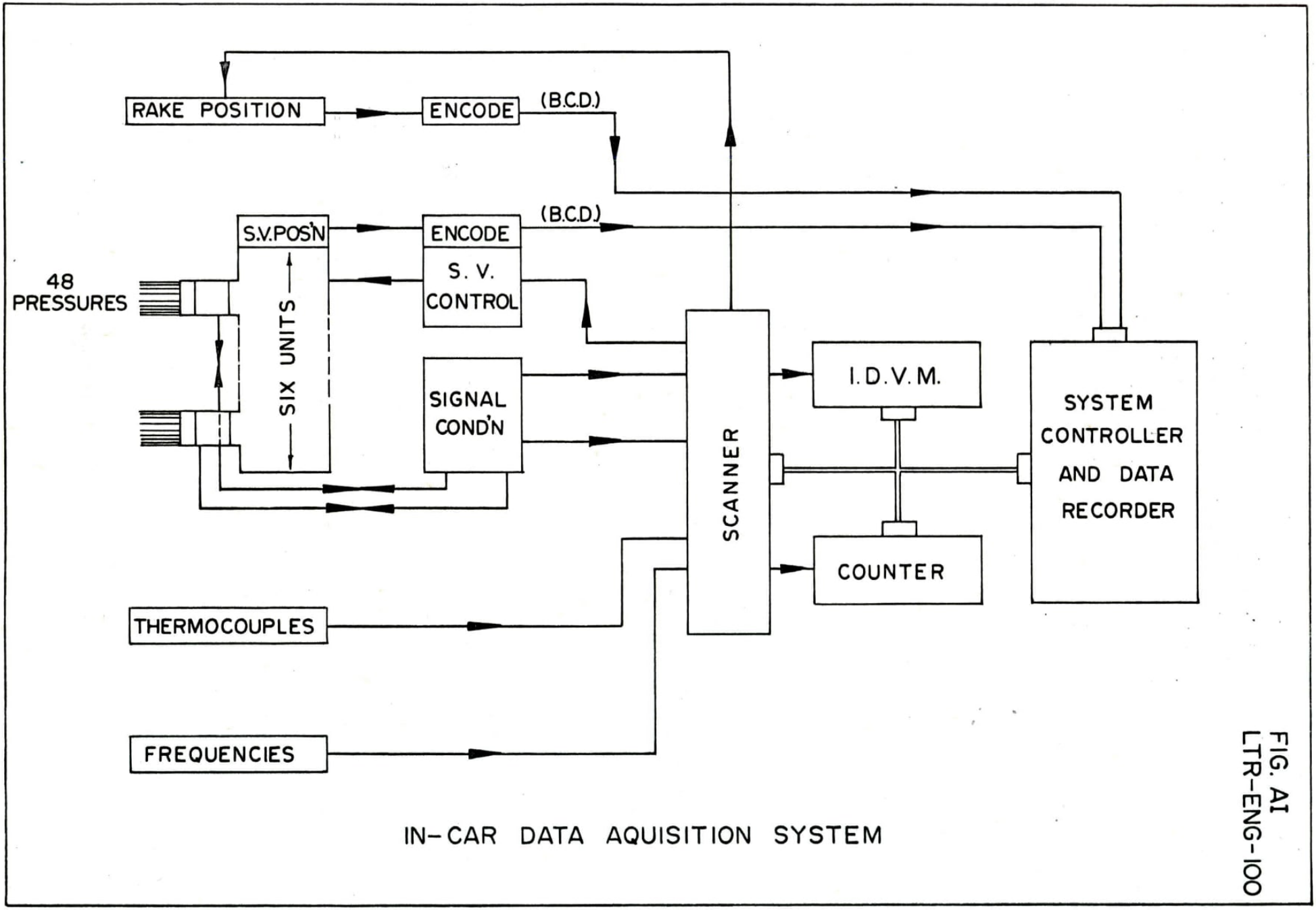

IN-CAR DATA AQUISITION SYSTEM

FIG. AI
LTR-ENG-100